

Below the surface

A laboratorial research to the vertical distribution
of buoyant plastics in rivers

By

Louise-Anne Zaat

To obtain the degree of

Master of Science

at the Delft University of Technology,
to be defended publicly on Thursday January 30st, 2020 at 4 p.m.

Student number:	4209656	
Thesis Chair:	Dr. T.A. Bogaard	TU Delft
Thesis Committee:	Dr. Ir. O. Hoes	TU Delft
	Prof. Dr. Ir. W.S.J Uijttewaai	TU Delft
	Dr. Ir. T.H.M. van Emmerik	Wageningen University

Cover photo: Retenue d'eau, Michel François.
Photo taken at Voorlinden Museum Wassenaar, October 2019

An electronic version of this thesis is available at repository.tudelft.nl

Preface

This MSc thesis gives first insights in the vertical distribution of plastic over the water depth, in relation with prevailing flow conditions. The research was carried out at the Delft University of Technology, with the support of a number of people involved, whom I would like to thank in this preface.

First of all, I would like to thank my graduation committee for their supervision and advice during this research. Thanks go out to Tim van Emmerik, for helping me find a subject fitting so perfectly to both the scientific needs, as my personal interests and desires. But also, for being so actively involved during the entire process. I would also like to thank Wim Uijttewaai, for challenging me to really understand the mechanisms behind the transport of plastic. I was forced to go outside of my own knowledge field and delve into the complex world of turbulent flows. Thanks go out to Olivier Hoes and his efforts for making this research stand out and to finally come to a structured, well understandable report. The strong advice to find a topic that really keeps my interest and motivates me, has been taken to heart. Even though the research path did take some unforeseen turns, which led to some hard times, I learned to enjoy doing this MSc research (which is often seen as a bitter pill at the end of the student's career). This is largely owed to my daily supervisor, Thom Bogaard, who played a crucial role in mentoring and motivating me. Thom helped me make decisions that were close to my intrinsic wishes to contribute to the great plastic issue, but that also kept the research within an overseeable scope.

Moreover, I would like to thank everyone whom I crossed paths with during my research. During my orientation phase I got help from Remco Pikaar and Harm Landman (Tauw b.v.). Many thanks for their time. Erik Mosselman brought me in contact with Marcel Liedermann - coauthor of one of the guiding researches I used for my own research - with whom I was able to interchange ideas on the subject. I want to thank the team of Dopper, for inviting me for their *Dopper thesis-challenge* and connecting me to many inspirational students working on similar topics as me. I enjoyed the positive work attitudes around this (less positive) subject of plastic pollution. Special thanks go out to Hans Brinkhof and Pepijn van Aubel of Rijkswaterstaat, and Rinze de Vries of the start-up Noria. I had the pleasure to work with them on a project in the Borgharen sluice of Maastricht. Even though this project did not lead to further research opportunities for my thesis, I have learned a lot from working with a team that is dedicated to reducing the plastic waste in rivers. Thanks to all these involved people, I learned so much more than expected. I feel really privileged to have had all these opportunities.

Lastly, special thanks go out to the people close to me who have endured my infinite talks about plastic, and who nevertheless have supported me throughout the entire process.

Louise-Anne Zaat
Delft, January 2020

Summary

Rivers are identified as main sources of plastic litter in oceans. About 65% of the plastic litter is buoyant in fresh waters, meaning it has the capability to float, making transport over rivers relatively easy. A better understanding of how plastic litter is transported via rivers is crucial. Both for quantification and mitigation of the plastic problem. Most research on quantification of the plastic flux is based on surface-measurements only, up till about 50 cm water-depth. Thereby, most cleaning strategies focus on skimming only the surface.

This research investigates the distribution of buoyant plastic litter over the water depth in rivers. Given the wide use of marginal buoyant plastics, it is hypothesized that a significant share of the plastic in rivers is transported below the first 50 cm surface-water, due to the mixing ability of turbulent flow. In such case, a great share of the plastic litter is overlooked in both flux estimates and riverine removal strategies. The question arises: How is plastic distributed over the water depth in rivers and how is this distribution related to prevailing flow conditions? The research is based on four pillars: Knowledge on the hydraulic **plastic parameters (1)**, in combination with **experimental observations (2)**, might lead to an explanation of the distribution with a **theoretical approximation (3)**, based on existing literature from neighboring research fields. Lastly, **manipulation (4)** of this plastic distribution by hydraulic interventions is investigated.

Two types of plastic sheets were used representing foil-like litter, referred to as HDPE and LDPE plastic. The *factory-density* of these two materials suggest a positive buoyant property ($\rho_{\text{plastic}} \approx 0.92 - 0.97 \text{ g/cm}^3$). The floating ability of the plastic is expressed as the average rise velocity (w_r), derived from stagnant water experiments. The rise velocity experiments showed two driving mechanisms: The *bulk-density* of the material together with the ability to trap or attach air, results in an *effective-density* determining the floating ability of the plastic. This effective-density can change over scales and is variable over time. Therefore, the distribution is also depending on many different (ambient) conditions and is variable over time and space.

The vertical distribution of plastic was investigated in a small-scaled flume setup which represented uniform river flow. Turbulence intensity was increased by increasing the average flow velocity. Results showed that it is reasonable to assume significant transport below the surface layer for common turbulent flow conditions; With an increase of the flow velocity in an average urban river, from 0.10 to 0.50 m/s, the surface share of the HDPE plastic decreased from 95% to 25%. For the LDPE plastic experimented with, both sinking and rising behavior was found, and the distribution observed was close to uniform. Here, the dual buoyancy property dominates the observed distribution, rather than the mixing ability of the flow. The differences observed between the two materials shows the sensitivity of the distribution of marginal buoyant plastics. Small changes in (ambient) conditions can influence the distribution. In general, due to the marginal buoyant properties, suspension is found to be relatively easy.

For in-depth comparison with existing theory, use is made of the well-known Rouse profile, describing the equilibrium distribution profile for sediments. A similar equation is established for the distribution profile of plastic particles. The profile is based on a balance between the inertial particle rise flux and the turbulent mixing flux, dictated by the ratio of particle rise velocity w_r over flow shear velocity u_* . From the theoretical analysis, a possible relation was found between the obtained average rise velocity and observed distribution profile, based on an estimate of the prevailing shear velocity: The shape parameters fitted through each observation follow the same trend as the theoretical estimate based on the w_r/u_* ratio. However, the extent to which the relation could describe and approximate the concentration distribution is not accurate and additional research is needed.

Lastly, the influence of hydraulic obstructions on the vertical distribution is explored. A lesser decrease of the surface share with increasing flow velocities was observed, implying a positive effect of obstructions on the surface share. The observed deviations in distributions could not be explained, though the results make it plausible that hydraulic structures can be intentionally applied in waterways to increase the surface share. Further research to application and design of supportive structures is advised.

With this research, a first insight is created on the vertical behavior of plastic in relation to the flow conditions. This study shows that marginal buoyant plastics can be sensitive to turbulent motions in flow and a significant amount of plastic might be transported below the surface. In order to create a complete picture of the behavior of different kinds of plastic in stream flows, more extensive research is needed.

Contents

Preface	iii
Summary	v
List of figures	ix
List of tables	x
Nomenclature	xi
Glossary	xiii
1. Introduction.....	1
1.1. Research context	1
1.2. Problem statement.....	3
1.3. Objectives and Research questions.....	3
1.4. Research approach and outline.....	5
2. Theoretical framework	6
2.1. Theoretical background on turbulent mixing	6
2.2. Similar research to the vertical distribution of particles	8
2.3. Conclusion theoretical framework	11
3. Methodology	12
3.1. Plastic parameters: Floating ability of plastic.....	13
3.2. Observation: Vertical distribution of plastic.....	14
3.3. Theoretical approximation: Concentration distribution profile	16
3.4. Manipulation: Influence of vertical obstructions	18
3.5. From lab experiment to reality: The scale issue.....	19
4. Results and discussion	21
4.1. Plastic parameters: Floating ability of the plastics	21
4.2. Observation: Vertical distribution of plastic.....	26
4.3. Theoretical approximation: Concentration distribution profile	31
4.4. Manipulation: Influence of vertical obstructions	37
5. Synthesis	40
6. Conclusions and Recommendations	42
6.1. Conclusions.....	42
6.2. Recommendations.....	45
Bibliography	47
A. In depth comparison with literature	50
A.1. Jakarta: Multi-trawl sampling (in depth comparison)	50
A.2. Danube: Sampling over entire depth	53
A.3. Thames: Samples near the riverbed.....	54
B. Additional Experiments	56
B.1. Density determination of the plastic.....	56
B.2. Time of submergence: changing properties.....	56
B.3. Additional experiments Gate structure	58

B.4.	Flume roughness: additional experiment	60
C.	Experiment setup and considerations.....	61
C.1.	Flume setup	61
C.2.	Flow development over flume.....	62
C.3.	Impression of lab experiments	64
D.	Fieldwork: Borgharen Sluice	65
E.	Plastic Problem in figures	67
F.	Photo impressions	70

List of figures

Figure 1.1: River plastic flowing into oceans in tons per year + mismanaged plastic waste (MPW) production per country (Lebreton et al., 2017a).	1
Figure 1.2: Triple-layered sampling net used for a study in the Danube (Hohenblum et al., 2015).	2
Figure 1.3: Four pillars form the base of this MSc thesis research	4
Figure 1.4: Four pillars form the base of this research. Short descriptions of the research per pillar is given.	5
Figure 2.1: Dye enters the turbulent region and is mixed over the water depth	6
Figure 2.2: Rouse profiles based on different β -values	9
Figure 2.3: (left) An example of the vertical profiles of pelagic fish eggs. (right) Schematic representation of the profiles	10
Figure 3.1: The outline of this chapter follows the four pillars as indicated	12
Figure 3.2: Used sizes in plastic experiments.	14
Figure 3.3: Flume setup for vertical distribution observations. Location B serves as measurement location, location A as reference.	15
Figure 3.4: The depth is divided in 10 sections. Section 1 and 2 form the surface-share (5 cm)	16
Figure 3.5: (left) Counts per section are translated to concentrations over depth, at half the section depth. (right) concentration distribution profiles are created, either fitted or approximated.	17
Figure 3.6: Setup of the obstruction experiment.	19
Figure 4.1: The outline of this chapter follows the four pillars as indicated	21
Figure 4.2: Probability density graphs of rise-time over 1-meter depth.	22
Figure 4.3: Probability density graph of rise-times per size of HDPE plastic.	23
Figure 4.4: Probability density graph of rise and settling times of 3x4 cm ² sheets.	24
Figure 4.5: Image showing the presence of air-bubbles on the plastic, with a diameter of about 1 mm	26
Figure 4.6: Histograms showing the count of sheets per section of HDPE, in % of the total, for each velocity experiment. Error bars are based on spatial averaging of the surrounding measurements.	28
Figure 4.7: HDPE surface share and bottom share (upper and lower 5 cm respectively) with increasing flow velocity.	28
Figure 4.8: Histograms showing the count of sheets per section of LDPE, in % of the total, for each velocity experiment. Error bars based on spatial averaging of the surrounding measurements are given.	29
Figure 4.9: LDPE surface share and bottom share (upper and lower 5 cm respectively) with increasing flow velocity.	29
Figure 4.10: Concentration distribution profiles fitted through the observation with estimator b (red lines), and approximated based on an estimate of the shape parameter β (b in graph) (blue lines).	33
Figure 4.11: fitted exponents (b) per velocity experiment vs the theoretical estimate of the shape parameter, β .	33
Figure 4.12: Concentration distribution profiles fitted through the observation with estimator b (red lines), and approximated based on an estimate of the shape parameter β (b in graph) (blue lines).	34
Figure 4.13: fitted exponents (b) per velocity experiment vs the theoretical estimate of the shape parameter, β .	34
Figure 4.14: optimized Rouse parameter with addition of parameter alpha = 0.64	35
Figure 4.15: normalized distribution profiles (to the near surface measurement Ca).	36
Figure 4.16: concentration distribution profiles normalized to the near surface measurement Ca for three velocities. The three obstructions are compared with the undisturbed distribution.	38
Figure 4.17: Distribution counts for the three obstructions, compared with the undisturbed distribution.	39
Figure 6.1: The four pillars of this research, with a short indication of the conducted experiments and analyses.	42

List of tables

Table 3.1: Summary of the experiment properties.....	13
Table 3.2: Experiment flow velocities and corresponding shear velocities (based on $c_f = 0.003$).....	14
Table 3.3: Main assumptions for the Rouse profile, that are adopted for the plastic distribution profile.....	16
Table 3.4: Concentration distribution profiles for Sediment, Fish-eggs and Plastic	17
Table 4.1: Found average rise velocities for plastic bags and foils.....	22
Table 4.2: Results from additional experiment to the material densities of the plastics (as presented in Appendix B.1.)	22
Table 4.3: Found average rise velocities of the scaled sheets, compared to the prototype bags	23
Table 4.4: Found average rise velocities for both plastics.	24
Table 4.5: Surface-shares of plastic found in experiments, for both HDPE and LDPE plastic, with respect to the average flow velocity and corresponding shear velocity.	27
Table 4.6: Observed surface-shares for HDPE plastic and observed downward movements between camera A and B	27
Table 4.7: Observed surface-shares for LDPE plastic and observed downward movements between camera A and B	27
Table 4.8: Surface-share for HDPE plastic as observed in the experiments, related to prototype river conditions. Based on $c_f = 0.005$ for the river, corresponding average flow velocities can be calculated.	30
Table 4.9: Upper and lower limits for the parameter estimates HDPE.....	32
Table 4.10: Upper and lower limits for the parameter estimates LDPE.....	32
Table 4.11: The observed and computed surface-shares for HDPE (%) under increasing flow (and shear) velocities	35
Table 4.12: Surface shares for HDPE found with obstructions, compared to the share found in undisturbed flow	37

Nomenclature

Abbreviations

HDPE	High-Density Polyethylene
LDPE	Low-Density Polyethylene
LMSE	Least Means Squared Error
PDF	Probability density function (area below function equals 1)
RMS	Root mean squared error
RSE	Relative standard deviation of the mean

Subscripts

p	Prototype
m	Model
1,5,10, ...	Percentage of the frontal area relative to the prototype plastic

Latin symbols

a	Reference height of near surface measurement	[m]
A _p	Frontal area of particle	[m ²]
b	Estimator of shape parameter (β) of concentration distribution profile	[-]
C	Chézy roughness coefficient	[m ^{1/2} /s]
C(z)	Concentration at depth z	[g/m ³]
		[#/m]
C _a	Reference concentration at reference height a near surface	[#/m]
C _D	Drag coefficient	[-]
C _f	Friction coefficient	[-]
d	Water depth under the surface	[m]
D _{T,z}	Turbulent diffusion coefficient	[mm ² /s]
D _z	Diffusion coefficient	[mm ² /s]
F _B	Buoyancy force	[N]
F _D	Drag force	[N]
F _G	Gravity force	[N]
Fr	Froude number	[-]
g	Gravitational acceleration constant	[m/s ²]
h	Water depth above the bed	[m]
i	Waterlevel gradient	[-]
n	Mannings friction coefficient	[s/m ^{1/3}]
R	Hydraulic radius	[m]
Re	Reynolds number	[-]
u	Flow velocity	[m/s]
u*	Shear velocity	[m/s]
U _{da}	Depth averaged stream velocity	[m/s]
V _p	Volume of particle	[m ³]
w _p	Particle rise (w _r) or settling (w _s) velocity	[m/s]
z	Vertical coordinate waterdepth	[m]

Greek symbols

α	Additional shape parameter in concentration distribution profile	[-]
β	Rouse parameter	[-]
$\Delta\rho$	Density difference	[g/cm ³]
ε_T	Eddy diffusivity coefficient	[m ² /s]
κ	Von Kármán constant (0.41)	[-]

ν_T	Eddy viscosity coefficient	$[m^2/s]$
ρ_f	Fluid density	$[g/cm^3]$
ρ_p	Particle density	$[g/cm^3]$
σ_i	Standard deviation over individual measurement	$[\#]$
σ_T	Schmidt number	$[-]$
τ_{bed}	Bed shear stress	$[N/m^2]$

Glossary

Bulk density	Density corresponding to an object including factors such as additives, coloring, combination of materials etc.
Buoyancy	Tendency of a body to float, to rise or to sink when submerged in a fluid at rest.
Developed flow	Constant in time and space
Diffusion	The process whereby particles of liquids, gases or solids intermingle as the result of their spontaneous movements and in dissolved substances move from a region of higher concentration to one of lower concentration
Effective density	Density difference between object and ambient water, resulting in the floating ability of the object
Equilibrium distribution	Statistic average distribution of particles over water depth under uniform, developed flow conditions
Factory density	Density corresponding to the raw, unprocessed material
Fitted distribution profile	The concentration distribution profile based on a fitted shape parameter (β) through the observed distribution
Floating ability	The ability of an object to float, quantified as the terminal rise velocity when ascending. Counteracting the mixing behavior of turbulent flow
Macroplastics	Plastics with a size > 5 mm
Marginal positive buoyant plastic	Plastic with a small density difference with respect to the ambient water resulting in a small floating ability
Microplastics	Plastics with a size < 5 mm
Model	The whole of lab-configuration and scaled objects used in the experiments
Pelagic eggs	Open ocean fish-eggs
Prototype	The whole of the situation a model is based on and compared to, often referring to the real-life situation and scale
Rouse profile	Equilibrium concentration distribution profile developed by H. Rouse (1937) in the field of Sediment Dynamics
Scale effect	Discrepancy between model and prototype resulting when one or more dimensionless parameters have different values in the model and prototype
Secondary flows	Flow deviating from the primary current. In natural rivers, they are significant at for example bends
Subcritical flow	Subcritical flows are controlled by the downstream flow conditions
Submerged	Descended below the surface of water
Surface-share	Share of plastic found in the upper 50 cm of the water-column
Theoretical distribution profile	The concentration distribution profile based on an approximated shape parameter (β)
Turbulent diffusion	Spreading of particles caused by turbulent movements
Turbulent flow	In turbulent flows the fluid particles move in very irregular paths, causing an exchange of momentum from one portion of the fluid to another. Turbulent flows have great mixing potential and involve a wide range of eddy length scales

1

Introduction

Forty years ago, marine plastic litter was seen more as an eyesore rather than a harmful risk (Derraik, 2002). Nowadays, about 8 million tons of plastic end up in our oceans every year, through multiple inputs including coastal industries, fishery and inland waste transported via rivers (Jambeck et al., 2015). Roughly 5 trillion pieces of plastic are floating at the ocean's surface (Eriksen et al., 2014). The abundance of plastic waste in the oceanic environment is not only due to the worldwide single-use of plastic, it is also a result of its persistence against degradation and the ability to float, making transportation over rivers relatively easy (Moore, 2008).

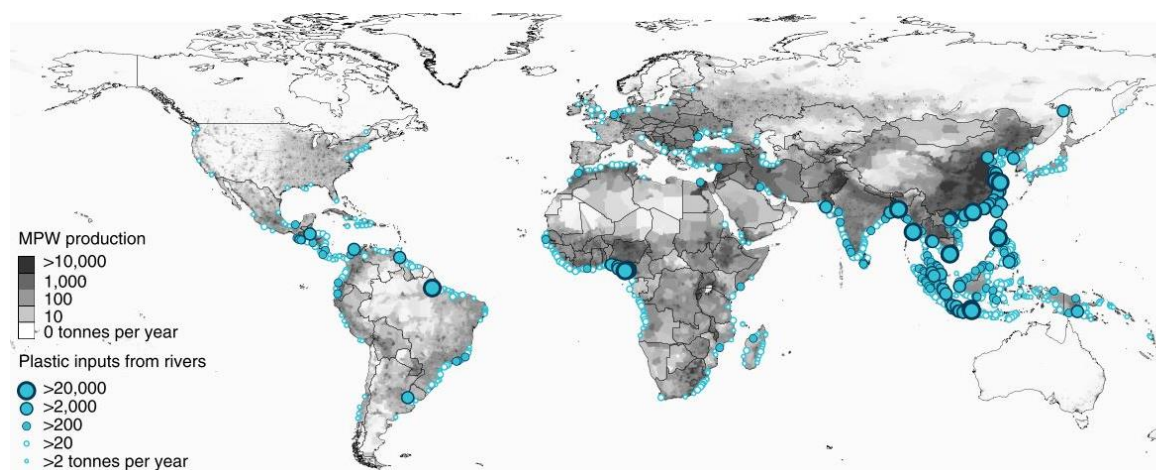


Figure 1.1: Riverine plastic flowing into oceans in tons per year + mismanaged plastic waste (MPW) production per country (Lebreton et al., 2017).

1.1. Research context

Contamination of waterbodies by these persistent plastics forms an environmental problem (van Emmerik & Schwarz, 2020). Effects range from the visible impacts such as entanglement of marine wildlife by macroplastics (> 5 mm), to the ingestion of microplastic fragments by organisms (< 5 mm). Even though the focus of research is mainly on the oceanic contamination, rivers are identified as the main sources of both oceanic- and coastal beaches litter (Rech et al., 2014). River networks may facilitate transport of plastic litter over long distances from land sources to the sea (Figure 1.1). Lebreton et al. (2017) and Schmidt et al. (2017) estimate that the global inflow of plastics from rivers into the ocean varies between 0.4-2.75 million tons plastic per year. These estimates are based on limited field data and subject to a substantial lack of knowledge on plastic behavior and transport, therefore great uncertainties are present.

The plastic problem has received a lot of attention over the last few years. Start-ups (such as *The Ocean Cleanup* and *Noria*), Governmental and Non-Governmental Organizations (e.g. *Rijkswaterstaat* and *4Ocean*) and multinationals (e.g. *Tauw*) are aiming for plastic free oceans and rivers, by setting up various studies and projects. Creating awareness against single-use plastic, and removal of the already present plastics, are both high profile topics. Both purposes ask for a better understanding of the behavior of plastic in water.

Creating awareness

In order to create awareness of the plastic problem, accurate and scientific-substantiated estimates of the plastic fluxes are crucial, which in turn give information for mitigation or policy strategies. Most research on

quantification of this flux is based on surface measurements only, up till about 50 cm water depth. This is partly due to sampling difficulties, as most sampling of macroplastic is done by visual counting or net sampling in the upper 30 to 50 cm of the water surface (González et al., 2016). A clear overview of plastic debris measurements is given by van Emmerik & Schwarz (2020). From the limited spatial and temporal information obtained, yearly average fluxes are estimated. Either a homogeneous distribution over the water column is assumed and the samples are spatially extrapolated (Dris, 2017; Lechner et al., 2014; Schmidt et al., 2017; Tramoy et al., 2018), or the transport below the surface is neglected, and the flux is solely based on the surface count (González & Hanke, 2017; Lebreton et al., 2017; Rech et al., 2015; Wilcox et al., 2017).

However, a study to the presence of plastic near the riverbed in the river Thames concluded that the *"unseen litter moving along river beds may represent an additional significant input to the marine environment"* (Morritt et al., 2014). Presumed floating plastics, such as plastic bags and food wrappers, were found in the lowest 40 cm of the water column. Along with other studies (Dris, 2017; Gasperi et al., 2014), this research called for a further investigation to submerged macroplastics in river catchments globally. To improve the flux estimates and thereby substantiate the call for awareness.

Two other studies stand out because of the focus on plastic found in deeper water layers. In a study conducted in the Danube, Austria, a multi-spot sampling method is applied (Figure 1.2). Samples over the entire cross-section are gathered from the surface water, the midwater and near the bottom, at two different sites. It was concluded that due to more turbulent flow at one of the locations *"plastic particles show properties of suspended particles rather than floating particles, and therefore can be encountered in the entire river profile"*. (Hohenblum et al., 2015). During a study in Jakarta, double-trawl samples were taken from the first meter below the surface. It was found that for marginal positive buoyant plastics, such as plastic bags, the surface-share of plastic sampled in the upper net relative to the lower net, decreased with increasing stream velocities. Highly positive buoyant plastics, such as foams, were only found in the upper net (van Emmerik et al., 2019). These results indicate the influence of the prevailing flow conditions, with respect to the floating ability of the specific plastic group. In both papers, a reference is made to flow conditions influencing the distribution of plastic over the water depth. Either the turbulence intensity or the average flow velocity. However, the objective of both studies is the determination of yearly fluxes of plastic to the ocean, and the mechanisms behind the behavior are not further discussed.



Figure 1.2: Triple-layered sampling net used for a study in the Danube (Hohenblum et al., 2015).

Removal of plastic

On top of the surface-focus in scientific research, most riverine cleaning techniques also focus on the floating plastics in the upper 50 cm of the water-column, e.g. *Mr Trashwheel* and *The floating barriers in Paris* as referred to in Gasperi et al. (2014). This 'surface plastic' is the pollution that we can see and therefore calls for immediate action. In addition, these skimming techniques are most practical in rivers as they can be installed near river banks, minimizing stream flow and navigation interruption. However, it is uncertain how effective these skimming techniques are since there is almost no knowledge on the amounts of plastic transported below the water surface.

A removal technique that stands out in the light of this 'surface focus' is the *Great Bubble Barrier*. In this design a curtain of air bubbles is released from the riverbed, directing plastic to the river banks without obstructing the waterflow. Because of the upward motion of the air-bubbles, it might be possible that the surface-share of plastic is increased. This is one of the only few examples in which there is a focus on vertical transport processes. More knowledge on the movement of (macro)plastic in water is needed, in order to react on the pollution with appropriate and efficient cleaning strategies.

1.2. Problem statement

A great share of plastic, about 65%, is positive buoyant in fresh and saline waters, meaning that it has the capability to float (Geyer et al., 2017). However, the density of these plastics is very close to the density of the ambient water, resulting in only a small buoyancy force ($\rho_{\text{buoyant plastics}} \approx 0.92 - 1.01 \text{ g/cm}^3$, $\rho_{\text{freshwater}} \approx 0.98 - 1.0 \text{ g/cm}^3$) (Appendix E). Because of additional factors such as the entrapment of air, the combination of plastic materials and the deformability of plastic items, it is hard to predict where the plastic litter is located over the water depth and whether it will float, sink, or can be found in suspension. Thereby, the effects of the ambient flow play a key role in the distribution. Various factors could influence the location of plastic over depth, be it only temporarily. An overview of relevant factors includes:

- Bed shear induced turbulent mixing (general turbulent flow)
- Constant secondary flows (e.g. spiral flow in bends and eddies and wakes from structures)
- Short term secondary flows (e.g. external forces by navigation)
- Wind-waves induced turbulent mixing (if there is a long enough fetch, mainly an oceanic factor)
- Density gradients (mostly salinity, but waste, temperature and turbidity could play a role)
- Material property change (e.g. ageing of the material itself, fouling and other organic processes)

Given the wide use of marginal positive buoyant plastic, and the preliminary results from previous studies to submerged plastics, the hypothesis of this research is that a significant share of the plastic litter in rivers is transported below the surface water of 50 cm depth. The commonly applied method for the yearly flux determination, in which it is assumed that the floating plastics contribute the vast majority of the flux, would then not suffice. In such case a great share of the plastic litter is overlooked in both flux estimates and removal strategies. The question arises how large this share is and what factors influence this share, summarized in the following problem statement:

***“How is plastic distributed over the water depth in rivers
and how is this distribution related to prevailing flow conditions?”***

1.3. Objectives and Research questions

With knowledge of the vertical distribution of plastic, we can not only improve flux estimates, but also look for methods to manipulate the vertical distribution of plastic. A goal can be to increase the surface-share of plastic relative to subsurface amounts, making surface skimming techniques more efficient. In addition, techniques can be applied at hotspots, were, based on the flow conditions, more plastic can be found near the surface. With the aim to contribute to the scarce knowledge on riverine plastic transport this master thesis research is responding to a pressing question: Are we missing the suspended plastics?

1.3.1. Objectives

The focus of this research is solely on the vertical distribution of positive buoyant macroplastics. This master thesis has two main objectives which are linked to the two requirements for the plastic problem, i.e. defining an accurate estimate of the plastic flux through rivers and developing effective removal techniques. The objectives of this MSc thesis are:

1. **Investigate the vertical distribution of plastic under normal turbulent flow, induced by bed shear stresses only:** Rivers and urban channels are subject to turbulent flows as a result of shear stresses. Under this turbulent flow condition, the floating plastic might be brought and kept in suspension, and an equilibrium concentration-distribution over the water depth may develop.
2. **Explore the influence of constant secondary flows on the vertical distribution, induced by hydraulic obstructions:** Trash racks and retention booms applied in rivers form an obstruction of the water flow and might affect the equilibrium concentration distribution, either increasing or decreasing the surface share of macroplastics in the stream. This can affect the removal efficiency. In addition, other hydraulic structures could play a role in the distribution as well and might even be intentionally constructed to increase the surface share.

These two described flow factors may also influence longitudinal and lateral movements of plastic over the horizontal plane. Lateral movements are out of the scope of this research.

An additional objective in this master thesis is to link existing literature on particle movement, such as sediment distribution and ecological research to fish-egg transport, to the rather new field of plastic-research. It was found that in the riverine-plastic studies, almost no references are being made to studies from neighboring research fields. An in-depth comparison is made with existing theory on turbulent mixing of matter, mainly originating from the field of sediment dynamics.

1.3.2. Research questions

In order to conduct this research, supportive information on the plastic properties is needed for there is no research available that describes or quantifies the floating ability of different types of plastic. In that light, this research is built upon 4 pillars, as illustrated in Figure 1.3. For objective 1, the first three pillars are of interest: knowledge on the hydraulic plastic parameters, in combination with experimental observations, might lead to an explanation of the distribution with existing theory. For objective 2 a fourth pillar is introduced: manipulation of the plastic distribution by hydraulic interventions.

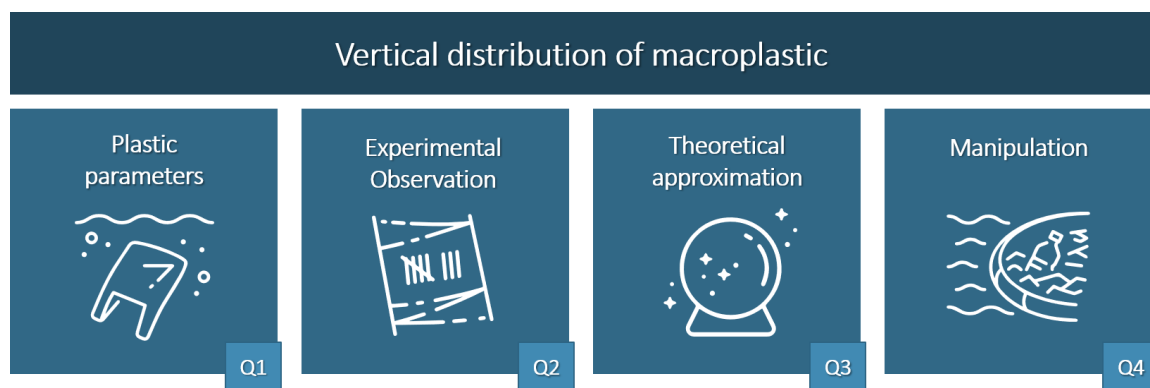


Figure 1.3: Four pillars form the base of this MSc thesis research and are guiding for the research questions

Based on the four pillars, four research questions are formulated. In Figure 1.4, a short description of the research conducted for each research question is given.

1. **How is the floating ability of the plastic defined and quantified, that counteracts the mixing behavior of turbulent flow?**
2. **How is the distribution of plastic over the water depth influenced by bed shear induced turbulence?**
3. **Can the vertical distribution of plastic be described with existing theory on turbulent mixing?**
4. **How is the vertical distribution influenced by a partial vertical obstruction of the river flow?**

1.4. Research approach and outline

Belonging to the marginal positive buoyant plastics is the Polyethylene plastic type (PE). In this material-group a distinction is often made between the types HDPE (high-density, $\rho = 0.93\text{-}0.97 \text{ g/cm}^3$) and LDPE (low-density, $\rho = 0.92\text{-}0.93 \text{ g/cm}^3$). Both materials are widely used for i.e. grocery- and shopping bags. Bags and foils form a great share of the plastic litter and are harmful to marine life (for additional information: Appendix E). Because of the small density difference with water ($\rho_{\text{freshwater}} = 0.98\text{-}1.0 \text{ g/cm}^3$), and their deformability, this plastic is an example of litter that could be sensitive to motions exerted on the object by flow. It could therefore be possible that common turbulent river flow results in mixing of these plastics over the water depth. The focus of this research will be on these two types of plastic foil-materials, originating from two different types of grocery bags that are commonly used. These two plastics represent only a part of the marginal positive buoyant plastics, for other plastic materials, such as Polypropylene (PP), are slightly buoyant as well. Thereby, many other products of the same factory-material (HDPE and LDPE) exist in many different shapes and configurations.

The research will be conducted in a small-scaled lab setup, using a flume with a maximum discharge of $0.1 \text{ m}^3/\text{s}$. This setup represents a free flowing, uniform river, in which flow velocities can be adjusted to vary the flow conditions. Because of the small scale, downsized plastic sheets will be used to represent the bag and foil materials. It can be expected that the trapping of air inside a bag has a great influence on the floating ability, which is eliminated when using single sided sheets. Research on plastic in a scaled lab setup is quite novel and therefore the issue of scaling will be a common thread throughout the report.

The research presented in this report is based on the four pillars. Following this introduction, a theoretical framework will be outlined in Chapter 2, in which the base concept of turbulent mixing is explained. The turbulent diffusivity principle is explained which will be used for the analysis of this research. Chapter 3 describes the methodology of this research, followed by the results and discussion in Chapter 4. These chapters are organized based on the four pillars. An overarching synthesis on the four sub-studies is presented in Chapter 5. Finally, conclusions and recommendations are drawn in Chapter 6. This chapter will provide answers to the stated research questions. In the Supplementary materials, additional experiments that are relevant for this research are described and discussed. References will be made throughout the report.

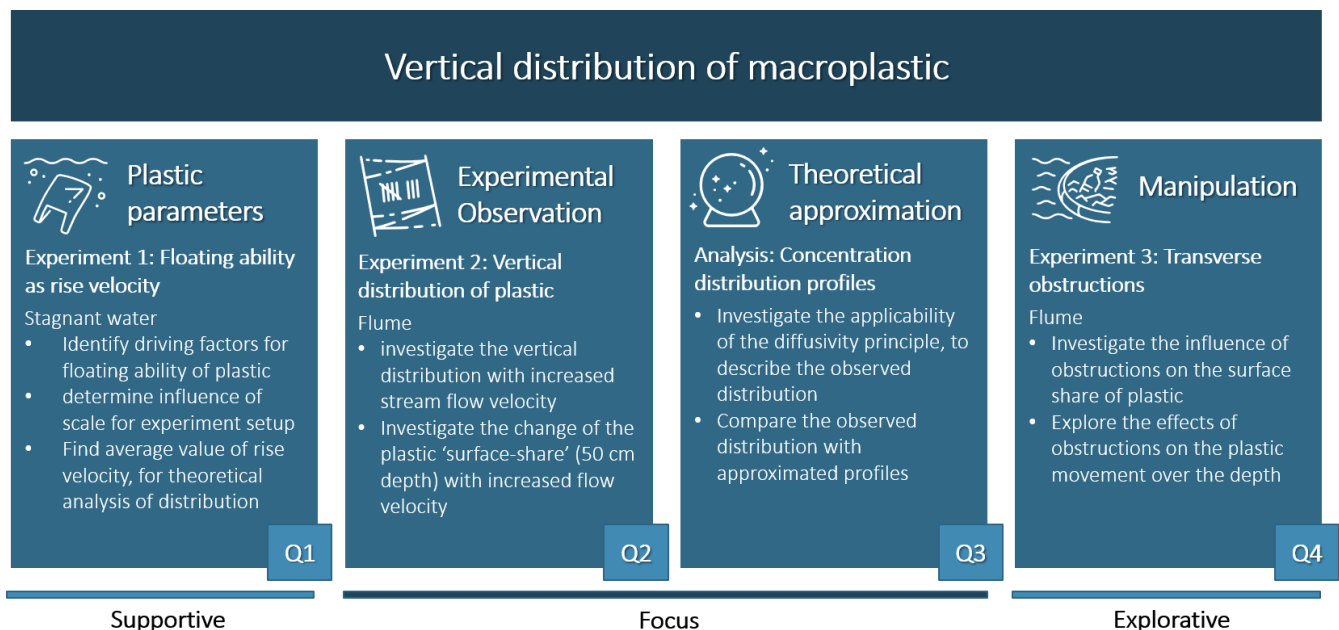


Figure 1.4: Four pillars form the base of this research. Short descriptions of the research per pillar is given.

Theoretical framework

As discussed in the problem statement (1.2), it is hypothesized that turbulent motions can bring and keep plastic materials in suspension. This chapter starts with a theoretical elaboration on the mixing ability of turbulent flow and continues with a discussion of the *turbulent diffusivity approach*, used to model turbulent fluxes of matter. This particle mixing phenomenon is frequently studied in other fields of research. The parallel literature is narrowed down to two fields, i.e. *Riverine sediment dynamics* and *Transport of positive buoyant (passive) fish-eggs in the open sea*. In section 2.1.3 a short review on this literature is given, in which parallels to the objectives and approach of this master thesis can be found. In Methodology (Chapter 3), an approach towards the theoretical description of the vertical distribution of plastic is introduced, based on the theory and parallel studies as presented in this chapter.

2.1. Theoretical background on turbulent mixing

2.1.1. Turbulent mixing

Most surface water systems are turbulent. As a rule, turbulence is fully persistent in open channel flow if the Reynolds number (the ratio of flow inertia over viscosity) is above 1000. If the conduit boundary is rough, fully turbulent flow can occur at lower Reynolds numbers. In turbulent conditions, eddies of many sizes are superimposed onto the mean flow. Figure 2.1 shows a schematic visualization of this turbulent movement. Dye that enters the turbulent region traces a path that is not only dictated by the mean flow, but also by the eddies and is mixed over the water depth, showing the movement of water particles (MIT, n.d.). Turbulent eddies create fluctuations in all velocity directions. In a uniform flow, without secondary flows, the average of the vertical velocity component equals zero. However, the fluctuation of the vertical velocity component around the mean, causes vertical movements of water.

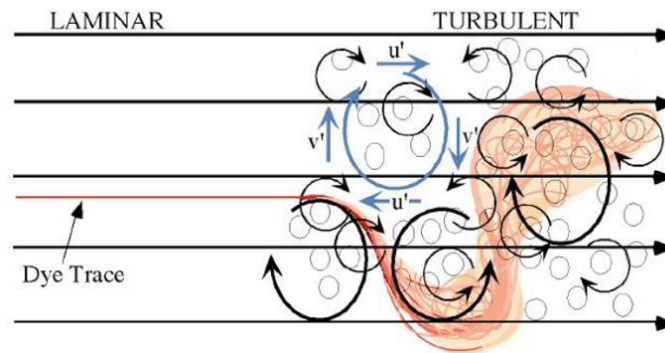


Figure 2.1: Dye enters the turbulent region and is mixed over the water depth by fluctuating eddies (MIT, n.d.)

Between the bed and the free stream, the velocity varies over the vertical coordinate. This velocity gradient is called *shear*. Turbulence is an instability generated by shear and the turbulence strength scales on the shear. Because this scale relationship is not dimensionally consistent, a velocity scale is introduced to represent the shear strength: The shear velocity, or friction velocity: u_* ('u-star'). The definition of u_* is based on the bed shear stress, τ_{bed} , as shown in equation (2.1).

$$\tau_{bed} = \rho u_*^2 \quad (2.1)$$

The bed shear stress is a measure of the force of friction from a fluid (moving water) on a body (the river bed), depending on slope, depth and water density. For uniform flow, the bed shear stress can also be

expressed as a function of the friction coefficient c_f and the depth average flow velocity, U_{da} (2.2). This results in equation (2.3) for the shear velocity. The equation shows that the shear velocity, and therefore also turbulence strength, increases with an increase in flow velocity.

$$\tau_{bed} = \rho g h i = \rho c_f U_{da}^2 \quad (2.2)$$

$$u_* = \sqrt{c_f} \cdot U_{da} \quad (2.3)$$

The bed friction coefficient is subject of many researches. The relation between Manning's n -value, Chezy's C -value and the c_f coefficient is given in equation (2.4). The friction coefficient c_f does not depend strongly on depth and for the TU Delft flume a constant c_f of 0.003 is assumed. Based on the geometrics of the conduit and Mannings estimate for several bed conditions and materials, other friction coefficients can be determined (Battjes & Labeur, 2017, p. 180).

$$\frac{1}{n} R^{1/6} = C = \sqrt{g / c_f} \quad (2.4)$$

2.1.2. Turbulent mixing modeled as a diffusion process

Turbulence can generate net transport, referred to as mixing. Solid substances such as sediments and (passive) organisms are distributed over the water depth due to this mixing ability of the flow. This could also apply for solid pollutions such as plastic particles. This mixing occurs from high concentration to low concentration; hence, the turbulent flux is always in the opposite direction of the concentration gradient. Therefore, turbulent mixing tends to homogenize a suspension. However, this smoothing effect is continuously disturbed by the buoyancy force of the considered material itself. For sediments with a higher density than water and therefore a negative buoyancy, this results in a higher concentration near the bed. For particles with a lower density than the surrounding fluid, this would result in a higher concentration near the surface. Theoretically, neutral buoyant particles would have a uniform concentration distribution due to turbulent mixing.

The turbulent flux can be modeled as an additional diffusion term in the equation of mass-conservation, given in equation (2.5), (MIT, n.d.). The additional term $D_{T,z}$ is determined by the strength of the turbulence and is much greater than the original diffusion term D_z , which is therefore ignored.

$$\frac{\partial \bar{C}}{\partial t} + \frac{\partial (\bar{u} \bar{C})}{\partial z} = \frac{\partial}{\partial z} (D_z + D_{T,z}) \frac{\partial \bar{C}}{\partial z} \quad (2.5)$$

For the vertical mixing of matter due to turbulence, a one-dimensional equation is considered and the variation over time is neglected, this results in the following simplification of the equation of mass-conservation:

$$\frac{\partial (\bar{u} \bar{C})}{\partial z} = \frac{\partial}{\partial z} (D_{T,z}) \frac{\partial \bar{C}}{\partial z} \quad (2.6)$$

Considering a balance between the settling flux and the turbulent flux, the vertical flux of particulate mass can be described by the differential equation (2.7). In which w_p is the settling velocity of the particle (m/s).

$$-w_p C(z) = D_{T,z} \frac{dC(z)}{dz} \quad (2.7)$$

The solution of this differential diffusivity equation is given in (2.8), which shows a concentration distribution equation. Where $C(z)$ is the suspended sediment concentration at height z above the bed and c_1 is the integration constant. The diffusion term $D_{T,z}$ is based on the assumption about the vertical profile of diffusivity, as does the resulting distribution profile (Heath et al., 2017). The settling velocity w_s of the particle depends on both properties of the particle and ambient environment.

$$C(z) = c_1 \cdot \exp \left(- \int \frac{w_p}{D_{T,z}} dz \right) \quad (2.8)$$

2.1.3. Counteracting buoyancy force

The terminal particle velocity w_p in equation (2.8) is determined by a balance between the buoyancy force, the gravitational force and the fluid drag force acting on the particle, given by equations (2.9)(2.8) to (2.12)(2.8). In which ρ_f and ρ_p are the fluid- and particle-density respectively (kg/m^3) and g is the gravitational acceleration constant (9.81 m/s^2), V_p is the particle's volume (m^3), A_p the particle's frontal area (m^2). In order to determine the terminal rise velocity w_p (m/s) numerically, the drag coefficient C_D (-) must be determined. The drag coefficient is mostly based on experimental data and varies with the particle's shape and also the particle's velocity (Chanson, 2004, p. 334).

$$F_B = \rho_f \cdot V_p \cdot g \quad (2.9)$$

$$F_G = \rho_p \cdot V_p \cdot g \quad (2.10)$$

$$F_D = \frac{1}{2} \cdot C_D \cdot \rho_f \cdot A_p \cdot w_p^2 \quad (2.11)$$

$$(\rho_f - \rho_p) \cdot V_p \cdot g - \frac{1}{2} \cdot C_D \cdot \rho_f \cdot A_p \cdot w_p^2 = 0 \quad (2.12)$$

For small (rigid) spherical particles ($d < 0.1 \text{ mm}$), the terminal particle velocity can be determined with Stokes' law, given in equation (2.13)(2.8). For bigger spherical particles, the particle velocity can be approximated by empirically defined equations for the drag coefficient, depending on the particle Reynolds number (Chanson, 2004, p. 334). For other shapes of particles and objects, a variety of drag coefficients is determined empirically. The coefficient of spherical particles is often estimated as 0.47, while the coefficient of a flat plate can lie around 2.0, partly depending on the orientation of the particle.

$$w_p = \frac{2}{9} \frac{g(\rho_f - \rho_p)}{\mu_f} d_p^2 \quad (2.13)$$

2.2. Similar research to the vertical distribution of particles

Research to the vertical distribution of suspended particles is nothing new. Two relevant fields of expertise, in which the vertical distribution of solid particles is considered, will be discussed and referred to further in this research:

1. **Sediment dynamics:** sediments are (mostly) negative buoyant, spherical particles, with a density difference $\Delta\rho$ in freshwater of around $1.0 - 1.7 \text{ g/cm}^3$. There is a great interest in understanding the movement of different types of sediment for the sake of land- and river-management. A well-known equation describing the vertical distribution is the Rouse Profile (Rouse, 1937). Although there will be resemblance between the suspended transport of sediments and plastics in rivers, there is a clear difference due to buoyancy. The density difference between sediments and the transport medium is relatively big compared to the case of the considered plastics ($\Delta\rho_{\text{plastic}} \approx 0.1 \text{ g/cm}^3$). Thereby, the suspension of positive buoyant plastic is inversed to that of negative buoyant sediments. The behavior of floating particles might differ substantially from that of suspended sediment, as the particles are affected by hydrodynamic phenomena that develop at the free surface.
2. **Ecology (the transport of fish eggs):** Another interesting link can be made with research to the transport of positive buoyant eggs, which is conducted from an ecological perspective; The spatial distribution of eggs determines the fate within specific geographical regions. A researcher that will be referred to in this thesis is Sundby (1983, 1991). The positive buoyant eggs considered in this research have a relatively small density difference, ranging from 0.0005 to 0.005 g/cm^3 . Computed terminal rise velocities range between 0.96 and 1.80 mm/s . Even though the focus of this specific research is on oceanic transport (pelagic eggs), the established profile is based on the same principle as the Rouse profile. However, different mechanisms play key roles in the open ocean, different assumptions are applied for the development of a concentration equation.

2.2.1. From Sediment Dynamics: The Rouse profile

In research to sediment dynamics, a well-known solution to the concentration distribution equation is given by H. Rouse (Rouse, 1937), the so-called Rouse profile. Many formulas have been developed sequentially, as summarized in the research of Huang et al. (2008). However, the Rouse formula is still the most extensively cited and will therefore be guiding for this research. This concentration profile is based on the assumption of a *parabolic diffusivity profile*, which is in line with a parabolic viscosity profile and corresponds with a logarithmic velocity profile.

The parabolic diffusivity profile is described by the eddy diffusivity coefficient ε_T and can be related to the eddy viscosity ν_T with the Schmidt number σ_T , which is often taken to be 1 (Heath et al., 2017). Resulting in equation (2.14). However, other relations can be applied; For sandy beds the parameter is suggested to be equal to 0.7 (van Prooijen et al., 2018). The κ is the von Kármán constant of 0.41, h the flow depth and z the height above the bed, increasing towards the surface.

$$D_{T,z} = \varepsilon_T = \frac{\nu_T}{\sigma_T} = \frac{\kappa u_*}{\sigma_T} z \left(1 - \frac{z}{h} \right) \quad (2.14)$$

Furthermore, for the derivation of the Rouse profile, a steady flow in a uniform channel is assumed and the settling velocity is considered as a constant (empirically defined) value. With implementation of the eddy diffusivity coefficient (ε_T) in equation (2.8), the concentration equation results in equation (2.15). The shape parameter (exponent of the equation) is called the Rouse parameter β , in which the settling velocity w_s , shear velocity u_* , von Kármán constant κ and Schmidt number σ_T are included. This parameter is a characteristic scale parameter for the resulting distribution profile (2.16).

$$C(z) = c_1 \left(\frac{h-z}{z} \right)^{\frac{\sigma_T w_s}{\kappa u_*}} \quad (2.15)$$

$$\beta = \frac{\sigma_T w_s}{\kappa u_*} \quad (2.16)$$

The integration constant c_1 can be solved by considering a reference concentration c_a that is measured at $z = a$. This reference concentration is taken as the near-bed concentration. The solution of the equation is as follows:

$$C(z) = C_a \left(\frac{h-z}{z} \frac{a}{h-a} \right)^\beta \quad (2.17)$$

Other sediment profiles exist as well. These profiles are based on different assumptions for i.e. the eddy viscosity profile (van Rijn, 1993).

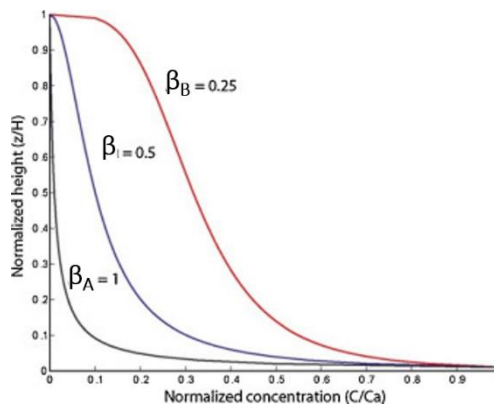


Figure 2.2: Rouse profiles based on different β -values ($\beta_A > \beta_B$): A bigger ratio of w_s over u_* implies a smaller influence of turbulent diffusivity. The settling velocity is the determining factor (figure from Teles et al., 2016)

2.2.2. From fish-egg studies: Positive buoyant particles

Based on the marginal positive buoyancy property of the considered plastics, studies to the distribution of (passive) fish-eggs resemble to this research on plastic distribution. The factors affecting the vertical distribution of eggs are studied and published in multiple papers (Sundby, 1983, 1991). These fish-egg studies are focused on the oceanic transport, and factors such as stratification and wind induced turbulence play a key role in the distribution. A comparison with these studies illustrates the possibilities in approaches towards a statistical approximation of concentration distributions and forms an important background for this thesis research. In the research conducted by Sundby (1983) the turbulent diffusivity theory also forms the base of the established distribution profile. However, since positive buoyant particles are considered, the particle flux is determined by the rise velocity (w_r) of the particles and the turbulent flux is in the opposite direction because of a higher concentration near the surface, equation (2.18). In the study of Sundby, the diffusivity coefficient D_T is assumed as a constant, rather than a parabolic profile described by ϵ_T . The solution to the diffusivity equation is then given by equation (2.19).

$$w_r C(z) = -D_{T,z} \frac{dC(z)}{dz} \quad (2.18)$$

$$C(z) = C_a \cdot \exp\left(-\frac{w_r}{D_T}(z - a)\right) \quad (2.19)$$

Furthermore, Sundby suggests a (Gaussian) distributed rise velocity parameter, instead of a constant average value. This results in an equation of higher order terms, depending on the depth considered for mixing (Sundby, 1983). By doing so, Sundby accounts for the variety of the rise velocity within a certain egg-group, which is due to differences in shape, size and particle density. This information was based on extensive preliminary research to the buoyancy of a variety of fish species of multiple authors referred to in Sundby (1983). With this approach, higher concentrations at deeper layers are computed because the more slower ascending eggs make a larger contribution at greater depths (Figure 2.3). The study focusses on pelagic (open ocean) fish-eggs, where wind induced turbulent mixing plays a key role and factors such as salinity and stratification are also considered. The assumption of the constant diffusivity coefficient D_T is based on the influence of wind and the absence of the bed influence on the turbulence intensity found at the surface. In the research conducted for this master thesis, the wind factor is of less relevance and neglected. The assumption of a constant uniform diffusivity profile is therefore not considered.

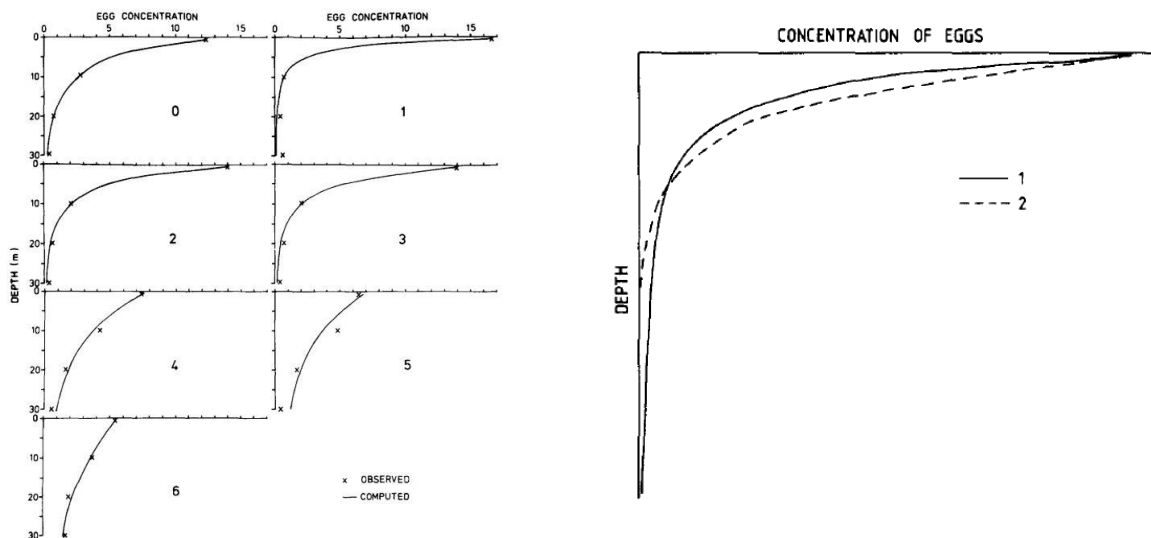


Figure 2.3: (left) An example of the vertical profiles of pelagic fish eggs. (right) Schematic representation of the profiles according to an average rise velocity (line 2) and a (Gaussian) distributed rise velocity (line 1) (Sundby, 1983)

2.3. Conclusion theoretical framework

Turbulent motions in the flow can induce mixing of solid matter, if the turbulent intensity is great enough with respect to the floating or settling ability of the considered particle. However, both the buoyancy of the particle as the turbulent intensities of the flow have spatial and temporal variations. A theoretical definition of the turbulent mixing of matter therefore only returns an indication of the probability of occurrence. The distribution profile of the suspended concentration gives an estimate of the average distribution over time. From the conducted literature review on fields with similar interests, it may be concluded that the turbulent diffusivity approach forms an appropriate base for describing the vertical distribution of suspended particles, for both negative and positive buoyant particles, with relatively small and big density differences compared to the transport medium ($|\Delta\rho_{\text{sediment}}| = 1.0 - 1.7 \text{ g/cm}^3$, $|\Delta\rho_{\text{fisheggs}}| = 0.0005 - 0.005 \text{ g/cm}^3$). Nonetheless, both fields that are discussed study the distribution of small sized ($< 5 \text{ mm}$), spherical particles. It is therefore likely that there are resemblances between the reviewed studies on sediments and fish-egg distribution, and this research to distribution of macroplastics, however, other effects might play key roles. In Chapter 3, the approach towards the development of plastic concentration-distribution-profiles is explained, which is mainly based on the assumptions considered for the sediment Rouse profile because of the focus on riverine transport.

3

Methodology

The sections in this chapter are organized based on the four pillars as introduced in the Introduction. The scheme is repeated below Figure 3.1. In additional section 3.5, attention will be given to the scale issue of the experiments. As a start, an overarching methodology for all experiments is presented below.

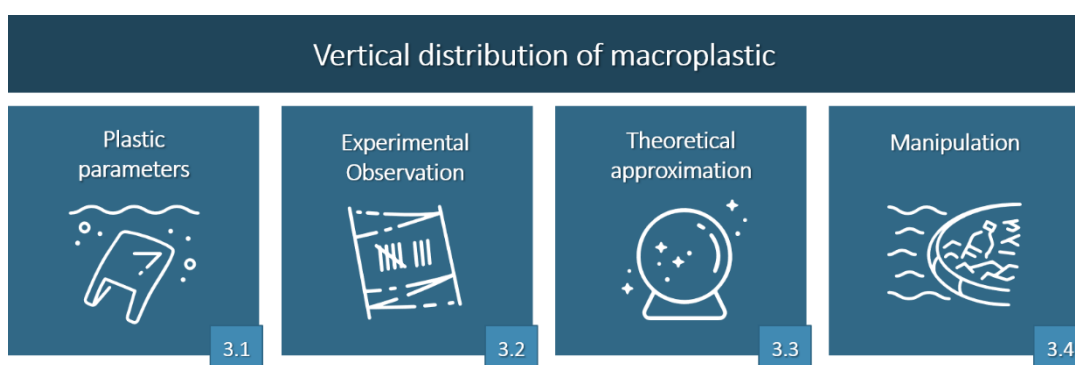




Figure 3.1: The outline of this chapter follows the four pillars as indicated

Overarching methodology

This research focusses on the vertical distribution of plastic bags and foils and is conducted in a small-sized flume of 40 cm width. Bags and foils are mostly made of the plastic types HDPE and LDPE (High- and Low-Density Polyethylene). These materials are characterized by a raw factory density between 0.93-0.97 g/cm³ for HDPE and 0.92-0.93 g/cm³ for LDPE. Plastic of both materials is investigated, originating from two different commonly used plastic bags as presented in Table 3.1. These plastics are not factory clean, untreated LDPE or HDPE materials. Because of factors such as additives, coloring, glue and even the combination of materials, the plastic is characterized by a *bulk density* that can differ from the *raw factory density*. Nonetheless, the bulk density is expected to be close to freshwater density and therefore result in a marginal-positive-buoyant property. A third density definition is introduced: the '*effective density*', defined as the density difference between the object and the ambient water. This effective density defines the floating ability of the plastic and is of interest for this research.

Because of the relatively small dimensions of the flume, it is not possible to experiment with plastic bags in their original form. Therefore, sheets of 3 x 4 cm² of the same materials are used in the flume experiments. In order to define the key factors that drive the floating ability, bags and foils are compared in preliminary experiments to the plastic parameters. For simplicity, bags are represented as foils with a single layer thickness in further experiments. Even though plastic bags and foils come in various sizes and shapes, especially when considering fragmentation of the litter, the full-sized plastics of the dimension 30 x 40 cm² are considered as prototype-plastic for this research. The two used bag-materials will be referred to as HDPE and LDPE plastic further in this research. The prototype-river is considered as an average urban river, with flow velocities between 0.1 – 0.5 m/s, and a friction coefficient of 0.005 (clean and straight river).

Table 3.1: Summary of the experiment properties

	Experiment setup	
	Flume	River
Range of flow velocities (m/s)	0.1 – 0.9	0.1 – 0.5
Friction coefficient c_f [-]	0.003	0.005
Depth (cm)	25	250
Plastic dimensions (cm ²)	3 x 4 *	30 x 40
	Plastic types	
	HDPE	LDPE
Raw factory density (g/cm ³)	0.93 – 0.97	0.92 – 0.93
Other Specifications (observed)	Thin, flexible	More thick, stiffer material
Originating from bag		

*these dimensions result from the preliminary research on the scale influence of plastic, as will be discussed in section 3.1.

3.1. Plastic parameters: Floating ability of plastic

As described in the Theoretical framework, Chapter 2.1, the floating ability of the plastic particle can be expressed as the particle's rise velocity (w_r). The terminal rise velocity results from a balance of forces on the particle (gravity, buoyancy and drag), as shown in equation (3.1) derived from equation (2.12). The rise velocity depends on factors such as the volume and shape of the particle and the density difference with the ambient environment. For known particle shapes and sizes, estimations of the drag coefficient C_D can be used to numerically determine the terminal particle velocity. According to equation (3.1), the change of the frontal area of the plastic (A_p) due to downsizing should not influence the terminal velocity of the plastic, since the thickness of the material remains the same and therefore the ratio V_p/A_p is constant. However, other factors such as (relative) flexibility of the material might play a role.

$$w_r = \sqrt{\frac{2g \cdot (\rho_f - \rho_p) \cdot V_p}{C_D \cdot \rho_f \cdot A_p}} \quad (3.1)$$

Since the drag coefficient for the plastic sheets is unknown, and other factors might play a key role, an average rise velocity was empirically determined in stagnant water rise-time experiments. The goal of these experiments is two-fold:

1. To understand what defines the floating ability of the plastic, and how this is influenced by scaling of the experiment.
2. To quantify the floating ability as an average rise velocity, that is needed for a theoretical approximation of the distribution profile.

The results from this experiment are also used for the setup of the flume experiments and will therefore be shortly mentioned at the end of this section.

3.1.1. Rise velocity of the plastic - experiment

Two rise-velocity-experiments were conducted, both in a different setup because of equipment limitations. The first experiment was conducted to investigate the difference between bags and equally sized sheets, in which we may assume that the ability to trap air plays a role. In a tank filled with 1 meter of water (2 x 2 m² footprint), bags and full-sized sheets were pushed to the bottom and released. The first 40 cm was taken as acceleration length and the rise time over the left 60 cm was manually measured with a stopwatch (± 1 sec). This was done for both types of plastic (HDPE and LDPE) and repeated 30 times per bag and sheet. Since it was found that the influence of air trapped in the bags can be of such a great influence that it overrules the plastic property, an 'average situation' was pursued by stirring the plastic underwater before testing. Big air-bubbles were released from the bags. This is considered as average situation for plastic that can be found in rivers.

In the second experiment, the influence of scale was explored. Multiple downscaled sizes of sheets were tested in a smaller container of $0.7 \times 1.1 \text{ m}^2$ and 0.5 m water depth. Because of the limited depth, acceleration length was not accounted for. Again, the rise time was manually measured and average rise velocities per sheet-size were computed. The sheet sizes used are depicted in Figure 3.2, in which the subscript indicates the scale of the plastic that is used in the experiment. For example: HDPE₀ represents the prototype bag in its full size and form. HDPE₁ indicates a single sided sheet of the same material, but with an area of 1% of the prototypes frontal area. All sheets were cut out of the original bag and therefore have the same thickness and material properties. The shape of the plastics was kept equal to the prototype bag.

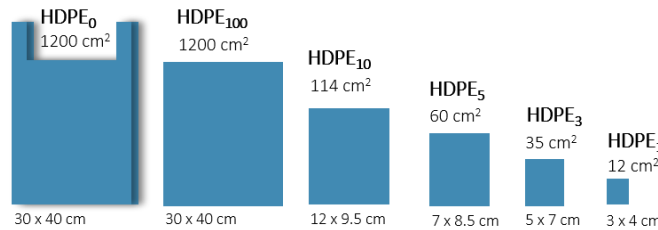


Figure 3.2: Used sizes in plastic experiments. The 1% sheet is used for further studies, based on the geometrics of the flume and results of the experiment.

For all experiments, ‘fresh’ bags and sheets were taken. This means it was new plastic that was not in contact with water before the experiments. The bags were wetted and stirred before each experiment in order to release big air-bubbles and pursue an average condition. The experiments were repeated 30 times. It may already be mentioned that the time the plastic spends in the water can influence its floating ability. A small side experiment to this effect was conducted and is elaborated on in Supplementary materials B.2. The influence of time on changes of the materials properties is neglected further in this research. All considerations for the methodology of the experiments were to pursue conditions that are ‘as average as possible’. In which average is based on assumptions on for example the ambient water conditions (fresh water, 20°C) and conditions of the plastic (not extensively used, no presence of big air bubbles).

3.1.2. Conclusion for flume-setup

Based on this scale-research and the flume dimensions, the sheets of 1% frontal area, $3 \times 4 \text{ cm}^2$, were chosen for the successive flume experiments. Based on the plastic-prototype definitions of $30 \times 40 \text{ cm}^2$, this results in a geometric scale factor of 1:10 for further experiments.

3.2. Observation: Vertical distribution of plastic

3.2.1. measurement of the plastic distribution over depth – flume experiment

The distribution of the plastic sheets over the water depth was measured in a flume setup. The flow in the flume represents river-flow, as can be found in a straight river reach with gradually varying flow. Therefore, the results of the experiments are to be considered as: *The distribution over depth through a uniform, straight river reach, without influences of secondary flows or obstructions*. The experiment was conducted under different average flow velocities (Table 3.2). Assuming a uniform flow over constant water depth (25 cm) and a constant friction coefficient (0.003), the distribution over depth can be assigned to a prevailing shear-velocity, which increases with an increase of the average flow velocity, equation (2.3). The two types of plastic, HDPE and LDPE, size $3 \times 4 \text{ cm}^2$, were used. The measurement was done by counting how many times plastic sheets were present in each depth-section. For each velocity (and corresponding shear-velocity), 100 plastic sheets were released in the flume, one by one to prevent interaction. The flume setup is illustrated in Figure 3.3 and associated considerations are explained below. A more detailed description of the setup can be found in Supplementary Materials C.1.

Table 3.2: Experiment flow velocities and corresponding shear velocities (based on $c_f = 0.003$)

Experiment number	1	2	3	4	5	6	7
Flow velocity (m/s)	0.10	0.20	0.35	0.45	0.55	0.65	0.95
Shear velocity (cm/s)	0.5	1.1	1.6	2.2	2.7	3.3	4.9

Based on the plastic sheets and flume dimensions, a geometrical scaling factor of 1:10 was chosen. The water depth in the flume was kept constant at 25 cm for every velocity experiment. The ‘surface-share’ of plastic in rivers is considered as the amount of plastic found in the first 50 cm below the surface. In the flume, this surface-section equaled 5 cm. The inlet depth of the plastic was kept constant and was mostly based on a set of preliminary trial and error experiments. The inlet near the surface (5 cm below) assured the possibility to monitor downward movements as a result of turbulent motion. At two locations, A and B in Figure 3.3, cameras were used to capture the position of the plastic sheet over depth. The depth was divided in 10 sections, of each 2.5 cm. The times that a sheet was present in each section was counted. However, only location B was considered as reliable measuring location. At this location, a developed flow and equilibrium profile is assumed, based on the configuration of flume length, flow velocities and average rise velocity of the plastic. Additional information on the flow profiles in the flume can be found in Supplementary Materials C.2. The data retrieved from location A was used to check whether a downward movement, linked to turbulent mixing, did occur in the velocity-experiment. A threshold of 10 % was chosen to indicate mixing, meaning that if less than 10 % of the tested sheets showed downward movement between location A and B, the distribution of the plastic at location B may have been due to effects of the inlet method rather than mixing ability of the flow. In that case the shear-velocity was considered as ‘below mixing threshold’.

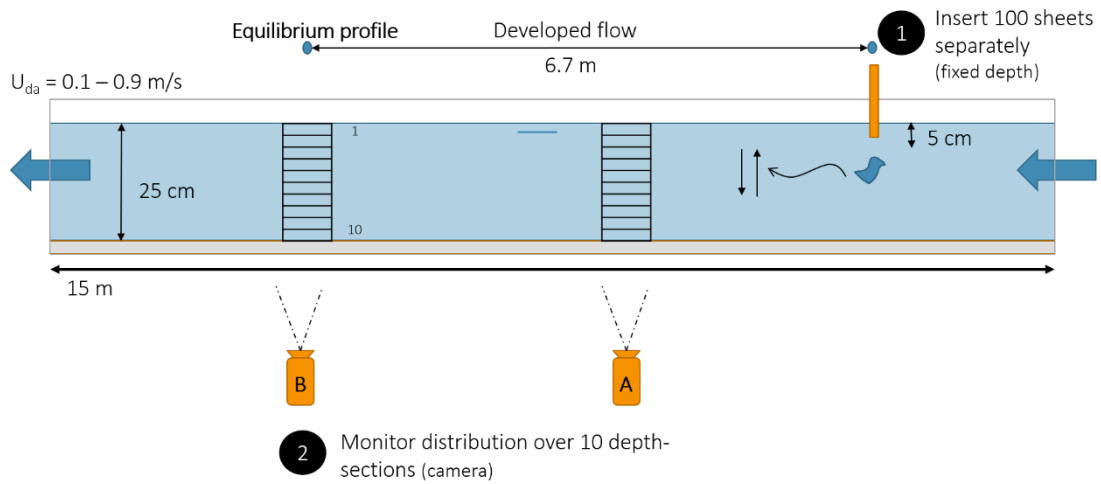


Figure 3.3: Flume setup for vertical distribution observations. Location B serves as measurement location, location A as reference.

For this research, several assumptions were made, summarized as follows:

- There is fully developed, uniform flow (constant in time and space).
- The vertical component of the average velocity is caused by bed-shear induced turbulence and can be expressed as the shear velocity u^* .
- An equilibrium distribution profile can be assumed at the measuring location (camera B). Meaning that the distribution that is measured here, is representative for the distribution that would be measured at any location over an infinity long distance after an infinity of time (neglecting the influence of time on the floating ability of the plastic).
- The floating ability of the considered plastic can be described with an average rise velocity w_r . Even though the rise velocity may vary due to the influence of air and ambient factors such as water temperature etc.

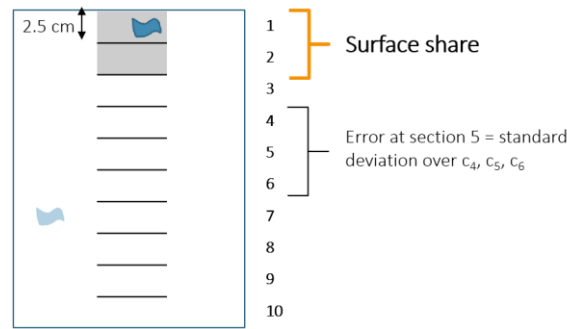


Figure 3.4: The depth is divided in 10 sections. Section 1 and 2 form the surface-share (5 cm)

3.2.2. Error definition of observation

A difficulty with the observation method is handling the perspective on camera images. Since the focus of the research is on the relation between surface plastic and subsurface plastic, the camera's horizon was set at section 1. As a result, the count was more prone to observation errors for deeper sections, because of the perspective. A count in section 10 could also have been in section 9. Each velocity experiment was conducted once, with 100 sheets. Therefore, it was not possible to compute a standard deviation over the individual velocity-measurements. Therefore, the uncertainty determination for the observation (the count per section) was defined as a spatial average over counts above and below the section of interest, as illustrated in Figure 3.4. A standard deviation over the three measurements was taken to compute the standard relative error of the middle observation, as given by equation (3.2), in which \bar{c} is the average count over the three considered sections. For the upper and lower boundary (section 1 and 10), the standard error of the section below (2), respectively above (9) was taken. This way, when the difference in count between the neighboring sections is big, we estimate a bigger error in count than when the difference is small.

$$\sigma_i = \sqrt{\frac{(c_{i-1} - \bar{c})^2 + (c_i - \bar{c})^2 + (c_{i+1} - \bar{c})^2}{3}} \quad (3.2)$$

3.3. Theoretical approximation: Concentration distribution profile

3.3.1. Theory: Plastic distribution modeled as diffusion process

The method for modeling the turbulent flux as a diffusion term, as described in Chapter 2.1.2, could theoretically be applied to the vertical distribution of (macro)plastics as well. This section discusses a proposed concentration equation to both analyze and approximate the vertical distribution of plastic over depth, based on the Rouse profile.

Table 3.3: Main assumptions for the Rouse profile, that are adopted for the plastic distribution profile

Main assumptions for the Rouse profile
<ul style="list-style-type: none"> • Steady flow in a uniform channel • Parabolic eddy viscosity profile • Constant and uniform Schmidt number • Constant and uniform settling velocity • An equilibrium concentration profile (steady state distribution)

Concerning the marginal positive buoyant properties of the considered plastic, there is a resemblance between the fish-egg studies and this research to plastic. However, the studies of Sundby (1983, 1991) are focused on open sea processes, including wind induced turbulent mixing. The assumption of a constant turbulent diffusivity profile used by Sundby does not suffice for this research. Therefore, the assumptions considered for the sediment Rouse profile are adopted. The parabolic diffusivity profile, based on a logarithmic velocity profile, is dictating the equation (Table 3.3). With these considerations, the concentration distribution equation for plastic equals the Rouse equation. However, because of the focus on positive buoyant plastics, rather than negative buoyant sediments, the settling velocity is replaced by the rise velocity (as was shown in the fish-egg studies). Therefore, the resulting concentration-distribution-profile is inversed with respect to the sediment profile. To cope with this change of directions of the fluxes, z is considered

increasing with depth and $z = 0$ now represents the water surface. The used equation in this research is then of the same form as the presented equation for the Rouse profile, equation (2.17), but distinguished by the use of a depth (d) rather than height (h) (3.3). The Schmidt number is taken as 1 and neglected. The reference concentration C_a is taken as a fixed near-surface measurement.

$$C(z) = C_a \left(\frac{d-z}{z} \frac{a}{d-a} \right)^\beta \quad \text{with} \quad \beta = \frac{w_r}{\kappa u_*} \quad (3.3)$$

The shape parameter β is dictated by the ratio of inertia of the particle versus the turbulence of the flow: rise velocity (w_r) over shear velocity (u_*). However, the shape and size of plastic has a great variation in comparison to spherical sediment and egg-particles and no analytical solution exists to predict the rise velocity. The empirical determination of the rise velocity was discussed in previous section (3.1.1) and will be used as input parameter in this analysis. An overview of the distribution profiles as described in Chapter 2, and as defined for the plastic distribution is given below (Table 3.4).

Table 3.4: Concentration distribution profiles for Sediment, Fish-eggs and Plastic

Sediment Rouse profile	Egg distribution profile	Plastic distribution profile
$C(z) = C_a \left(\frac{h-z}{z} \frac{a}{h-a} \right)^\beta$ $\beta = \frac{\sigma_T w_s}{\kappa u_*}$	$C(z) = C_a \cdot \exp \left(-\frac{w_r}{D_T} (z-a) \right)$	$C(z) = C_a \left(\frac{d-z}{z} \frac{a}{d-a} \right)^\beta$ $\beta = \frac{w_r}{\kappa u_*}$
D_T = parabolic turbulent diffusivity profile	D_T = constant turbulent diffusivity profile	D_T = parabolic turbulent diffusivity profile
z = height above bed (increases towards surface) C_a = near-bed concentration w_s = settling velocity	z = depth (increases towards bottom) C_a = near-surface concentration w_r = rise velocity	z = depth (increases towards bottom) C_a = near-surface concentration w_r = rise velocity

3.3.2. Analysis: From section-counts to a distribution profile

The distribution of plastic over depth was measured over a 2.5 cm interval. In order to convert this discrete dataset in a continuous concentration-distribution profile, the count per section was first divided by the depth interval and then translated to point-measurements at half the depth sections (Figure 3.5). The datapoints are to be considered as concentrations (%/cm) and used to compute a concentration-distribution-profile according to the equation based on turbulent diffusivity principle, repeated below (3.4). The reference concentration C_a was taken as the near-surface observation at $a = 1.25$ cm for each individual experiment.

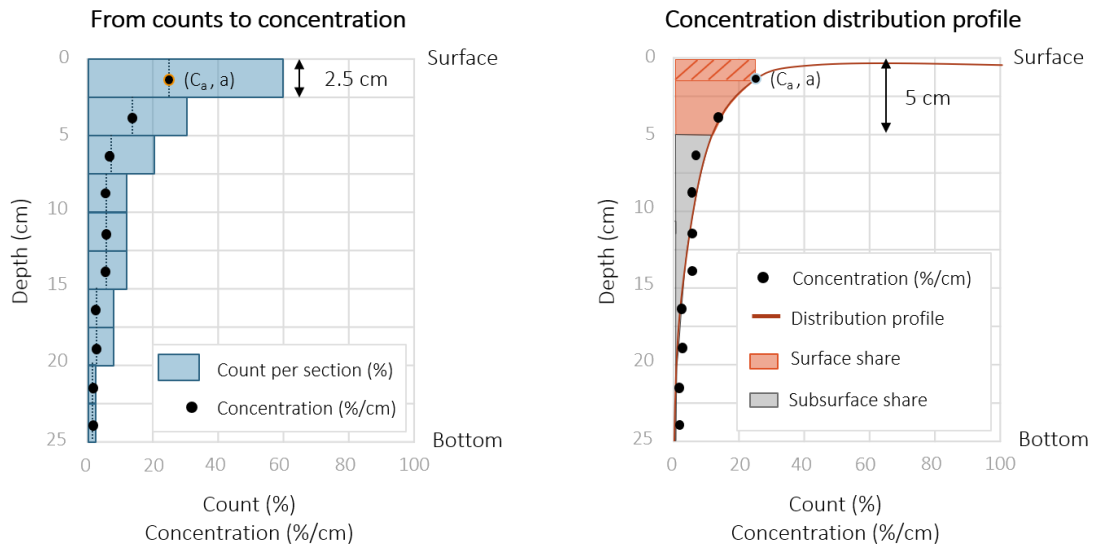


Figure 3.5: Left: Counts per section are translated to concentrations over depth, at half the section depth. Right: concentration distribution profiles are created, either fitted or approximated. The surface share can be calculated.

Two profiles based on this equation were developed per velocity-experiment. The first profile is an optimized fit of the concentration equation through the observed datapoints. The fit was optimized with a Least Mean Squared Error method (LMSE) for each velocity-experiment separately, with the shape parameter as estimator, called b . This was done in order to investigate the ability of the concentration equation to describe the observed distribution. This fitted profile was then compared to the theoretical profile, in which the shape exponent β is based on an estimate of the average rise velocity of the plastic w_r (as determined) and the shear velocity u_* (based on the prevailing flow velocity). This later profile will be referred to as the theoretical profile with the Rouse parameter β as shape parameter. κ represents a constant of 0.41.

$$C(z) = C_a \left(\frac{d-z}{z} \frac{a}{d-a} \right)^\beta \quad \text{with} \quad \beta_{\text{estimator}} = b \quad \text{or} \quad \beta_{\text{theory}} = \frac{w_r}{\kappa u_*} \quad (3.4)$$

In this analysis, no required conditions to the area below the distribution curve were given and therefore the profile loses its probability density attribute. The profile describes the relative concentrations over depth regarding the measured near-surface concentration (C_a). To compare the profiles of the different velocity experiments, the equation can therefore also be normalized over the near-surface observation, as shown in equation (3.5).

$$\frac{C(z)}{C_a} = \left(\frac{d-z}{z} \frac{a}{d-a} \right)^\beta \quad (3.5)$$

In order to determine the surface share from the concentration distribution profiles, the following equation was established (3.6)), as illustrated in Figure 3.5 (right side). Because of the asymptotic behavior of the equation towards the surface, the concentration between the surface and first measurement (0, a) was considered as uniform. Else, the surface shear would be overestimated.

$$\text{Surface share} = \frac{C_a \cdot a + \int_0^a C(z) dz}{C_a \cdot a + \int_0^d C(z) dz} \quad (3.6)$$

3.4. Manipulation: Influence of vertical obstructions

In the final experiment, the influence of obstructions on the surface-share of the plastics, relative to the undisturbed equilibrium distribution, was investigated. The underlying goal of this research was to investigate the influence of a surface skimming technology itself, which is in fact a permeable gate structure (such as a trash rack). Thereby, the potential of hydraulic structures to increase (or decrease) the surface share of plastic was studied. Three obstruction-scenarios with a crosswise orientation towards the waterflow were tested, all obstructions were sharp-crested, solid obstructions.

1. Sluice gate submerged till 5 cm underwater ($1/5^{\text{th}}$ water depth)
2. Bottom sill (bump) of 5 cm height
3. Half-depth obstruction of 5 cm height

Both the distribution 50 cm in front of the obstruction and at the obstruction (above or below) were monitored. In order to investigate the influence of the obstruction relative to the equilibrium distribution, the approach conditions and measurement location were the same as in the undisturbed experiments as described in 3.2.1. The obstruction was placed downstream of measurement location B. For each scenario, three of the 7 velocities were investigated: 0.1 m/s, 0.3 m/s and 0.5 m/s. In all cases, the flow was subcritical. The obstruction effects propagate upstream and therefore the downstream conditions were used to set the experiment conditions equal to the undisturbed conditions, which were a water depth of 0.25 m and a set flow velocity per experiment. Since we cannot assume uniform conditions with obstructed flow, we cannot assume equilibrium concentration profiles for these scenarios. The focus is on the change of the surface share and deviation of the equilibrium profile, as found in the previous experiments, due to the obstructions.

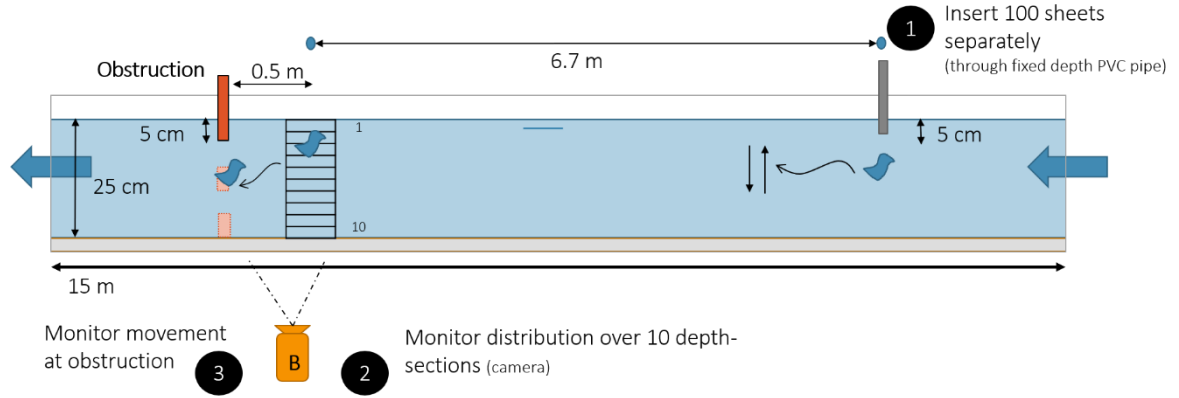


Figure 3.6: Setup of the obstruction experiment, similar to the previous experiment with undisturbed flow

The behavior of the plastic behind the obstruction was also of interest. However, due to limited length in this setup between the obstruction and the outlet of the flume, this downstream behavior was monitored in a different setup. In this setup, a sluice gate was placed more upstream of the flume and the downstream behavior of the plastic as monitored. Based on the results from this experiment it was decided to not test this for the other scenarios. The results are presented in Supplementary materials 0

Lastly, two additional orientations of the sluice gate were tested, in order to investigate the influence of secondary flows near the obstruction such as a wake formation in front and behind the sluice gate. The three following configurations of the sluice gate were compared:

1. Perpendicular to the water, 90° orientation.
2. 70°, oriented against the flow direction.
3. 110°, oriented with the flow direction.

These results will be presented in Supplementary Materials 0 as well, for this study was very explorative.

3.5. From lab experiment to reality: The scale issue

All experiments were scaled, and results might deviate from reality. The possibility of plastic to mix over the water depth can be explained by the ratio of the vertical forces acting on the plastic. This ratio is used as kinematic scale factor. Considering only primary turbulent flows (induced by bed shear stresses), the ratio can be described as:

1. The floating ability of the plastic itself, expressed as the rise velocity (w_r).
2. The vertical component of the flow velocity expressed as the shear-velocity (u_*).

We assume that, if the shear velocity is greater than the rise velocity of the plastic ($u_* > w_r$), a net downward force is possible, and mixing over the water depth can occur. Both components can be influenced by scaling of the experiment. To relate the flume experiments to reality, the ratio between the two acting vertical velocities should be equal (3.7). Hence, information about these two velocities (w_r and u_*), for both model and prototype, is needed. Under uniform conditions, the shear velocity is a result of the average flow velocity and the bed friction: $u_* = \sqrt{c_f} \cdot U_{da}$. This results in the following kinematic scale factor between experiment and prototype flow velocities (3.8):

$$\frac{u_{*,p}}{w_{r,p}} = \frac{u_{*,m}}{w_{r,m}} \quad (3.7)$$

$$U_{da,m} = U_{da,p} \cdot \frac{w_{r,m} \cdot \sqrt{c_{f,p}}}{w_{r,p} \cdot \sqrt{c_{f,m}}} \quad (3.8)$$

In this research, rough assumptions for a prototype river were made to be able to link the experiment to reality. It is assumed that the distribution is linked to the prevailing shear velocity. However, multiple configurations exist to come to equal shear velocities and therefore the experiments represent a possible river condition rather than a one-to-one comparison with a case-study. The prototype river can be described as a shallow urban river or channel, with a velocity range between 0.1 and 0.5 m/s. The bed friction coefficient (c_f) is estimated as 0.005 (straight clean river). The flume has a friction coefficient of 0.003 (PVC bottom). Consequently, the shear velocity in the flume is relatively low with respect to the prevailing flow velocity, when compared to real-conditions. Apart from the fact that subcritical flow was a requirement for the flume experiments, in which the Froude number is below 1 (3.9), other effects from scaling on for example the relative importance of plastic elasticity or fluid viscosity, are considered as less important and neglected.

$$Fr = \frac{U_{da}}{\sqrt{g \cdot d}} \quad (3.9)$$

Results and discussion

Because of the iterative approach of this research, results and discussion are treated together. The sections are divided by the four sub-studies (Figure 4.1). In each section, first the results and observations are presented, the section ends with a discussion of the sub-study. In Chapter 5, an overall synthesis is given in which underlying relations and influences between the studies are discussed, together with relations found with discussed literature. Note that the two plastic materials used for this research are referred to as HDPE and LDPE plastic. The used material originates from prototype plastic bags and therefore properties can deviate from the raw form of the materials.

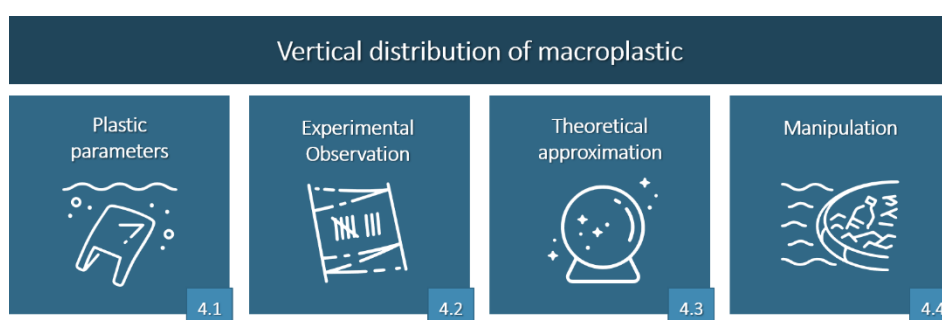


Figure 4.1: The outline of this chapter follows the four pillars as indicated

4.1. Plastic parameters: Floating ability of the plastics

As described in section 2.1.2, the floating ability can be expressed as the rise velocity (w_r) of the particle, which depends on the effective density, the volume, shape and other (ambient) factors. Experiments to the rise velocities were conducted with two different plastic materials from the types HDPE and LDPE. Before extrapolating the vertical distribution of macroplastics, as found in lab experiments, to a real-world river prototype, it is of importance to investigate the effects of scaling. Section 4.1.1 presents the differences between bags and single-sided foils of the same dimension, in which the ability to trap air is important. In Section 4.1.2 the scale of the plastic sheets is investigated and rise velocities are compared. Based on these scale-results, a geometric scale factor of 1:10 was chosen for further experiments, and sheets of $3 \times 4 \text{ cm}^2$ were used as model-plastic for further experiments. In Section 4.1.3, the information on the rise velocity of this model-plastic (both HDPE and LDPE sheets) is presented separately. These average rise velocities are needed in the approximation of the concentration-distribution profile, as will be discussed in Section 4.3.

4.1.1. Define the floating ability: from bags to sheets

Because of the open form of bags, air and water can be trapped inside, influencing the bulk density of the object. To investigate this factor, the rise velocity of bags is compared to the rise velocity of foils with equal material and equal dimensions of $30 \times 40 \text{ cm}^2$ (simply bags cut in single sided sheets). Figure 4.2 shows the probability density curves of the rise time over 1-meter depth, for respectively the HDPE and LDPE plastic bags and foils. The results are based on 30 experiments for each plastic type. The average rise velocities determined from these experiments are given in Table 4.1.

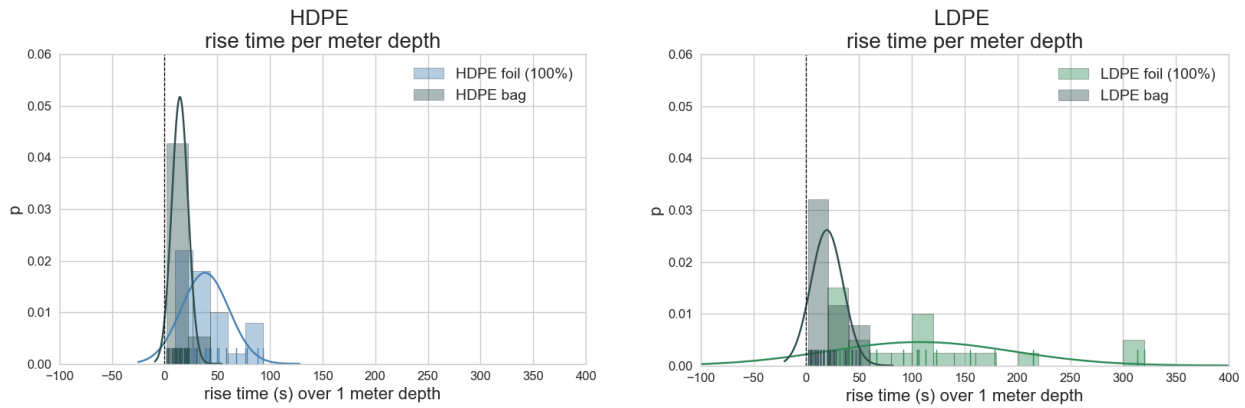


Figure 4.2: Probability density graphs of rise-time over 1-meter depth, assuming a normal distribution (the area below both graph line and bars equals 1). For HDPE plastic (left) and LDPE plastic (right).

Table 4.1: Found average rise velocities for plastic bags and foils

	HDPE		LDPE	
	Plastic Bag	Foil (full size)	Plastic Bag	Foil (full size)
Average rise velocity (cm/s)	6.6	2.6	5.0	0.9
RSE*	7.9%	10.9%	12.4%	18.8%
min velocity (cm/s)	2.3	1.1	1.7	0.3
max velocity (cm/s)	30.0	10.0	30.0	5.0

*RSE = Relative standard deviation of the mean

The main observations from these results are as follows:

- For the HDPE material, the average rise velocity of the bag equals 6.6 cm/s and for the foil the rise velocity equals 2.6 cm/s. There is a factor of 2.5 in between the HDPE plastic forms.
- For the LDPE material, the bag rise velocity is 5.0 cm/s, whilst the foil rise velocity comes to an average of 0.9 cm/s, resulting in a difference of factor 5.6.
- For the HDPE plastics the rise velocity is higher than for LDPE plastics. Furthermore, the HDPE rise-times show less spreading than the LDPE rise-times, for both the bag and foil experiments.
- To determine the average rise velocity and spread of the dataset, a uniform distribution profile is used. However, the datasets appear to be positively skewed.
- Only rising behavior of these full-size plastic is observed, and therefore the used plastics are considered as positive buoyant plastics.

A noteworthy difference between the two materials, is that the LDPE plastics have a lower average rise velocity than the HDPE plastics, while LDPE is made of a material with a lower factory density than the HDPE plastic. Assuming the density plays a determining role in the buoyancy of the plastic, it was expected the LDPE plastic would show higher rise velocities. From these counterintuitive results, a question on the assumed factory-properties arose. A side experiment to the materials' density is conducted and explained in Supplementary materials B.1. This experiment showed relatively high bulk density estimates for both plastics, as showed in Table 4.2 . Therefore, it is important to bear in mind that the names of the both plastics, High-Density and Low-Density Polyethylene, are not descriptive for the material plastic's properties in this research.

Table 4.2: Results from additional experiment to the material densities of the plastics (as presented in Appendix B.1.)

	HDPE	LDPE
average density (g/cm³)	1.01	1.03
min density	0.85	0.95
max density	1.21	1.12

4.1.2. The influence of scale on the floating ability

In the results mentioned above, the difference in terms of floating ability between the bags and their corresponding flat sheets was shown. The effect of scaling is investigated in this section. However, it appeared this experiment was only valid for the HDPE plastics. A short explanation based on observations is as follows:

While conducting experiments with different sizes of sheets, it appeared that the LDPE plastic is sensitive for scaling regarding the influence of air. For the downsized sheets, both rising and sinking behavior was observed. Small air-bubbles (diameter ± 1 mm) were seen to be attached to the material under water for both the HDPE and LDPE plastic. However, for the downsized sheets of LDPE plastic, all air-bubbles could be released, and the sheets were able to lose their rise-ability. This effect seemed to be depended on scale: smaller sheets lose their air more quickly; and variable for each individual attempt: the difference between settling or rising of the plastic was defined by the attachment of just one single air-bubble. In this experiment setup, it was not possible to monitor both sinking and rising velocities simultaneously. For that reason, the results of the scale experiments are applicable for the HDPE plastics only and these results are guiding for the experiments that will follow. The observed sinking behavior does support the results of the density experiments showed in the previous section (Table 4.2).

For HDPE plastics, the rise velocity is investigated for 5 different scales and for completeness again compared to the rise velocity of the prototype bag Figure 4.3. Since the sheets are all cut out from the original prototype bag, the material properties and thickness of all scales is equal. For practical reasons, the setup of this experiment differs from the experiment setup used for the results in section 4.1.1. The results also differ from the results mentioned earlier. The results from this experiment will be considered guiding for further experiments.

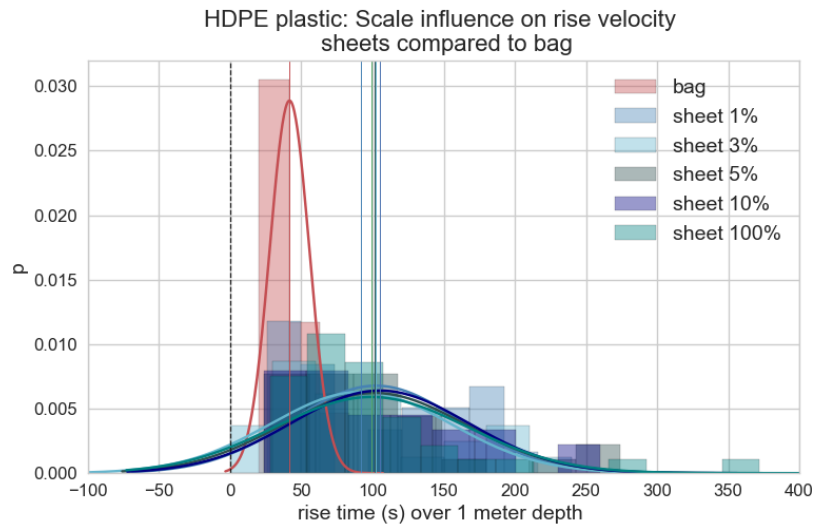


Figure 4.3: Probability density graph of rise-times per size of HDPE plastic, including comparison to the prototype bag. Assuming a normal distribution (the area below both graph line and bars equals 1).

Table 4.3: Found average rise velocities of the scaled sheets, compared to the prototype bags

	Bag	Sheet(% frontal area)				
	HDPE ₀	HDPE ₁₀₀ (= foil)	HDPE ₁₀	HDPE ₅	HDPE ₃	HDPE ₁
Dimensions (cm ²)	30 x 40	30 x 40	12 x 9.5	7 x 8.5	5 x 7	3 x 4
Average rise velocity (cm/s)	2.4	1.0	1.0	1.0	1.0	1.0
RSE	7.6%	11.7%	11.0%	12.0%	12.4%	11.7%
min velocity (cm/s)	1.2	0.3	0.4	0.4	0.4	0.5
max velocity (cm/s)	5.0	3.6	4.12	4.2	4.2	3.9

On can observe the following from the results:

- All sheet sizes show an equal average rise velocity of around 1.0 cm/s (± 0.05), with similar minimum and maximum rise velocities.
- All sheets of the material HDPE show rising behavior in stagnant water and are therefore considered positive buoyant.
- Between the bag and sheet rise velocities in this experiment, there is a factor of 2.4 difference. For the results presented in Section 4.1.1, the factor difference between the HDPE bag and its sheet is about the same (≈ 2.5). However, the average rise velocity differs between the experiments. Above mentioned results will be guiding for further research.
- As well for these experiments, the datasets are positively skewed. However, a uniform distribution is assumed for simplicity.

Based on the results of the HDPE plastic, and in conjunction with the possibilities in the flume, the 1% sized sheets of 3 x 4 cm² are used in further research to the vertical distribution of plastic, resulting in a geometric scale factor of 1:10 for the flume experiments.

4.1.3. Quantify the floating ability: Average rise velocity of plastic

In this section the rise-velocity results of the plastic that is used for further experiments, which are both HDPE and LDPE sheets of 3 x 4 cm², are presented separately for a clear overview (Figure 4.4). The HDPE sheet has an average rise velocity of 1.0 cm/s. The LDPE 3 x 4 cm² sheets showed settling behavior in stagnant water. However, rising motion was observed under flow conditions. Based on this observation and for the sake of simplicity, the LDPE sheets are considered as *neutrally buoyant* with a rise velocity of 0.0 cm/s. LDPE will be used for further experiments, even though the effect of scaling could not be properly investigated. The LDPE sheets represent the lower limit of this research to positive buoyant plastics (Table 4.4).

Table 4.4: Found average rise velocities for both plastics. A velocity of 0 cm/s is assumed for the LDPE plastic

	HDPE	LDPE*	LDPE _{assumed}
Average rise velocity (cm/s)	1.0	-0.4	0.0
RSE	11.7%	6.7%	-
min velocity (cm/s)	0.5	-0.2	-
max velocity (cm/s)	3.9	-0.9	-

*These results will be neglected, for the focus is on positive buoyant plastics.

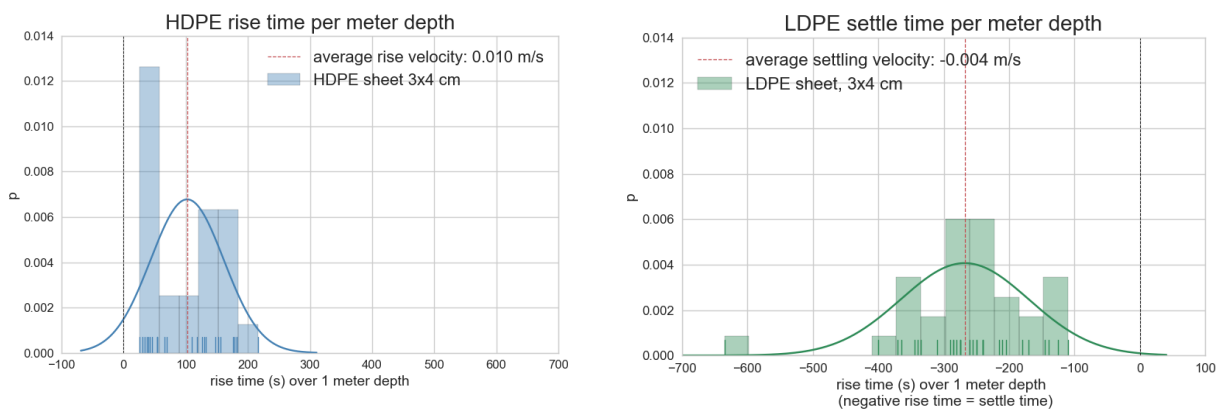


Figure 4.4: Probability density graph of rise and settling times of 3x4 cm² sheets, assuming a normal distribution. HDPE (left) and LDPE (right). The red line indicates the average rise time over depth (s/m), which is converted into an average rise velocity (m/s).

4.1.4. Discussion of results: plastic parameters

It is clear that air bubbles are of great influence on the rise velocity of the plastics. Not only the entrapment of air inside the bags, but also the attachment of air to the material was found to be important. On the surface of both plastics, multiple small air-bubbles (diameter ± 1 mm) are attached to the material and can be released while underwater (Figure 4.5). Based on the conducted experiments, two driving mechanisms for the floating ability of the plastic can therefore be distinguished:

1. The floating ability of the plastic defined by its own properties, relative to ambient conditions such as the water density.
2. The influence of air trapped inside the shape or attached to the material, which is considered as an average condition for riverine plastic.

However, the ability to attach air to the material can also be seen as a material property and both mechanisms are strongly interrelated. Observations are discussed thematically below. Note that the plastic is referred to as HDPE and LDPE plastic. The material however originates from bags and is not to be considered as raw material. The results are therefore also not general for these two types of plastic but show bandwidths of results that are representative for the group of marginal positive buoyant plastics with similar properties such as the air-attachment ability, flexibility of material, shape and dimensions.

Influence of the plastic itself: From the full-sized experiments it can be concluded that trapped air can be the key factor for the rise velocity. Since twice-as-high rise velocities for the bags relative to the foils were found, and the maximum rise velocities of both plastic types is equal. However, the minimum and average rise velocities differ between the two plastic types (with about 25%). So, when little to no air is trapped inside the form, the object properties are dictating the floating ability. However, the ability to attach air to the materials' surface was found to be a property as well. As was seen, the LDPE plastic bag had less attached air-bubbles on the material than the HDPE bag material did on average. We can say the air-attachment ability is less for the LDPE plastic bag. This is clearly seen in the decrease of average rise velocities from bags to foils. The factor difference between the LDPE bag and sheet rise velocity ($= 5.6$) is greater than the factor found for the HDPE plastic ($= 2.5$). In other words, for the LDPE plastic, the floating ability decreases greatly when the opportunity of trapping of air-bubbles inside the form is eliminated. Thereby, the used HDPE material is more flexible and therefore more prone to folding. In between folds, bigger air-bubbles can be trapped as well. In conclusion, the HDPE plastics used in the experiments have a greater floating ability in general.

Positive buoyancy due to air: It is striking that the LDPE plastic shows settling behavior and therefore a smaller floating ability than the HDPE plastic, since the material definitions presume differently. The side experiment to the materials densities clarifies this observation. Even though the experiment was rudimentary and prone to large errors, it can be concluded that the factory densities of the plastic material do not match the actual bulk densities. This could be due to used additives and coloring in the production of the bags. Both materials have a bulk density that lies within the range of fresh water and could therefore also be negative buoyant based on purely their product bulk density ($\rho_{\text{particle}} > \rho_{\text{fluid}}$). However, it was observed that all full-sized foils and bags do show rising behavior. The positive buoyancy can therefore be ascribed to the average effect of air-attachment and is considered as an average property of the plastic. These results show that the classification of plastic litter based on the base-material and corresponding factory density could suggest other behavior than reality.

Influence of scale on air attachment: For downsized LDPE plastic, it was seen that with scale the air concentration on the plastic was variable. Air bubbles literally roll over the surface and are released mostly at the edges of the sheet, as was visually observed during the experiments. On a smaller surface, the air-bubbles roll off the material more easily (less distance relative to the air-bubble size). For a material that has less adhesion properties, this can result in a total loss of air-bubbles. Because of this phenomenon, the plastic can show both rising and settling behavior and the behavior can change over time. For the downsized HDPE plastics, the average air attachment appeared to be independent of the scale; the rise velocity is equal over all scales and so is the spreading around the average. Therefore, we can conclude there is no change in the driving mechanisms causing the floating ability of this plastic type. However, for smaller scales it might be possible this material loses its floating ability as well.

Variability over time makes floating ability complex: In a side-experiment it is found that the average ability of the plastic to attach air, and therefore the floating ability, decreases with the time of submergence underwater. Foils and bags were submerged for 5 weeks and the rise-time experiment was repeated. This

experiment and results can be found in Supplementary materials B.2. One can imagine that the plastic properties can change over time as well, due to deterioration of the material. Thereby, multiple additional driving factors for the floating ability can be thought of. Such as organisms that attach to the material, fouling effects and trapping of e.g. sediments. These other effects are not considered in this research, but the combination of these driving factors add to the complexity of the definition of an 'average rise velocity' for a certain type of plastic. The floating ability of a plastic is therefore a time-dependent property and should be considered when ascribing properties to plastic litter.

Positively skewed dataset: The rise-time data shows outliers towards longer rise times and therefore towards lower rise velocities. The average rise velocity cannot become higher than its maximum velocity under air-saturated conditions. In these cases, the presence of air is considered as 'overruling the plastic property'. But with the lack of air-bubbles, either trapped or attached, the rise velocity can decrease remarkably, causing a wider variety towards longer rise-times.

Scaling to reality: Downsized LDPE sheets are not representative for the defined prototypes of plastic (bags and 30 x 40 cm² foils), since the mechanisms of floating ability change with scale. As such, the further research conducted to the LDPE plastic represents the lower limit of buoyant plastics: neutral buoyant plastics. The HDPE plastics are representative for the prototype foil material, since it was shown scaling does not have effects on the floating ability. However, since the influence of scaling was found to be variable with the plastic type, it is better to not consider the downsized plastic as a representation of full-scaled plastic, but merely as a representation of a certain type of plastic with a certain found floating ability defined as the average rise velocity.



Figure 4.5: Image showing the presence of air-bubbles on the plastic, with a diameter of about 1 mm

4.2. Observation: Vertical distribution of plastic

In this section, only the vertical distribution under bed shear induced turbulence is considered. If the turbulent intensity of the flow is big enough with respect to the floating ability of the plastic, particles should be able to get in suspension and be distributed over the water depth. In flume experiments the influence of an increasing shear velocity on the vertical distribution of plastic was investigated, both for HDPE and LDPE plastic sheets (3 x 4 cm²). The focus is mainly on the surface-share; the plastic found in the upper 50 cm of the river. The results for the HDPE and LDPE plastic are presented separately, an overview of the found surface-shares is given in Table 4.5. For comprehensibility, the average flow velocity is used to identify each experiment in the figures, rather than the corresponding shear velocity. However, it must be kept in mind that multiple configurations of average flow velocities with friction coefficients are possible to achieve equal shear velocities and, as reasoned in this research, would lead up to equal distribution profiles.

Table 4.5: Surface-shares of plastic found in experiments, for both HDPE and LDPE plastic, with respect to the average flow velocity and corresponding shear velocity.

Experiment number	1	2	3	4	5	6	7
U_{da} flow velocity (m/s)	0.10	0.20	0.35	0.45	0.55	0.65	0.95
U* shear velocity (cm/s)	0.5	1.1	1.9	2.5	3.0	3.6	5.2
HDPE Surface share (%)	95	74	52	34	28	25	17
LDPE Surface share (%)	28	15	33	22	10	15	25

Noteworthy is the decrease of the surface-share for HDPE plastic, with increasing flow- and shear-velocities. While the surface share of LDPE plastic does not show a visible trend with increasing velocities.

4.2.1. HDPE plastic

Table 4.6: Observed surface-shares for HDPE plastic and observed downward movements between camera A and B

Experiment number	1	2	3	4	5	6	7
U_{da} av. Velocity (m/s)	0.10	0.20	0.35	0.45	0.55	0.65	0.95
U* shear velocity (cm/s)	0.5	1.1	1.9	2.5	3.0	3.6	5.2
HDPE Surface share (%)	95	74	52	34	28	25	17
Downward movements (%)	1	15	26	37	32	45	45

From the results in Figure 4.6, one can observe the following:

- For a flow velocity of 0.10 m/s, the threshold of mixing ($\geq 10\%$) is not met. For the experiment with 0.20 m/s flow the threshold is met, and the observed distribution is related to turbulent mixing.
- The surface share decreases with an increasing flow velocity U_{av} and shear velocity u^* . The surface share decreases from 95% to 25% between a flow velocity of 0.10 - 0.65 m/s.
- For experiment 1 to 3, the surface-share is above 50% of the total amount of plastic. From $U_{da} = 0.4$ m/s, the surface share is below 50% of the total. In Figure 4.7 the surface share decline is visualized.
- Counts in section 10 (between 22.5 and 25 cm depth) are below 2% at all time.

4.2.2. LDPE plastic

Table 4.7: Observed surface-shares for LDPE plastic and observed downward movements between camera A and B

Experiment number	1	2	3	4	5	6	7
U_{da} av. Velocity (m/s)	0.10	0.20	0.35	0.45	0.55	0.65	0.95
U* shear velocity (cm/s)	0.5	1.1	1.9	2.5	3.0	3.6	5.2
LDPE Surface share (%)	28	15	33	22	10	15	25
Downward movements (%)	36	40	32	44	47	39	29

The most particular observations in Figure 4.8 are as follows:

- The threshold of downward movements between the two observation points is met in all experiments, which should indicate the role of turbulent mixing in the distribution of plastic.
- For the LDPE plastic, there is no surface decrease with an increase in flow velocity. The surface share is always lower than 30% of the total.
- There is no clear pattern in the change of the distribution over depth. This is illustrated in Figure 4.9, in which surface, midwater and bottom share are presented.
- The count in section 10 is below 2% in all experiments.

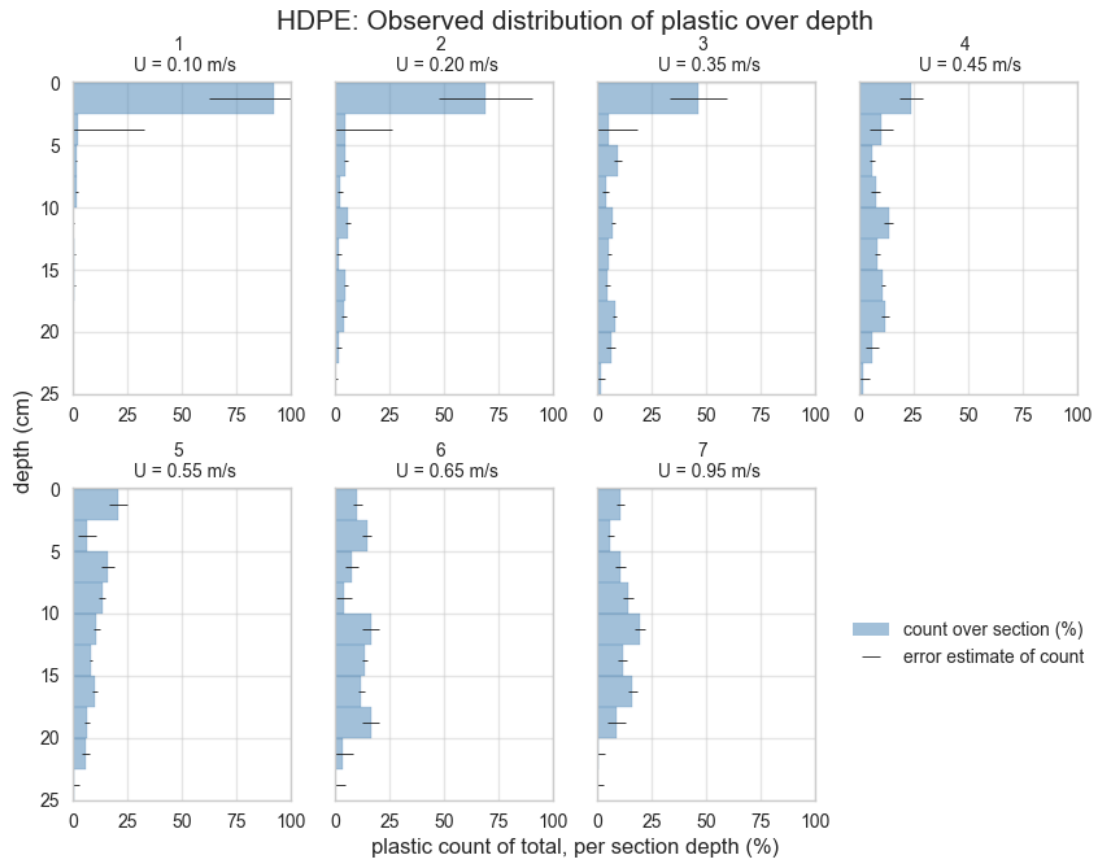


Figure 4.6: Histograms showing the count of sheets per section of HDPE, in % of the total, for each velocity experiment. Error bars are based on spatial averaging of the surrounding measurements.

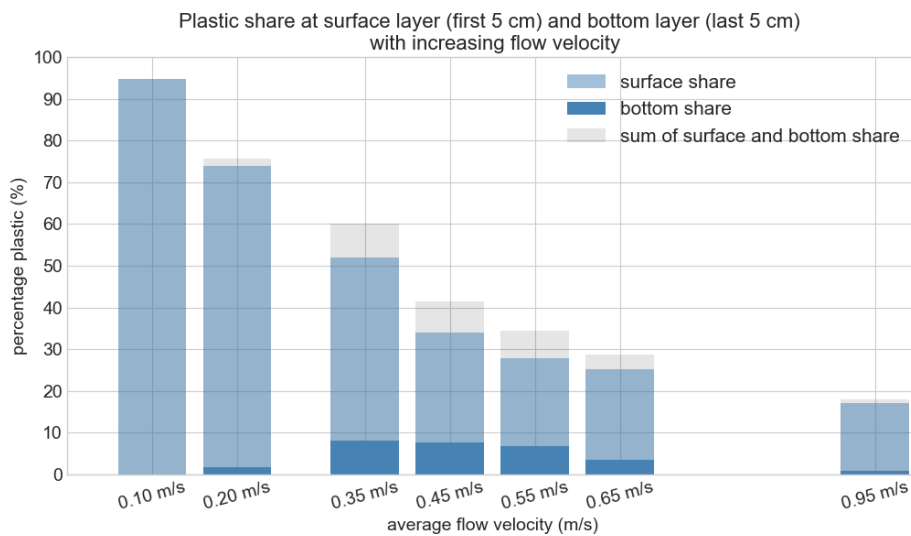


Figure 4.7: HDPE surface share and bottom share (upper and lower 5 cm respectively) with increasing flow velocity. A decrease of the surface share with increasing flow velocities is clearly visible. The remaining share is the plastic share found in the middle water layer (between 5-20 cm depth).

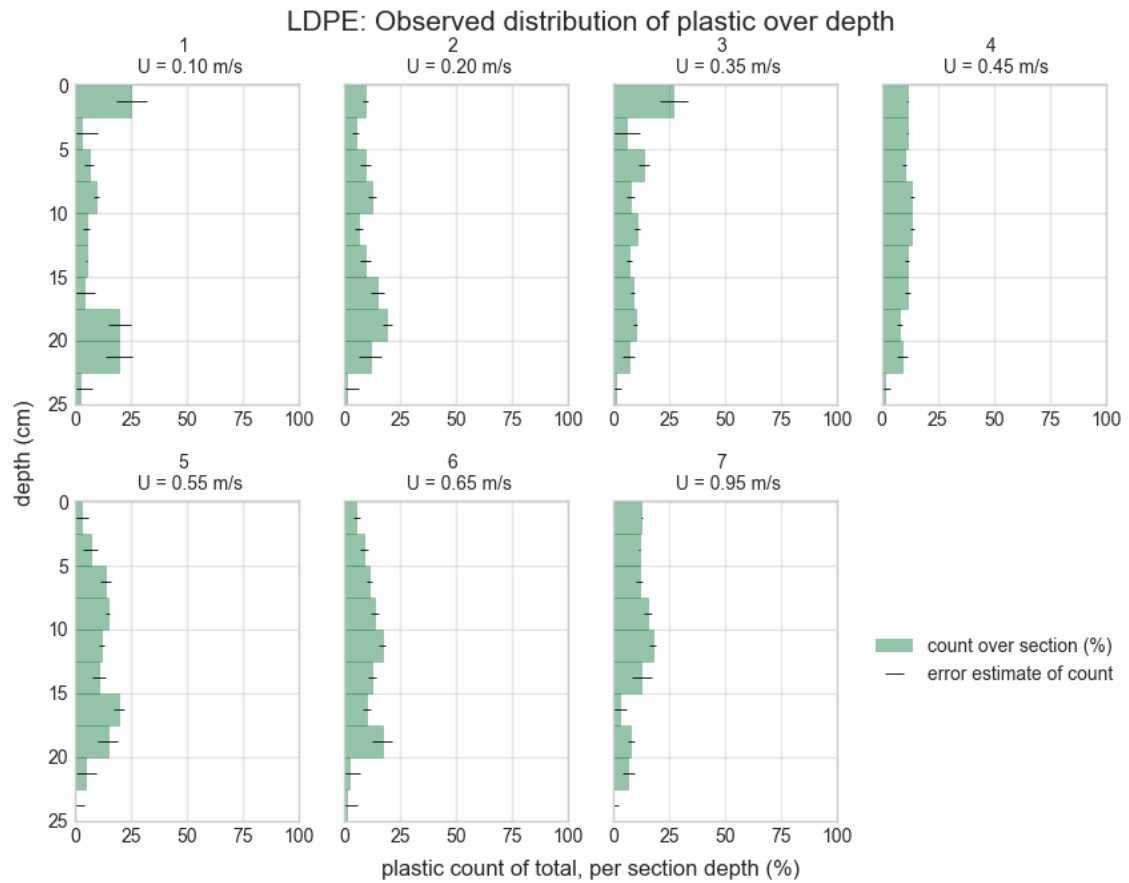


Figure 4.8: Histograms showing the count of sheets per section of LDPE, in % of the total, for each velocity experiment. Error bars based on spatial averaging of the surrounding measurements are given.

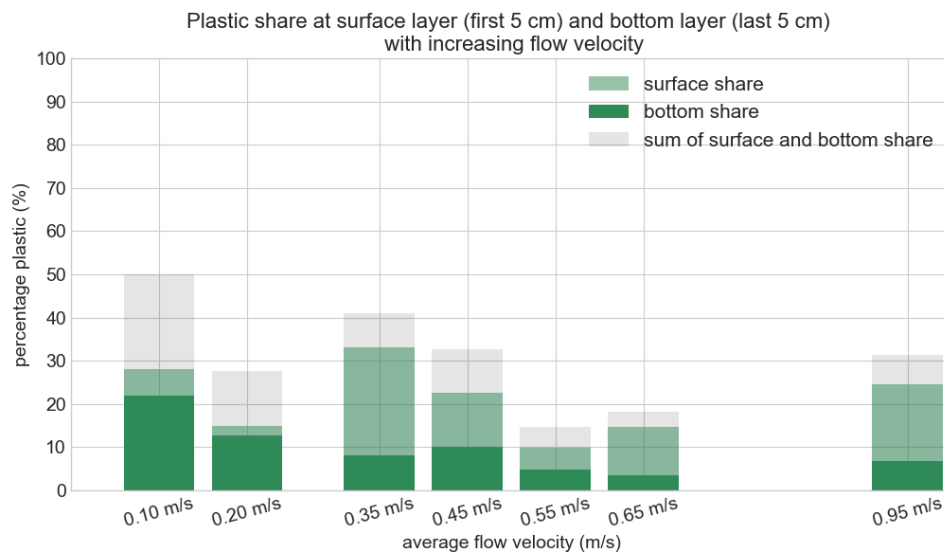


Figure 4.9: LDPE surface share and bottom share (upper and lower 5 cm respectively) with increasing flow velocity. No clear trend for either surface or bottom share is visible. The remaining share is the plastic share found in the middle water layer (between 5-20 cm depth).

4.2.3. Discussion of results: Observation

The results found per experiment can be translated to real-scale situations, as proposed in Methodology Section 3.5. A decrease of about 75% of the surface share can then be observed for the HDPE plastic with an increase of the average flow velocity in the prototype river from 0.10 to 0.50 m/s approximately (Table 4.8). For this calculation it is presumed that the rise-velocity is independent of scale, as was found for the HDPE plastic. Therefore, the corresponding flow velocity in the prototype river is based on the difference in friction coefficients only, with $c_{f,flume} = 0.003$ and $c_{f,river} = 0.005$ (the equation is repeated below (4.1)). For the LDPE results, no trend was observed, and a translation from observations to prototype river flow velocities is irrelevant. It can only be concluded that this plastic can be found all over the water depth, possibly due to both the great variability in buoyancy and the near-neutral buoyancy property which allows for the homogenizing property of turbulent flow.

Table 4.8: Surface-share for HDPE plastic as observed in the experiments, related to prototype river conditions. Based on $c_f = 0.005$ for the river, corresponding average flow velocities can be calculated.

Experiment number	1	2	3	4	5	6	7
U_{da} av. Velocity flume (m/s)	0.10	0.20	0.35	0.45	0.55	0.65	0.95
U* shear velocity (cm/s)	0.5	1.1	1.9	2.5	3.0	3.6	5.2
HDPE Surface share (%)	95	74	52	34	28	25	17
U_{da} av. Velocity river (m/s)	0.08	0.15	0.27	0.35	0.43	0.50	0.74

For the HDPE plastic, it is assumed that the same distribution of the used plastic would be found if the same shear velocity applies. However, this assumption is arguable, other scale effects could play a role. Thereby, the determination of the shear velocity is based on rough assumptions on uniform flow and bed conditions. In practice, it is very difficult to estimate a bed friction coefficient over an entire river reach. The results do show a clear decrease of surface share with increasing shear velocity. This indicates that plastic that is close to neutral buoyant has a great chance of being mixed over the water depth due to turbulent motions, which can be found under average flow conditions in urban rivers. Additional relevant observations and results are thematically discussed below.

$$U_{da,m} = U_{da,p} \cdot \frac{w_{r,m} \cdot \sqrt{c_{f,p}}}{w_{r,p} \cdot \sqrt{c_{f,m}}} \quad (4.1)$$

Threshold of mixing: Shear velocity represents the vertical component of the flow. Therefore, if shear velocity and rise velocity are in the same order of magnitude, mixing of the plastic should become possible. This hypothesis seems to be substantiated by the results found for the HDPE plastic. As stated in Chapter 3.2.1, mixing is concluded when at least 10% downward movement is observed. HDPE had an average rise velocity of 1.0 cm/s, the threshold of mixing is found to be between a shear velocity of 0.5 cm/s and 1.1 cm/s: At 0.5 cm/s, no mixing is concluded for there was only 1% downward movement, at 1.1 cm/s, this was 15% and mixing is concluded. In case of the LDPE plastic, the threshold is met for every experiment, but there is no clear trend with an increasing average flow velocity. For LDPE, the dual buoyancy property could be a cause of the distribution rather than the mixing ability of the flow.

Plastic at the bottom: counts in section 10 are barely made. For the positive buoyant plastic (HDPE) this is expected: Because of the net upward flux, there is only a slight chance sheets will be found near the bed. However, for the assumed neutral buoyant LDPE plastics, we expect a uniform distribution and therefore also plastic in the lowest sections. Especially considering that the sheets showed settling behavior in stagnant water. The absence of observed plastic close to the bed could partly results from the observation methodology: Due to the perspective and the focus of the camera on the surface sections, plastics passing in section 10 could easily be assigned to section 9. Another more physical explanation might be because of stronger upward motions near the bed, counteracting the symmetrical behavior of turbulence. Lastly, it is not certain if the observed decrease over depth is independent of the total water-depth, or that the suspension can only occur over a limited depth. The influence of water depth should be investigated further.

Inlet depth of the plastic: all plastic sheets are released at 5 cm below the water surface. Assuming there is an equilibrium distribution achieved at the observation location (camera B), the inlet depth should not be relevant; the plastic is distributed over the water depth due to the equilibrium state of the rising flux and

turbulent flux. However, it is possible that the equilibrium distribution is not yet achieved over the available length (6.7 m). In this case, releasing the plastics more near the flume bottom could result in a higher count of plastics near the bottom sections and therefore indicate more suspension of the positive buoyant plastics. It was found that the releasing of plastic at the water surface did not result in mixing at all. Sheets would remain at the surface due to surface tension. With the inlet just below the surface, at 5 cm depth, it is possible to clearly observe downward movements that are assumed to occur due to turbulent mixing.

Reproducibility of the experiment: Each experiment is only conducted one single time, with 100 sheets per experiment. The velocity experiments should be repeated in order to prove the equilibrium condition and ensure reproducible results.

4.3. Theoretical approximation: Concentration distribution profile

Distribution profiles based on the turbulent diffusivity principle can be established for each velocity-experiment. The first profile is fitted through the observed distribution, in which the shape parameter is estimated with estimator b . The second profile is the theoretical profile, based on the empirically found average rise velocities of the plastics (in Section 4.1.3) and the prevailing shear velocity per experiment. The equations are repeated below (4.2). In which k is the von Karman constant ($= 0.41$), w_r is the average rise velocity of the considered plastic (m/s) and u^* is the shear velocity of the flow (m/s), based on the friction coefficient of $c_f = 0.003$. The value for C_a at $z = a$ is represented by the observed concentration nearest to the surface, at depth $a = 1.25$ cm.

$$C(z) = C_a \left(\frac{d-z}{z} \frac{a}{d-a} \right)^\beta \quad \text{with} \quad \beta_{\text{estimator}} = b \quad \text{or} \quad \beta_{\text{theory}} = \frac{w_r}{k u^*} \quad (4.2)$$

The two profiles are plotted for each velocity experiment. The fitted profile is investigated on its ability to describe the observed distribution and then compared to the theoretical approximation. For each fitted profile, a shape parameter b_i is found. The parameter is compared to the theoretical β parameter, by plotting both against the average flow velocity, in which $w_r = 1.0$ cm/s for the HDPE plastic and 0.0 cm/s for LDPE are taken. Uncertainties regarding the found rise velocity and calculated shear velocity are considered. The results are presented separately per plastic type (HDPE and LDPE). On the x-axis the percentage of occurrence over depth is given (%/cm). However, with the fitted profiles, the area does not equal 100%, because of under- and overestimations of the fitted profiles. The percentage should be considered as an absolute concentration.

4.3.1. HDPE plastic

From Figure 4.10 the following overarching observations can be made:

- For each experiment, the best-fit profile through the observed datapoints indicates more plastic in suspension, than estimated with the theoretical approach. The theoretically approximated profile underestimates the observed suspension.
- The estimator b decreases with an increasing flow velocity and is always lower than β (and therefore the predicted profile shows less suspension than the fitted profiles).
- There is no uniform increase or decrease in the computed RMS (Root Mean Square deviation) for the fitted profile with increasing flow velocity. The RMS of the theoretical profile increases over the experiments, except between experiment 4 and 5.

HDPE – shape parameter

The shape parameters, b_i and β are plotted against the average flow velocity in Figure 4.11. The average flow velocity is related with the shear velocity through the friction coefficient c_f . It is important to notice that the theoretical parameter β is defined by an estimate of the friction coefficient c_f , and an estimate of the average rise velocity of the plastic w_r . Upper and lower limits can be defined for these estimates according to their errors (given in Table 4.9).

Table 4.9: Upper and lower limits for the parameter estimates HDPE

	Lower	Upper
Wr (m/s)	0.009	0.011
Cf (-)	0.002	0.004

Based on the rise-velocity experiments of the plastic sheets, a standard error of ± 0.001 m/s is found. The upper and lower limits for β according to this error are shown in Figure 4.11.B. The estimate of the friction coefficient in the flume is based on empirical data from the TU-Delft flume. Manning's friction coefficient n lies between $0.010 - 0.014 \text{ m}^{-1/3}\text{s}$ for glass, plastic and smooth concrete walls (Battjes & Labeur, 2017). Therefore, a friction coefficient c_f range is chosen between $0.002 - 0.004$, based on a hydraulic radius of the flume $R = 0.11 \text{ m}$ (Figure 4.11.C). These limits combined result in an error range as illustrated in Figure 4.11.A.

4.3.2. LDPE plastic

For the LDPE plastic, the theoretical profile is based on a rise velocity of 0.0 cm/s , resulting in $\beta = 0$. The theoretical approach results in a homogeneous distribution with the measured concentration C_a as a constant over the entire depth. From Figure 4.12, the following observations can be made:

- The distribution profile varies greatly, without a visible trend with an increasing shear velocity.
- For exp. 5 and 6, it appears the distribution flips over the vertical, with higher concentrations at lower water depths. This profile is possible for the best fit equation, resulting in a negative shape parameter b . For the theoretical profile, this would however not be possible due to the assumed boundary condition of 'no concentration at the bottom'.

LDPE plastic – shape parameter

The average rise velocity of the LDPE plastic is considered as 0 m/s . Because this estimation is based on a combination of observations and measurements, there is no applicable uncertainty range. Instead, the found settling velocities for the downsized sheets is considered as lower boundary, while the rise velocity for the full-sized foils is considered as upper boundary. For the uncertainty of the c_f value, the same range applies as is used for the experiments with HDPE plastic. The upper and lower limit range based on the rise- and settling velocity of the LDPE plastic, show the difficulty of the combination of both positive and negative buoyant properties. The uncertainty is big and entirely different profiles are estimated when using other assumptions than the neutral buoyant property.

Table 4.10: Upper and lower limits for the parameter estimates LDPE

	Lower	Upper
Wr (m/s)	-0.4	0.9
Cf (-)	0.002	0.004

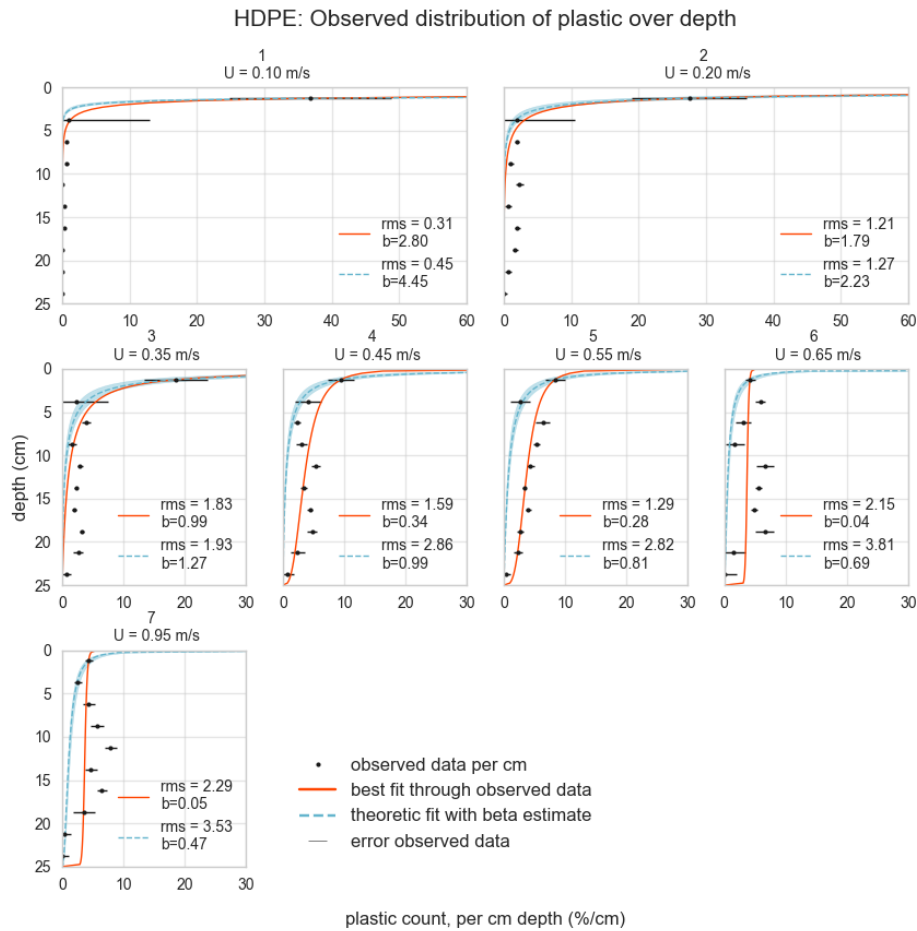


Figure 4.10: Concentration distribution profiles fitted through the observation with estimator b (red lines), and approximated based on an estimate of the shape parameter β (b in graph) (blue lines). For the approximated profile, the error of the observation C_a at a is considered and an envelope around the profile is given.

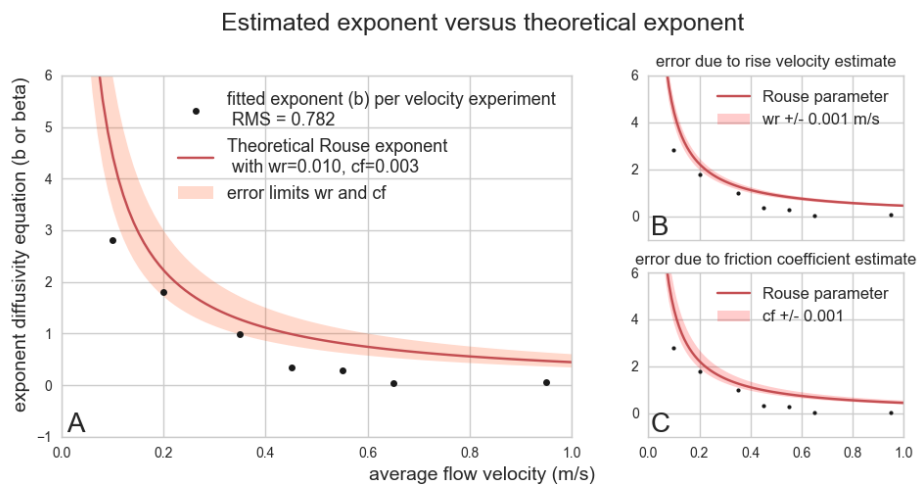


Figure 4.11: fitted exponents (b) per velocity experiment vs the theoretical estimate of the shape parameter, β . In A, a combination of both uncertainty limits is given, based on the uncertainty in the rise velocity (B) and friction coefficient (C)

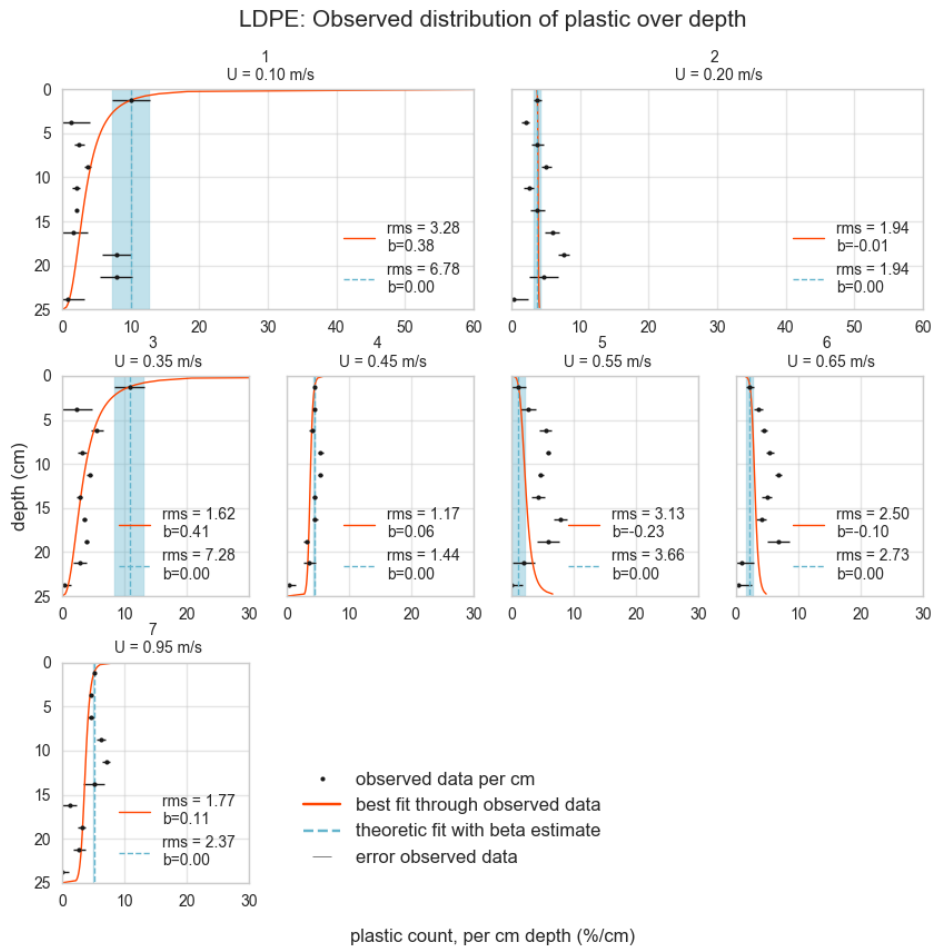


Figure 4.12: Concentration distribution profiles fitted through the observation with estimator b (red lines), and approximated based on an estimate of the shape parameter β (b in graph) (blue lines). For the approximated profile, the error of the observation C_a at a is considered and an envelope around the profile is given.

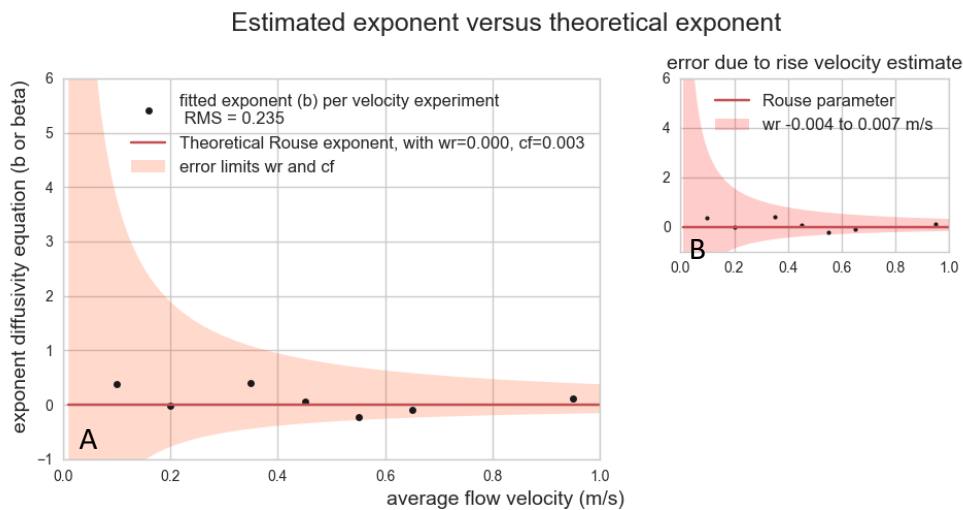


Figure 4.13: fitted exponents (b) per velocity experiment vs the theoretical estimate of the shape parameter, β . In A, a combination of both uncertainty limits is given, based on the uncertainty in the rise velocity (B) and friction coefficient.

4.3.3. Iteration of results

For the LDPE plastic, the concentration equation cannot properly describe the observed distribution. For the HDPE plastic however, it was found that the concentration equation shows an accurate fit through the observed counts, with a maximum RMS value of 2.29%. The surface-shares defined by the distribution profiles are computed according to the method stated in Chapter 3.3.2. The found shares under both the fitted profiles and approximated profiles are given in Table 4.11. The shares found with the fitted profile generally agree with the observed share (except for experiment 2 and 3, where there is a difference of about 20%).

Table 4.11: The observed and computed surface-shares for HDPE (%) under increasing flow (and shear) velocities

Experiment number	1	2	3	4	5	6	7
U_{da} average velocity (m/s)	0.10	0.20	0.35	0.45	0.55	0.65	0.95
U* shear velocity (cm/s)	0.5	1.1	1.9	2.5	3.0	3.6	5.2
observation (%)	95	74	52	34	28	25	17
fitted profile (%)	99	93	73	38	35	22	23
approximated profile (%)	100	96	84	74	66	59	46
with additional α-value (%)	99	87	68	59	52	46	37
U_{da} prototype river (m/s)	0.08	0.15	0.27	0.35	0.43	0.50	0.74

The theoretical profile underestimates the suspension of the plastic sheets in all HDPE-experiments. In this subsection, an additional parameter is added to the Rouse parameter, by fitting a profile through the found exponent parameters b . The additional shape parameter, α , is defined as in equation (4.3). A LMSE-curve fit of the alpha value results in $\alpha = 0.64$. The plot is shown in Figure 4.14, in which the upper and lower limits for the HDPE experiments are shown, based on the uncertainties mentioned before.

$$\beta_{\text{optimized}} = \alpha \cdot \beta \quad (4.3)$$

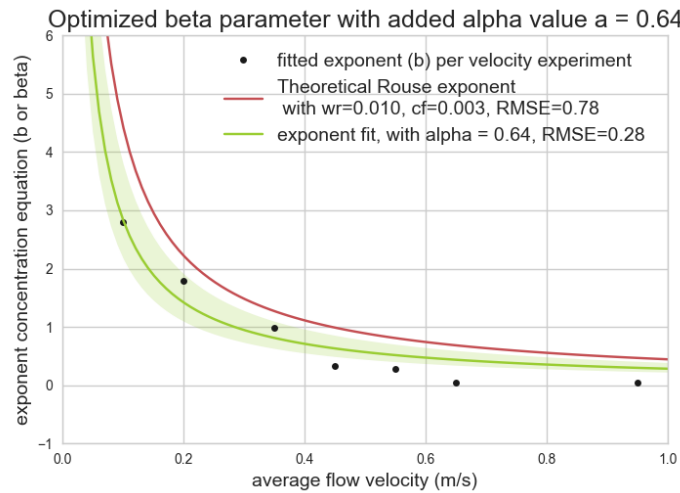


Figure 4.14: optimized Rouse parameter with addition of parameter $\alpha = 0.64$

In Figure 4.15 three sets of profiles are plotted, normalized over the concentration c_a (x-axis), so that the development of the profiles over the average flow velocity is clearly visible. The first graph (A) shows the theoretical evolvement of the profile, with β as shape parameter. Graph B shows the best-fit profiles through the observed datapoints. The last figure shows a new estimate for a theoretical profile in which the additional parameter α is considered (the surface share values are added to Table 4.11). From Figure 4.14 and Figure 4.15, it may be observed that with the use of the additional parameter α , the approximated profiles move towards the observation. However, for the higher flow velocity experiments, the approximation still heavily underestimates the suspension of the plastic as observed.

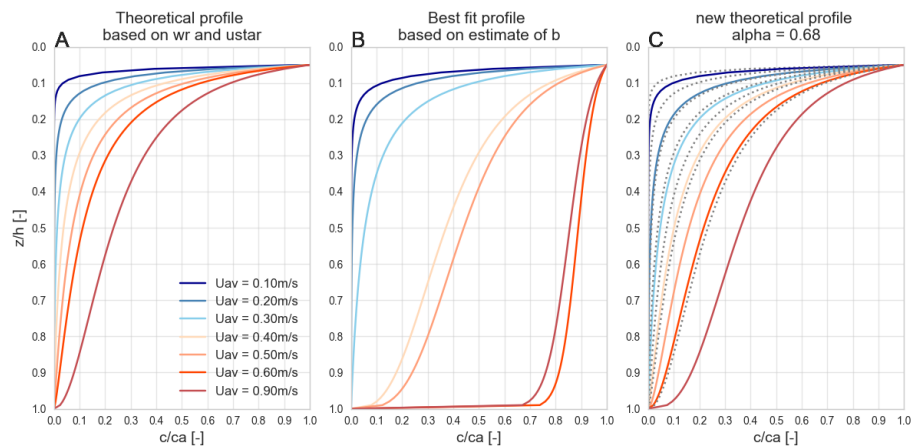


Figure 4.15: normalized distribution profiles (to the near surface measurement C_a). A: based on β . B: optimized fits with b_i . C: based on additional parameter α and β . In grey lines, the original profiles of A are given.

4.3.4. Discussion: Approximation of the distribution profile

The analysis of the vertical distribution of the LDPE plastic showed the consequences of the dual-buoyancy behavior found for this plastic: It is not possible to describe the distribution profile with the diffusivity equation, for which either a positive or negative concentration-gradient is assumed. For the HDPE plastic however, it appears the proposed equation can describe the observed distribution profile. Nevertheless, the estimated shape parameter does not match the theoretical defined parameter; the resulting profile underestimates the suspension of plastic as observed. Possible reasons are discussed below.

Rouse parameter is debatable: The theoretical defined parameter is subject of many uncertainties, since the inner parameters are based on empirical measurements and estimations. Thereby, the Rouse approach that forms the base of the equation is subject of many studies still and other profiles have been developed. Additional parameters could be needed in order to describe plastic rather than spherical small sized sediment particles.

Turbulent diffusivity relation: For the HDPE plastic, one of the reasons for the underestimation of the suspension could be the assumed relation between the eddy diffusivity and eddy viscosity. For the conducted analysis, the relation is considered as one to one (Rouse, 1937, van Rijn 1984, 1993) and the additional Schmidt parameter (σ) in the Rouse parameter is neglected. However, this relation is subject of many studies. In sediment dynamics, a constant of $\sigma = 0.7$ is considered for sandy beds (van Prooijen et al., 2018), decreasing the overall Rouse parameter and therefore suggesting more suspension. The found value for α could indicate this relation.

Additional effects on the plastic: There is however another reason that could explain this deviating behavior, which lies in the factor of air-attachment: It was found that for higher shear velocities the fitted profile deviates more from the theoretical approximation, more plastic is found in suspended than would be estimated. It could be plausible that with an increase of turbulent mixing, and therefore movement of the plastic, more air is released during the transport. The floating ability would therefore also decrease when in more turbulent flow.

Other uncertainties: The observations itself are prone to uncertainties, in order to compare approximations with observations, more observations are needed. Another uncertainty lies in the assumption for the near-surface measurement C_a at a . The count over the section is translated to a point-measurement at $z=1.25$ cm, by dividing the count over section depth. Therefore, a linear or constant distribution over the section depth is implicitly assumed. Lastly, as discussed earlier, the inlet height of the plastic could influence the observed distribution. If the equilibrium distribution is not yet developed over the available length, the choice of the inlet near the surface could influence the distribution. The observed distribution could in this case show less suspension with respect to the equilibrium. The underestimation of suspension that was seen in the theoretical approximated profile, can therefore not be ascribed to a possible effect of the inlet height.

4.4. Manipulation: Influence of vertical obstructions

In urban rivers, hydraulic structures such as weirs, bottom sills and sluice gates can be frequently found. Secondary flows evolving around the structure can influence the vertical distribution of the plastic approaching the structure, relative to the undisturbed equilibrium distribution under bed shear influenced conditions as investigated in Chapter 4.2. From the results in the previous chapters, it is decided to only experiment with the HDPE plastic in this sub-study. The obstructions that were investigated in this research are listed below.

1. A solid gate with a depth of 5 cm ($1/5^{\text{th}}$ water depth).
2. A bottom sill of 5 cm is placed at the bottom.
3. A half-depth obstruction of 5cm. Flow passes above and underneath the structure.

4.4.1. Surface share

Figure 4.17 shows the distribution count of plastic per section for all obstructed experiments compared to the previous experiments in undisturbed flow. Three velocities are tested. The first row shows the distribution as was found for the undisturbed flow situation, presented in chapter 5.2, the rows below consist of the results from the obstructed scenarios. The hatched areas in the figures show the 5 cm high structure at the surface, halfway and at the bottom respectively. Both the distribution 50 cm in front of the structure (blue) and at the structure (red) are measured. Plastic cannot go through the obstruction and always passes underneath or above. The surface share of plastic, comprising of the count in both section 1 and 2 (5 cm), is given in Table 4.12 for the different scenarios.

Table 4.12: Surface shares for HDPE found with obstructions, compared to the share found in undisturbed flow

Experiment number	1	3	5
Approach velocity	0.10 m/s	0.35 m/s	0.55 m/s
Undisturbed flow (%)	95	52	25
Gate (%)	84	72	55
Bottom Sill (%)	94	84	75
Halfway obstruction (%)	65	56	65

From the results in Figure 4.17, summarized in Table 4.12, the following observations are noteworthy:

- In the case of the surface and bottom obstruction, the surface share decreases with an increasing flow velocity, as was seen for the undisturbed condition as well.
- However, in the halfway-obstruction scenario, the surface share stays more or less equal (56-65%). The distribution does clearly change between section 1 and 2 for the halfway-obstruction.
- For the surface and bottom obstructions, the decrease of the surface-share over increasing flow velocities, is smaller than for the undisturbed scenario: Over the velocities (0.10-0.55 m/s), there is a difference of 30% and 20% respectively for the gate and sill obstruction. While the difference for the undisturbed flow is 70%.
- In case of the sluice gate, with a relative low velocity (0.10 m/s) plastic is mostly passing just underneath the gate. With higher velocities more plastic is passing in deeper layers.

4.4.2. Concentration profile development

In order to compare the distributions, the best-fit profiles through the observations are plotted in Figure 4.16 as relative concentrations. The results show the following:

- For a low velocity of 0.1 m/s, all profiles lie close to each other. The same applies for the surface shares as was shown in Table 4.12. Only the results of the halfway obstruction show noteworthy differences (65% surface share).
- No clear trend is visible for the halfway obstruction. Not relative to the other profiles or surface shares, neither based on the own development. Even though the surface share appears to be about equal ($\pm 60\%$), the suspension underneath the surface seems to increase and then decrease again.

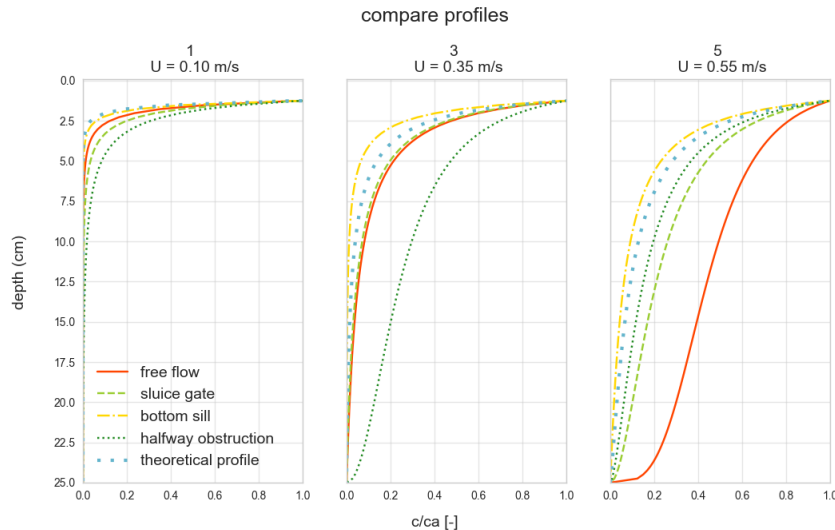


Figure 4.16: concentration distribution profiles normalized to the near surface measurement C_a for three velocities. The three obstructions are compared with the undisturbed distribution.

4.4.3. Discussion of results: Manipulation

Obstructions seem to result in higher surface shares, relative to undisturbed conditions. An explanation is sought in two mechanisms:

1. An additionally created upward motion in the water brings more plastic to the surface.
2. The overall shear velocity decreases when the flow is obstructed, resulting in lower mixing abilities.

Additional vertical motions: The first mechanism does not explain the increased surface share in case of the sluice gate, since the sluice gate causes an additional downward motion of water flowing underneath rather than an additional upward motion. There is however a notable difference between the surface shares found in the gate scenario and the bottom sill scenario. The surface share of the gate decreases with an absolute of 25% over the experiments, the surface share under bottom sill conditions decreases with 15%. This difference could be related to the additional downward motion below the gate and the opposite effect of the additional upward motion above the bottom sill. The effect of the half-way obstruction is not clear.

Decrease of shear velocity: The second mechanism could be theoretically possible: An obstruction introduces a backwater curve. The upstream depth increases and therefore the flow velocity decreases, which results in a lower shear velocity. However, the backwater curve in front of the obstructions was negligible small, with ± 1 mm water-level difference between plastic inlet and in front of the obstruction. This increase in water-depth is too small to explain the increase of surface share relative to the undisturbed conditions.

Effects of an obstruction: There is no reason to assume a decrease of surface-share due to obstructions, such as a trash rack. However, with a solid sluice gate, almost all plastic eventually passes underneath the gate. When a permeable trash rack or net gets clogged, it starts to behave as a solid obstruction and will cause plastic to pass underneath and be mixed over the entire water depth, where after it will need time to find its original distribution. In an additional experiment, the orientation of the sluice gate is altered to 70° and 110° with respect to the waterline. The surface share did not differ noteworthy. The movement of the plastic underneath the gate however is clearly influenced, with a counter-stream orientation (70°), more plastic passes under the gate via deeper sections. These results are presented in Supp. materials B.3.

Setup limitations: All in all, the found results could indicate a positive effect of obstruction on the surface share. However, the setup of the experiment forms limitations. For example, it is not possible to investigate a developed distribution profile simultaneously with the effects of obstructions, due to length limitations. Thereby, these experiments are exploratory and great simplifications of the real-life situations are applied. The results do encourage further research to the layout and dimensions of litter retention structures, and also to plausible supportive obstructions such as a bottom sill, that could increase the surface share by forcing suspended plastic towards the surface.

Observed distribution, comparison of structures

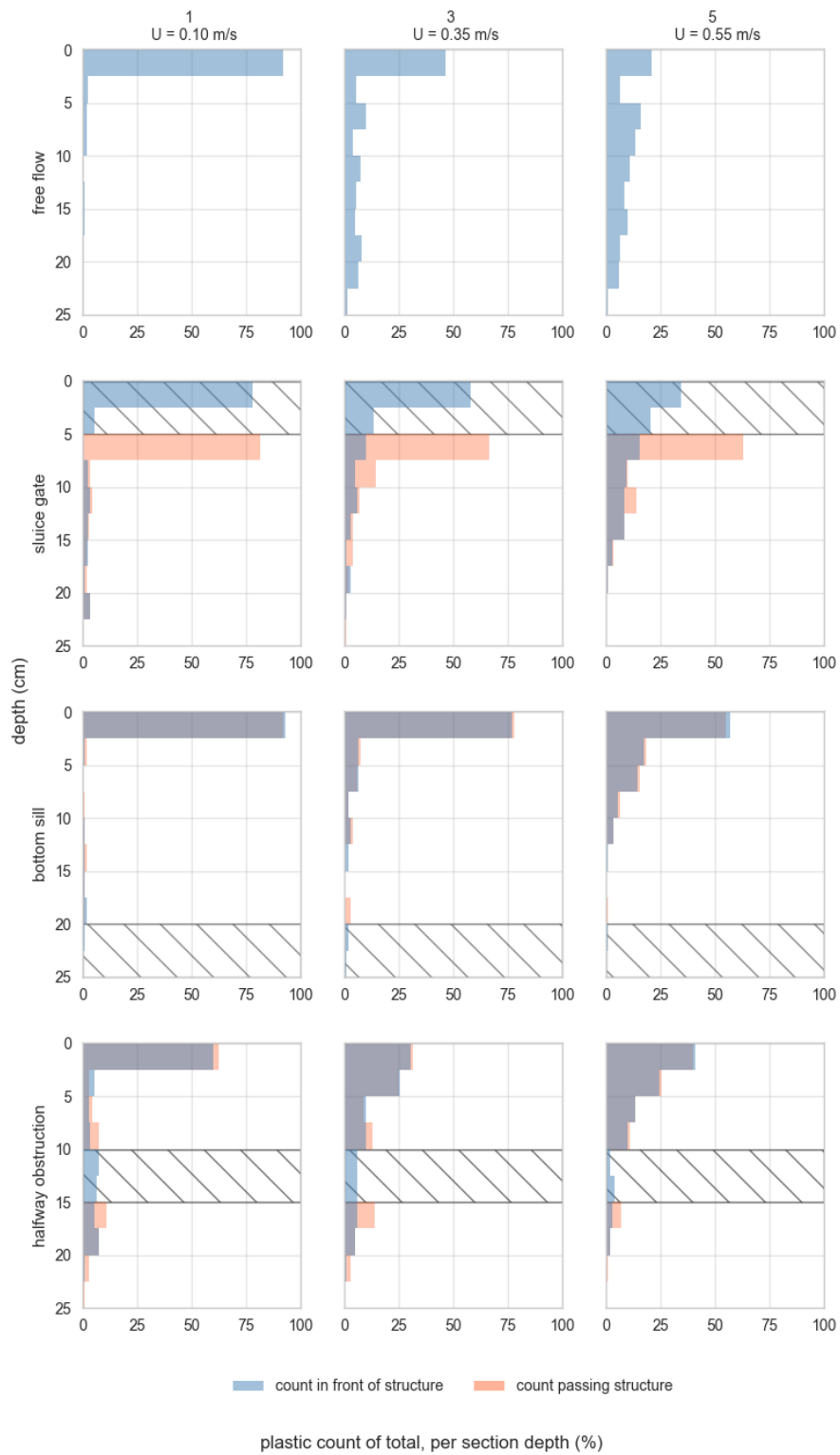


Figure 4.17: Distribution counts for the three obstructions, compared with the undisturbed distribution. The hatched area indicates the obstruction, plastic cannot go through the hatched areas and the red bars are equal to zero.

5

Synthesis

In this chapter, an overarching discussion is given. The relation between the four presented sub-studies is discussed and results are compared to literature. References will be made to studies of colleague-students that are of interest in combination with this research.

Plastic floating ability in relation to the vertical distribution

It was found that a large variability of the rise velocity was driven by the fluctuating amount of air attached to the plastic (Chapter 4.1). For the LDPE plastic, this resulted in both settling and rising behavior, which could be the main cause of the observed vertical distribution (Chapter 4.2), rather than the mixing ability of the flow. The theoretical distribution based on the diffusivity equation (Chapter 4.3) makes use of the empirically found average rise velocity. Deviations between the observation and approximation could partly be explained by the uncertainty and variability of the rise velocity. In a study to the vertical distribution of fish-eggs (Sundby, 1983), the distribution of the particles' rise velocity is accounted for. With supportive information from previous studies to the buoyancy of a range of egg-species, a Gaussian distributed rise velocity was computed. This distribution was inserted in the diffusion equation, instead of a constant average value. The more slowly ascending particles contributing to the concentration found in deeper water layers are thus accounted for. The underestimation of the approximated plastic distribution could partly be explained by the use of an average rise velocity, since the rise velocities for the plastics was skewed towards slower upward motion. In order to account for a distributed rise velocity, more extensive research to the floating ability of specific plastics is needed.

Particle velocities are strongly dependent on ambient factors, such as water temperature and salinity. Additional results on several of these factors may be found in appendix B.2. With a great share of the plastic litter being marginally buoyant, small changes in ambient water could influence the floating ability and therefore the vertical distribution. This is an attribute that could especially become interesting considering tidal rivers. Additionally, factors such as the arbitrary shape of the plastic, deterioration over time and the influence of organisms, drive further complexity of determining the vertical distribution with a theoretical approximation. Importantly, these plastic characteristics change continuously over time. The rise velocities found for the HDPE and LDPE plastic in this research are therefore not to be considered as general material properties but give insights in a certain scenario.

In conclusion, the uncertainties of the rise velocity measurements are great. In reality, these uncertainties are even greater due to e.g. the wide variety of shape, size, local (heterogeneous) flow conditions etc. The experiments however do show a possible relation between the found average rise velocity and observed distribution profile, based on an estimate of the prevailing shear-velocity: The fitted shape parameters follow the same trend as the theoretical estimate. The extent to which the relation could describe and approximate the concentration distribution is however not accurate, development of an additional parameter, such as was intended with the fitted parameter α (Chapter 4.3.3), could improve the estimation.

From controlled lab research to a greatly varying reality

Firstly, there is little information on the consequences of scaled research to plastic behavior. In this research, sheets were cut out of the bags to use in the flume. With that, the ability to trap air and water inside the volume is eliminated. It was found that the extent of the influence of shape and scale is dependent on the specific type of plastic, e.g. for HDPE it was found the scale is of no importance with respect to the air-attachment, for LDPE the scale was of great importance. Reasoning back from the experiment results to the distribution of the prototype bags in the prototype river is not recommended.

Secondly, only two types of plastic materials are tested in a controlled ambient environment. The experiments give information on a scenario, in which the distribution of a plastic with a specific floating ability is investigated under a shear velocity, which could in turn be found in different configurations of river-systems. In the light of the variable effective density, grouping plastics based on the original (presumed) material properties, as is mostly done in literature, may not be efficient. There are a lot of dimensions in plastic that define the floating ability and possibility to scale, additionally to the base material. For an understanding of the behavior of plastic in rivers, the range of effective densities is of interest and plastic should be grouped by the average floating ability as is found on site. With extensive information on the floating abilities of a wide spectrum of plastics found in rivers, expectations on the vertical distribution of these plastics can be established, in relation with the prevailing flow conditions.

Possibilities for the approximation of the distribution

Assuming the concentration distribution profile could be approximated with the right adjustments of the diffusivity equation, it is good to understand what the applicability of this approximation is. First of all, the approximation could return an estimate of the total flux of plastic with only measurements of the surface-share of plastic (C_a). This is convenient, since there are a lot of difficulties concerning the monitoring of plastics. In order to then compute an estimate of the distribution profile, sampled plastic must be clustered and the floating ability per cluster should be determined. Data collected from the discussed studies in Austria (Danube river) and in Jakarta (Hohenblum et al., 2015; van Emmerik et al., 2019) were used in an effort to test the applicability of this approach. In case of the Danube research, no distinction of plastic types is made, and it is not possible to estimate an average rise velocity for the bulk of plastic. Based on the concentrations found over the three depth sections, the composition of the samples is probably made up of both positive and negative buoyant plastics (Supp. Materials A.2.). It was found that at the “turbulent” sampling site about 60% of the sampled plastic was found below the surface-section (50 cm). At the second sampling location, flow was considered “less turbulent”, 75 % of the total plastic was located at the surface. In case of the Jakarta research, a distinction on plastic types was made. However, only double-trawl measurements of the first 1-meter water depth are available, and apart from the average flow velocities, information on the river conditions are lacking. Based on rough assumptions, a profile through the two surface-measurements is computed for the PO_{soft} group, where plastic bags belong to. The analysis can be found in Supplementary Materials A.1. In general, an increase of suspension with an increasing flow velocity may be observed.

A second approach for the use of distribution profiles, is to measure the concentration of plastic over the entire water-depth and approximate the corresponding diffusivity coefficients, in order to create an understanding of the distribution that can be found under certain flow conditions. This approach could help in the understanding of the additional factors determining the profiles, such as an additional shape parameter that was explored in this research. For this objective, the multi-spot sampling method as described by Hohenblum et al. (2015) could be applied. Another method is currently being investigated by colleague master student Broere. Broere studies the ability of acoustic sensing to identify submerged macro plastics in rivers, with the use of a *Fishfinder* (deeper chirp+).

The presented results substantiate the findings from the studies in the Danube and Jakarta, in which it is hypothesized that surface-share of the plastic decreases with an increase of the turbulent intensity and therefore also with an increase of the average flow velocity (Supp. Materials A). One can imagine that interaction of litter can influence the distribution of the plastic. Especially when imagining the extreme rivers covered in plastic, the possibility to determine a distribution profile decreases, as well does the relevance.

Influence of obstructions

The influence of obstructions on the plastic distribution is explored. It is found that the surface and bottom obstructions increase the surface share with respect to the corresponding undisturbed conditions. The structures could indirectly influence the floating ability of the plastic, by an additional vertical velocity term. An interesting example of a removal technology responding on the suspension of plastic, is the Great Bubble Barrier. The curtain of air forms an obstruction for the plastic, adding an upward flow motion that could trap plastic and bring it to the surface. It could even be possible that the use of air for this cause increases the floating ability of the plastic by adding air to the material, either trapped in folds or attached to the material. However, in this research, this phenomenon is not further investigated. An interesting, more elaborated study on the effects of an obstruction at the surface, is conducted by Honingh (2018). This study shows the effects of clogging in front of a trash rack.

Conclusions and Recommendations

For this research, two objectives were stated. The first objective was to investigate the vertical distribution of plastic under normal turbulent flow, induced by bed shear stresses only. In order to generalize the results of this research for the overall plastic problem, an in-depth comparison was made with existing theory on turbulent mixing of suspended matter. The second objective was to explore the influence of obstructions on the depth-distribution of plastic. The extent of surface-share changes due to obstructions, and the manner by which the distribution is altered compared to undisturbed equilibrium distribution, was investigated. In this chapter, conclusions are structured according to the two objectives. Recommendations are given in Section 6.2.

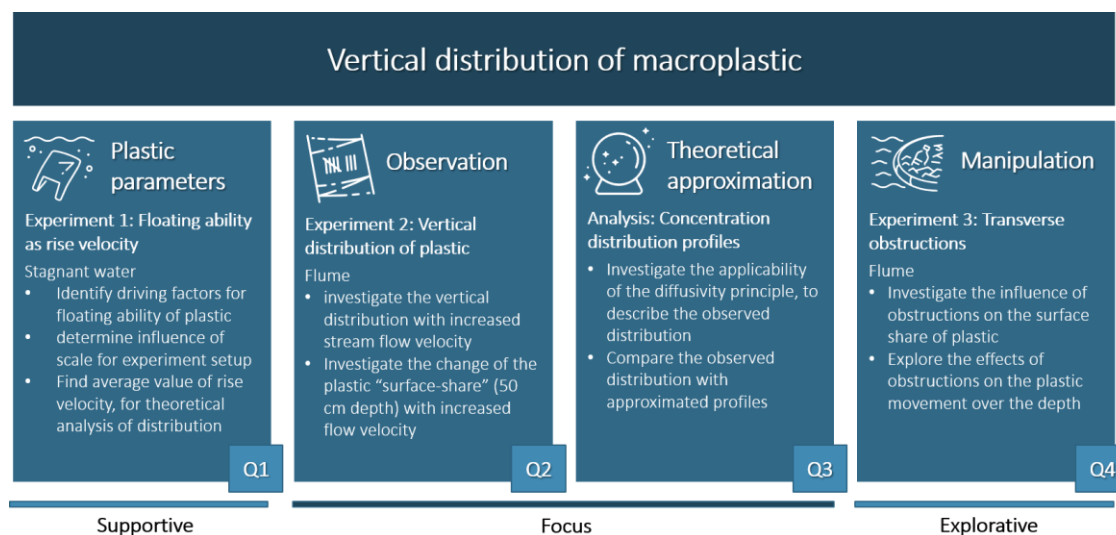


Figure 6.1: The four pillars of this research, with a short indication of the conducted experiments and analyses.

6.1. Conclusions

Vertical distribution of plastic

The results of this laboratory study showed that it is reasonable to assume a considerable amount of plastic transport below the surface layer, for average turbulent flow conditions found in urban rivers. It was demonstrated that with an increase of the shear velocity (u_* from 0.5 to 3.6 cm/s), which is an indicator of turbulence intensity and scales on the average flow velocity (U_{da}), the surface-share of the positive buoyant plastic of the type HDPE decreased from 95% to 25%. For the defined prototype river, the 25% surface-share would go with an average flow velocity of 0.5 m/s. In multiple studies on the yearly fluxes of riverine plastic transport, the hypothesis of a uniform vertical distribution was used, e.g. the studies of Dris and Schmidt et al., (2017; 2017). The results of this research would substantiate this hypothesis.

However, the conducted research was focused on only two types of marginally positive buoyant plastics: foils of the material HDPE and LDPE. The floating ability of these plastics is relatively small and therefore these plastics are sensitive to turbulent mixing. Other plastics come with other floating abilities, depending on much more than the density and size only. Thereby, the experiments were scaled and the plastic was downsized. From the experiments it was found that the presumed buoyant plastics of the material LDPE even showed settling behavior for downsized sheets, implying a material density higher than the ambient water density ($\rho_{\text{water}} = 0.98\text{--}1.00 \text{ g/cm}^3$). It became clear that the floating ability of the plastic used in these

experiments is highly dependent on the influence of air. It can be expected that for bigger sheets of plastic, and especially for plastic bags, air trapped inside the shapes and folds can dominate the vertical movement through the water and more plastic would be found near the surface than was found in the scaled experiments. If we however consider the fragmentation of these bags over time, there would be more resemblance with the experimented small-scaled sheets (3 x 4 cm).

In this paragraph, the influence of air on the floating ability is elaborated on, and an answer will be given to the first research question stated in this thesis: **“How is the floating ability of the plastic defined and quantified, that counteracts the mixing behavior of turbulent flow?”**. It was found that small air-bubbles are attached to the materials’ surface, for both the HDPE and LDPE plastic. If all air was released, which was observed for the downsized LDPE sheets, the plastic would lose its floating ability. Therefore, two driving mechanisms can be distinguished that define the floating ability of the plastic: 1. The properties of the plastic itself in relation to the ambient water properties (e.g. density difference, shape and size) and 2. The influence of air, either trapped in the shape or attached to the surface of the plastic. Technically, the ability to attach air to the material could also be defined as a material property and was found to be either dependent or independent of scale. Additionally, in supplementary research it was found that this air-attachment decreased over time of submergence of the plastic, slower rising motions were observed for ‘older’ plastics. In conclusion, the floating ability of the plastic is quantified as an empirical average rise velocity. Because of the limitations of this research on only positive buoyant plastics, it was decided to consider the dual-buoyant LDPE plastic as neutral buoyant for further analysis, with an average rise velocity of 0.0 m/s. The HDPE plastic was found to be positive buoyant in general and an average rise velocity of 1.0 cm/s was found.

As an answer to the second research question: **“How is the distribution of plastic over the water depth influenced by bed shear induced turbulence?”**, the following conclusions are drawn: When the shear velocity is low, the distribution is mainly governed by the floating ability of the plastic whereas turbulent mixing plays a minor role. For higher shear velocities, which correspond with higher flow velocities, the role of turbulent mixing gets more substantial and a uniform distribution can develop. The two materials showed different floating abilities in terms of average rise velocities, mainly due to the ability to attach air. Because of this, different developments of the vertical distribution can be distinguished. For the HDPE plastic, air-attachment was found to be an average condition. The distribution developed to a more uniform spread: an increase in shear velocity resulted in a decrease of the plastic surface-share. For the experiments conducted with the LDPE plastics however, it was found the air-attachment ability of the plastic was dependent on scale and the floating ability was extremely variable. Under flow these plastic sheets would show both rising and settling behavior. This great variety in floating ability could explain the random distribution of this plastic found under the investigated flow conditions, in which no trend could be concluded. It is possible that the resulting distribution is governed by primarily the chance of air attached to the tested sheet, rather than the effect of turbulent motions of the flow.

In order to generalize the results from this research, an in-depth comparison of the observed results is made with existing theory on the vertical distribution of suspended matter. In the following paragraph, answer will be given to the third research question: **“Can the vertical distribution of plastic be described with existing theory on turbulent mixing?”**. Concentration distribution profiles were fitted through the observed distributions, for each velocity experiment separately. The profiles were based on a concentration distribution equation, adapted from the *Rouse profile*. The shape of the theoretical Rouse profile is dictated by the ratio between the shear velocity and the rise velocity of the plastic ($\beta = w_r / \kappa u^*$). This represents the ratio between the floating ability and turbulent mixing. The optimal LMSE-fit through the observed data per velocity-experiment is based on an estimator for β for each experiment, b_i , and the measured concentration near the surface (C_a at $z = a$). The optimal estimators (b_i) were then compared to the theoretical Rouse parameter, β , which is based on an empirically determined rise velocity and a calculated shear velocity. For the LDPE plastic, this theoretical shape parameter equals 0, since the rise velocity was set as 0 cm/s on average. The theoretical profile for this plastic therefore shows uniform distributions over depth in all cases. This was not observed in the experiments, but deviations can be explained by the dual buoyancy behavior of this plastic. For the HDPE plastic, it was seen that the fitted concentration equation can accurately describe the observed distribution. The theoretically approximated profile however underestimated the suspension of the HDPE plastic in all cases. But, even though the fitted and theoretical profiles for each velocity-experiment showed strong deviations, the fitted shape parameters (b_i) do follow a similar trend as the theoretical parameter β when plotted against the flow velocity. This indicates a possible relation between

the observed distribution and the ratio of velocities w_r/u^* . This result suggests that it is possible to describe the distribution with existing knowledge, based on the turbulent diffusivity principle. Additional parameters to describe the distribution of plastic might be needed. An attempt was made by optimizing the shape parameter β with an additional parameter α , for which a value of 0.64 was found. However, the deviations between observed and approximated profiles remains large. An explanation could lie in the possible variation of the floating ability under flow conditions: higher shear velocities and more mixing may cause air to be released from the plastic. An additional parameter should then be variable with the flow condition. It would also be possible to consider the entire distribution of rise-velocities rather than an average value, as applied in research of Sundby to the distribution of fish-eggs (1983). The great variability due to the role of air-attachment could then be accounted for. Important note is the fact that the equation can only be applied to either positive buoyant or negative buoyant particles, with neutral buoyancy as a limit. A combination of both is not possible.

Influence of obstructions on vertical distribution of plastic

In addition to the investigation of the equilibrium distribution of plastic, the influence of obstructions on the distribution was studied. A sluice gate, bottom sill and half-way obstruction with the size of $1/5^{\text{th}}$ of the water depth were placed in the flume setup, with the requirement of subcritical flow fulfilled. The underlying goal of this second part of the research was to investigate both the influence of a surface skimming technology itself, which is in fact a permeable gate structure (such as a trash rack), and the potential of hydraulic structures to increase (or decrease) the surface share of plastic. This sub-research was explorative. All obstructions were solid, sharp crested structures and the design and layout of the structures is not experimented with. In the following paragraph, answer will be given to the final research question: **“How is the vertical distribution influenced by a partial vertical obstruction of the river flow?”**. From the results it was seen that the plastic surface-share is greater with the presence of a sluice gate and a bottom sill. With increasing shear velocities, the surface-share still decreases, but to a lesser extent than was observed under undisturbed conditions. The observed surface-share decrease does imply the increasing relevance of turbulent mixing. However, in case of the half-way obstruction this trend was not observed. The surface share was about equal over a range of 0.1 to 0.5 m/s flow velocity. The cause of this discrepancy is not clear. It is possible that limitations of the flume- and obstruction-setup resulted in the observed distribution. Even though, no negative effects were observed, and the results make it plausible that hydraulic structures can be intentionally applied in waterways to increase the surface share. Further research to application and design of supportive structures is advised.

Relevance of research placed in context

A better understanding of how plastic litter is transported via rivers is crucial. Both for quantification and mitigation of the plastic problem. This research contributed to the overall knowledge on the behavior of plastic in rivers, by investigating the overarching problem statement: **How is plastic distributed over the water depth in rivers and how is this related to prevailing flow conditions?** Even though this study is not extensive enough to create a complete picture of the influence of turbulence on the behavior of plastic, it does show that marginal buoyant plastics can be sensitive to turbulent motions in flow. There is a chance of missing these suspended plastics when focusing on only the surface share, causing underestimations of the yearly fluxes. With this research, a first insight is created on the vertical behavior of plastic in relation with flow conditions. This insight can however not stand on its own, due to the complexity of river flow. More extensive research on the 3D-transport mechanisms of plastic is needed. It was shown that there are possibilities to approach the vertical distribution according to existing theory, based on studies on sediment dynamics and more ecological minded research. This link to neighboring fields is missing in the field of plastic research. Collaboration between different expertises is therefore encouraged.

6.2. Recommendations

The hypothesis of this research is that a significant share of the plastic litter in rivers is transported below the surface water of 50 cm depth. It is recommended to either strengthen this hypothesis by further laboratorial research to a wider variety of plastic materials, or to test the hypothesis in a real-life context. For both options, main recommendations that should be considered in a follow-up research proposal are discussed.

Strengthen hypothesis with laboratorial research

For the first option, more extensive research to the floating ability of the plastic tested could be of interest. One can imagine that the properties of the plastic, such as stiffness, rigidity and texture, can result in different (key-)driving mechanisms for the floating ability. The method of grouping plastics based on their material type (HDPE, LDPE, PVC etc.) is debatable and other classifications might give more information on the behavior of the plastic group. Additionally, variations in ambient conditions such as water temperature and salinity levels, could be added to the research scope. These factors could especially be of interest in tidal areas and lakes, where stratification plays a role. Furthermore, the applicability of the Rouse profile, or other distribution profiles found in literature, can be further investigated. If chosen to continue in line with the conducted experiments in this research, some main recommendations on the methodology are given:

- The main improvement is the scale of experiment. Firstly, the length of the flume is of importance, since an assumption is made on an equilibrium plastic distribution. Ideal would be an infinite flow, so that the equilibrium distribution can be ensured. This could be imitated with a carousel flume. However, the floating ability of the plastic could form an issue in this set-up. Secondly, in more deep and wide flumes bigger plastics could be experimented with and the effects of deformability of the plastic could be investigated. Thereby, the bigger the scale, the lesser the scale influences.
- In order to properly investigate the effect of obstructions relative to the undisturbed distribution, a longer flume would be needed. There should be enough length to reach a developed, undisturbed distribution before the plastic reaches the obstruction and is influenced. Behind the obstruction, enough length is needed to achieve the equilibrium distribution once again.
- Since it was found that the theoretical approach towards the distribution is promising, but needs improvement, it might be interesting to study plastic particles that are more easily confined within this theory, e.g. spherical particles (pellets). So that factors such as orientation and deformation of shape are excluded.

Test hypothesis in real-life context

In order to test the hypothesis in a real-life context, fieldwork measurements of the vertical distribution of plastic are needed. In the study of Hohenblum (2015) a multi-spot sampling approach is introduced. However, this method is quite expensive and labor intensive. The sampled plastics should be investigated on site, so that the floating ability corresponding to the local ambient conditions can be defined. The methodology described in this thesis can be applied on site; see through containers can be filled with water retrieved from the location and the rise velocities of sampled plastic can be measured. It is advised to test the plastics immediately after retrieval, to prevent warming of the water and other changes. The depth-location of each sampled plastic should be noted, and the plastics should then be grouped on the found rise velocity, in order to establish a distribution profile that is based on the rise velocity of the plastic in relation to the prevailing flow condition. Determination of the prevailing flow conditions, expressed as the shear velocity, is difficult. The roughness coefficient must be estimated and is prone to great uncertainties. The average stream flow velocity can be measured on site.

During this thesis research, an attempt was made to investigate the plastic distribution in a real-scale scenario, namely in a sluice: The Borgharen Sluice in Maastricht is not in use and Rijkswaterstaat is developing this sluice into a river-test-facility at the moment. As further explained in Supplement D, the sluice could serve as a 1:1 flume model. However, the turbulent vortex flows that were found during the fieldwork made further investigation in this sluice not suitable. The flow conditions should be altered in order to be able to do scientific research in this sluice. Rijkswaterstaat is working on improvements of this test-facility and is happy to help students and startups to conduct research and pilot projects at this location. This study would serve as a step between controlled laboratorial research and uncontrolled reality

Recommendations for implementation

For practical applications in line with this research, such as cleaning strategies based on surface skimming, the following recommendations are given:

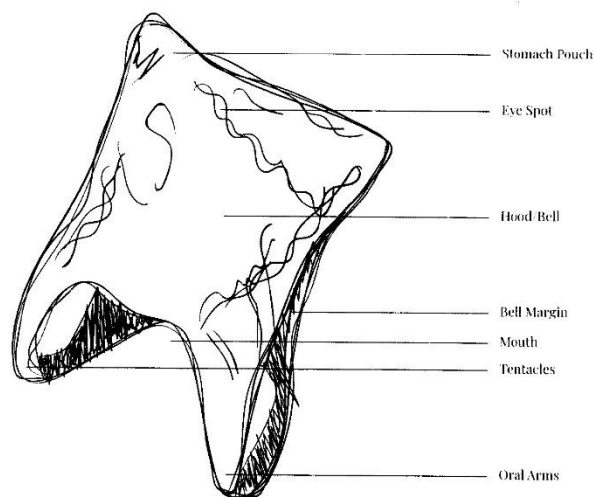
- It was found that higher turbulent flow conditions significantly increase the chance on plastic suspension, and therefore this litter might be overlooked in cleaning strategies. Surface skimming techniques should therefore be placed at locations where the flow is less turbulent (lower flow velocities or at locations that have a smoother conduit) and mixing due to external factors (such as navigation or behind a hydraulic structure) does not occur.
- In line with previous recommendation, an open question exists: Is most plastic present at the locations where we see the most accumulation? For example, in stagnant water such as in harbor basins, often accumulation of litter is seen. A technique such as the Shoreliner of Tauw acts on this observed accumulation. However, the plastic we observe is a snapshot in time. It could be that at the locations where flow velocities are higher, more plastic passes per time interval and hotspots would actually be where we do not expect them to be. For this question, a focus on both vertical as horizontal distribution would be needed. The focus is less on the behavior of the plastic, more on the quantity.
- It might be interesting to investigate the influence of obstructions in the 1:1 flume of Borgharen. For example, the influence of a ramp, that could guide plastic to the surface where it is more easily removed.
- Lastly, within the context of this research, the following question may arise: should all plastic be made in such a way that it always floats? Since it was concluded that we might miss a great amount of plastic. If all plastic would stay afloat, it would be easier to remove. Industries should then focus on the use of low-density plastics for example. However, floating plastic is seen as prey for animals such as birds and seals. Thereby, the ability to float makes the transport mobile and easily transported to the ocean.

Bibliography

- Battjes, J., & Labeur, R. J. (2017). *Unsteady flow in open channels*. Cornwall: Cambridge University Press.
- Chanson, H. (2004). *Environmental Hydraulics of open channel flows*. Oxford: Elsevier Butterworth-Heinemann.
- Derraik, J. G. . (2002). The pollution of the marine environment by plastic debris: a review. *Marine Pollution Bulletin*, 44(9), 842–852. [https://doi.org/10.1016/S0025-326X\(02\)00220-5](https://doi.org/10.1016/S0025-326X(02)00220-5)
- Dris, R. (2017). *First assesement of sources and fate of macro and micro plastics in urban hydrosystems : Case of Paris megacity*. 248.
- Eriksen, M., Lebreton, L. C. M., Carson, H. S., Thiel, M., Moore, C. J., Borerro, J. C., ... Reisser, J. (2014). Plastic Pollution in the World's Oceans: More than 5 Trillion Plastic Pieces Weighing over 250,000 Tons Afloat at Sea. *PLoS ONE*, 9(12), e111913. <https://doi.org/10.1371/journal.pone.0111913>
- Gasperi, J., Dris, R., Bonin, T., Rocher, V., & Tassin, B. (2014). Assessment of floating plastic debris in surface water along the Seine River. *Environmental Pollution (Barking, Essex : 1987)*, 195, 163–166. <https://doi.org/10.1016/j.envpol.2014.09.001>
- Geyer, R., Jambeck, J. R., & Law, K. L. (2017). Production, use, and fate of all plastics ever made. *Science Advances*, 3(7). <https://doi.org/10.1126/sciadv.1700782>
- González, D., & Hanke, G. (2017). Toward a Harmonized Approach for Monitoring of Riverine Floating Macro Litter Inputs to the Marine Environment. *Frontiers in Marine Science*, 4(March), 1–7. <https://doi.org/10.3389/fmars.2017.00086>
- González, D., Hanke, G., Tweehuysen, G., Bellert, B., Holzhauer, M., Palatinus, A., ... and Oosterbaan, L. (2016). *Riverine Litter Monitoring - Options and Recommendations. MSFD GES TG Marine Litter Thematic Report*. <https://doi.org/10.2788/461233>
- Heath, M., Sabatino, A., Serpetti, N., McCaig, C., & O'Hara Murray, R. (2017). Modelling the sensitivity of suspended sediment profiles to tidal current and wave conditions. *Ocean and Coastal Management*, 147, 49–66. <https://doi.org/10.1016/j.ocecoaman.2016.10.018>
- Hohenblum, P., Frischenschlager, H., Reisinger, H., Konecny, R., Uhl, M., Mühlegger, S., ... Rindler, R. (2015). *Plastik in der Donau*.
- Honingh, D. F. (2018). *Riverine debris : interactions between waste and hydrodynamics*. TU Delft.
- Huang, S. H., Sun, Z. L., Xu, D., & Xia, S. S. (2008). Vertical distribution of sediment concentration. *Journal of Zhejiang University: Science A*, 9(11), 1560–1566. <https://doi.org/10.1631/jzus.A0720106>
- Jambeck, J. R., Geyer, R., Wilcox, C., Siegler, T. R., Perryman, M., Andrady, A., ... Law, K. L. (2015). Plastic waste inputs from land into the ocean. *Marine Pollution*, 347(6223), 768–771. <https://doi.org/10.1126/science.1260879>
- Lebreton, L., Egger, M., & Slat, B. (2019). A global mass budget for positively buoyant macroplastic debris in the ocean. *Scientific Reports*, 9(1), 1–10. <https://doi.org/10.1038/s41598-019-49413-5>
- Lebreton, L., Van Der Zwet, J., Damsteeg, J. W., Slat, B., Andrady, A., & Reisser, J. (2017). River plastic emissions to the world's oceans. *Nature Communications*, 8, 1–10. <https://doi.org/10.1038/ncomms15611>

- Lechner, A., Keckeis, H., Lumesberger-Loisl, F., Zens, B., Krusch, R., Tritthart, M., ... Schludermann, E. (2014). The Danube so colourful: A potpourri of plastic litter outnumbers fish larvae in Europe's second largest river. *Environmental Pollution*, 188, 177–181. <https://doi.org/10.1016/j.envpol.2014.02.006>
- MIT. (n.d.). Basics of Turbulent flow. Retrieved from <http://www.mit.edu/course/1/1.061/www/dream/SEVEN/SEVENTHEORY.PDF>
- Moore, C. J. (2008). Synthetic polymers in the marine environment: A rapidly increasing, long-term threat. *Environmental Research*, 108(2), 131–139. <https://doi.org/10.1016/j.envres.2008.07.025>
- Morritt, D., Stefanoudis, P. V., Pearce, D., Crimmen, O. A., & Clark, P. F. (2014). Plastic in the Thames: A river runs through it. *Marine Pollution Bulletin*, 78(1–2), 196–200. <https://doi.org/10.1016/j.marpolbul.2013.10.035>
- Rech, S., Macaya-Caquilpán, V., Pantoja, J. F., Rivadeneira, M. M., Campodónico, C. K., & Thiel, M. (2015). Sampling of riverine litter with citizen scientists — findings and recommendations. *Environmental Monitoring and Assessment*, 187(6). <https://doi.org/10.1007/s10661-015-4473-y>
- Rech, S., Thiel, M., Jofre Madariaga, D., Macaya-Caquilpán, V., Rivadeneira, M. M., & Pantoja, J. F. (2014). Rivers as a source of marine litter – A study from the SE Pacific. *Marine Pollution Bulletin*, 82(1–2), 66–75. <https://doi.org/10.1016/j.marpolbul.2014.03.019>
- Rouse, H. (1937). Modern conceptions of the mechanics of fluid turbulence. *Trans ASCE*, 102, 463–505.
- Schmidt, C., Krauth, T., & Wagner, S. (2017). Export of Plastic Debris by Rivers into the Sea. *Environmental Science and Technology*, 51(21), 12246–12253. <https://doi.org/10.1021/acs.est.7b02368>
- Sebille, E. Van, Aliani, S., Law, K. L., & Maximenko, N. (2019). *The physical oceanography of the transport of floating marine debris*. 1–54.
- Sundby, S. (1983). A one-dimensional model for the vertical distribution of pelagic fish eggs in the mixed layer. 30(6).
- Sundby, S. (1991). *Factors affecting the vertical distribution of eggs*. (1), 33–38.
- Tramoy, R., Gasperi, J., Dris, R., Colasse, L., Fisson, C., Sananes, S., & Rocher, V. (2018). *Assessment of the Plastic inputs from the Seine Basin to the Sea using statistical and field approaches*. 1–16.
- van Emmerik, T., Loozen, M., van Oeveren, K., Buschman, F., & Prinsen, G. (2019). Riverine plastic emission from Jakarta into the ocean. *Environmental Research Letters*, 14(8), 084033. <https://doi.org/10.1088/1748-9326/ab30e8>
- van Emmerik, T., & Schwarz, A. (2020). *Plastic debris in rivers*. (October 2019). <https://doi.org/10.1002/wat2.1398>
- van Prooijen, B., van Maren, B., Chassagne, C., & Winterwerp, H. (2018). Sediment Dynamics. In *Lecture Notes*. Delft: Delft University of Technology.
- van Rijn, L. (1993). *Principles of Sediment Transport*.
- Wilcox, C., Maximenko, N., Harari, J., Hardesty, B. D., Vethaak, A. D., Potemra, J., ... Lebreton, L. (2017). Using Numerical Model Simulations to Improve the Understanding of Micro-plastic Distribution and Pathways in the Marine Environment. *Frontiers in Marine Science*, 4(March), 1–9. <https://doi.org/10.3389/fmars.2017.00030>

Supplementary Materials



Jellyfish ([B]eg for no bag)

Jellyfish are mainly free-swimming or floating marine animals with umbrella-shaped bells and trailing tentacles. The tentacles are armed with smothering plastic layers and may be used to capture prey and defend against predators. Most animal species suffocate after coming into contact with a plastic jellyfish.

Because they are made from plastic, **they will be existing forever without any purpose, and they end up destroying nature.**

Postcard by Daphne Persoon, participant of the Doppler Challenge 2019

In depth comparison with literature

A.1. Jakarta: Multi-trawl sampling (in depth comparison)

In Jakarta, double-trawl samples were taken from the first meter below the surface, divided in two depth sections (van Emmerik et al., 2019). The objective of the study of van Emmerik et al (2019) in Jakarta was to provide an estimation of macroplastic emission from rivers and canals that run through the city of Jakarta into the sea. A part of the research was conducted with a double-trawl, which sampled from 0 to 0.35 m and 0.5 to 1.0 meter below the surface simultaneously. In a supplementary analysis retrieved from Emmerik, the relative concentrations (%) sampled in the surface net with respect to the total of the two nets, are plotted against the measured flow velocities (Fig. 1). The results are presented per plastic type (as classified in the paper of van Emmerik et al). It was observed that with an increasing flow velocity (from about 0.1 up till 0.4 m/s) the surface-share of the PO-soft plastic, to which plastic bags belong, decreases from around 80% to below 60% (with respect to the lower net). For highly positive buoyant plastics, such as foams, belonging to the group PS-E (expanded polystyrene), there is no plastic found in the lower net. On average for all sampled plastics, the measured concentration in the upper layer was found five times as high as in the lower net. Even though the plastic concentration was found to vary considerably in time, the concentration in the upper net was always higher than in the second net.

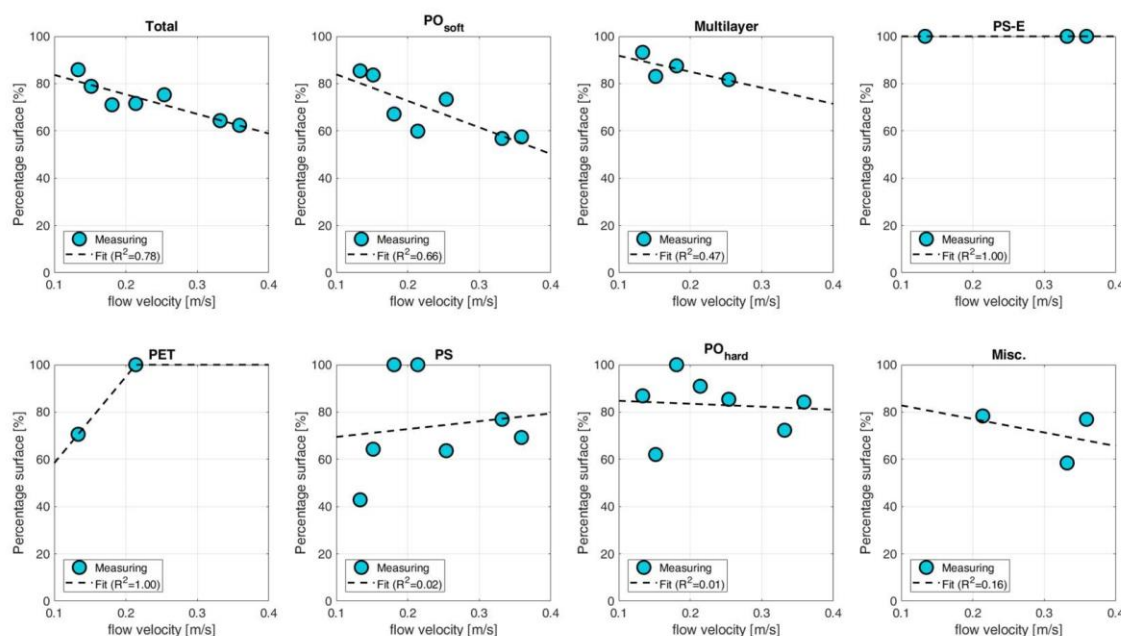


Fig. 1: Daily average results of the relative percentage found in the upper trawl (0-0.5 m) with respect to the lower trawl (0.5-1 m). Bags belong to the PO_{soft} group. With higher flow velocities, the share measured in the upper trawl seems to decrease. (Supplementary analysis retrieved from van Emmerik (2019))

Analysis on Jakarta measurements

The results of the PO_{soft} group are analyzed based on the proposed approach in this thesis. This data set only comprises of 2 measurements over depth (near the surface), for 7 different measured velocities. In Chapter 3.3.1 the diffusivity principle is used to define a concentration equation for positive buoyant plastics, this equation is applied on the retrieved dataset of Jakarta. Since no additional information on the river conditions or sampled plastic is given, rough assumptions are made:

- The river depth is set on 5 m, the width was measured (from Googlemaps) and equals 50 m.
- An assumption for the friction coefficient is based on a n-value of 0.035 (weedy river), this results in a friction coefficient $c_f = 0.007$.
- The plastic classified as PO_{soft} are assumed to have equal floating abilities as was found for plastic sheets in this MSc research, and the rise-velocity is set equal to 0.01 m/s.

Based on these assumptions, the corresponding shear velocity for each measured flow velocity is computed. It was hypothesized that the ratio of the prevailing shear velocity and the rise velocity of the plastic dictates the concentration profile and its shape parameter β . Therefore, the equation is fitted through the two observation points (upper trawl and lower trawl) and the optimized parameter b_i for each velocity is plotted against the shear velocity (Fig. 3 and Fig. 4). The found shape parameters are compared to the shape parameters found in this MSc research. The optimized profile of the shape parameter, with an additional factor of $\alpha = 0.64$ (as found in Chapter 4.3.3), is plotted as well for comparison (dashed green line). The initial profile of the theoretical parameter β shows an underestimation of suspension for all velocities. The optimized theoretical parameter ($\alpha\beta$) shows an improvement of the approximation.

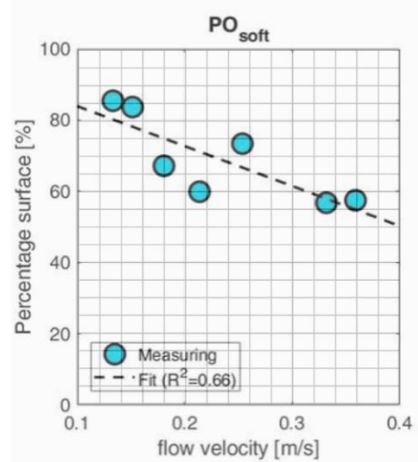


Fig. 2: Plastic bags were classified as PO_{soft} . These measurements (surface share versus average flow velocity) are taken as input data to compute distribution profiles over the entire depth.

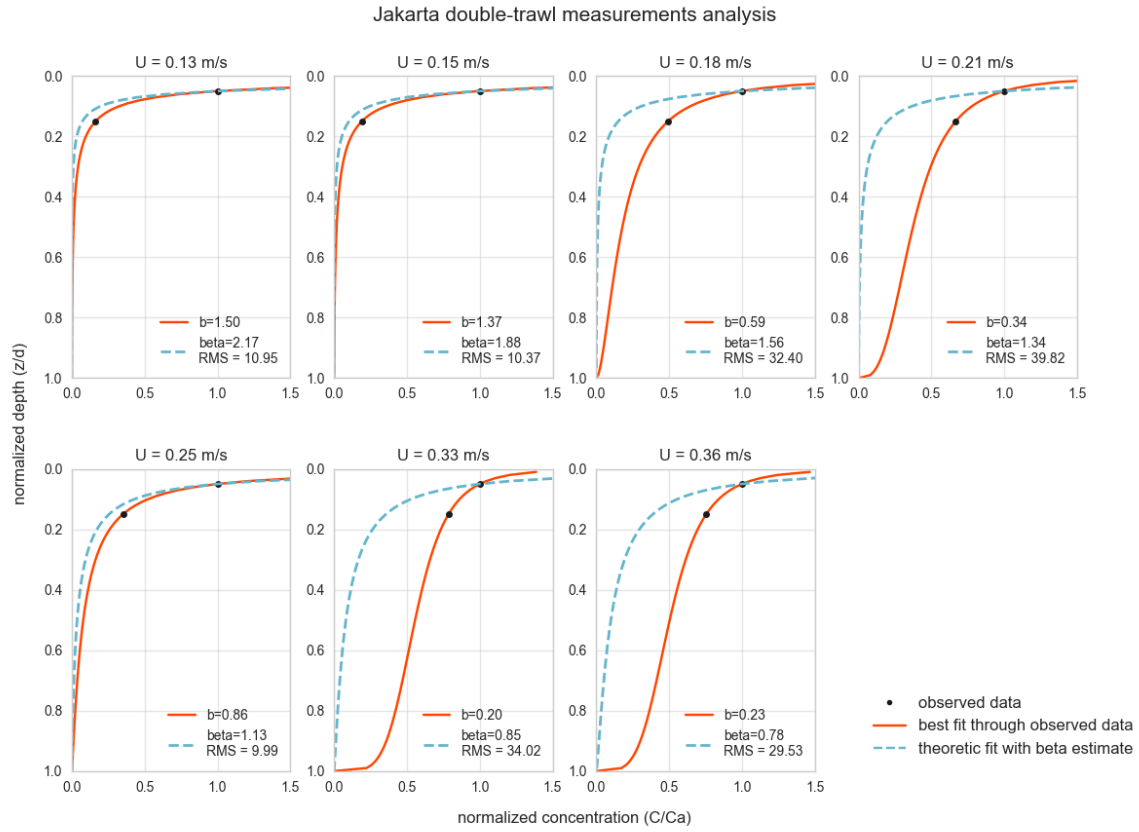


Fig. 3: Concentration distribution profiles of the 7 measured velocities in Jakarta (normalized to the near-surface measurement). Since two observed measurements are used for the fit, the RMS of the fit equals zero. The theoretical profile, based on rough assumptions on the shear velocity and rise velocity, is plotted as well.

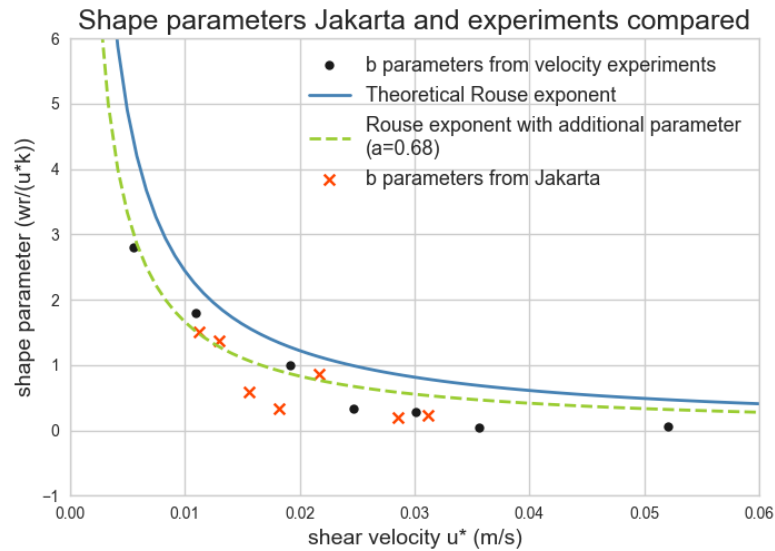


Fig. 4: Optimized shape parameters for each flow velocity are plotted against the corresponding shear velocity, so that comparison with the found shape parameters of the experiments is possible.

A.2. Danube: Sampling over entire depth

In a study conducted in the Danube, Austria, the horizontal and vertical variability of plastic transport is investigated by using a multi-spot sampling method (Hohenblum et al., 2015). With a triple-layered sampling net, samples are gathered from the surface water, the midwater and near the bottom at two locations (Hainburg and Aschach). From these samples, an annual average of plastic transport was calculated. The focus of this research was not particularly on the influence of flow conditions on the found distribution. However, it was concluded that due to more turbulent flow at the sampling site of Hainburg, “*plastic particles show properties of suspended particles rather than floating particles, and therefore can be encountered in the entire river profile*”. Based on the data presented in this study, it was found that at the location of Aschach (the less turbulent location) about 75% of the total sampled plastic concentration (mg/m^3) was found at the surface, while for Hainburg the surface-share equaled about 40%. There is however no elaboration on the definition of the turbulent intensity for both sampling sites, it is only stated that the location of Hainburg was “*more turbulent*”.

The gathered data from the study of Hohenblum et al. could not be used for a comparison with the found results in this research, since the plastic samples were not classified by type or buoyancy. The samples exist of a variety of plastic, most probably both positive and negative buoyant. A profile based on either a positive or negative concentration gradient does not suffice. In Fig. 7 it can be seen that the relative concentrations (with respect to the total) varies over the horizontal coordinate. Variation of flow conditions over the width, depth and length of a natural river exist.

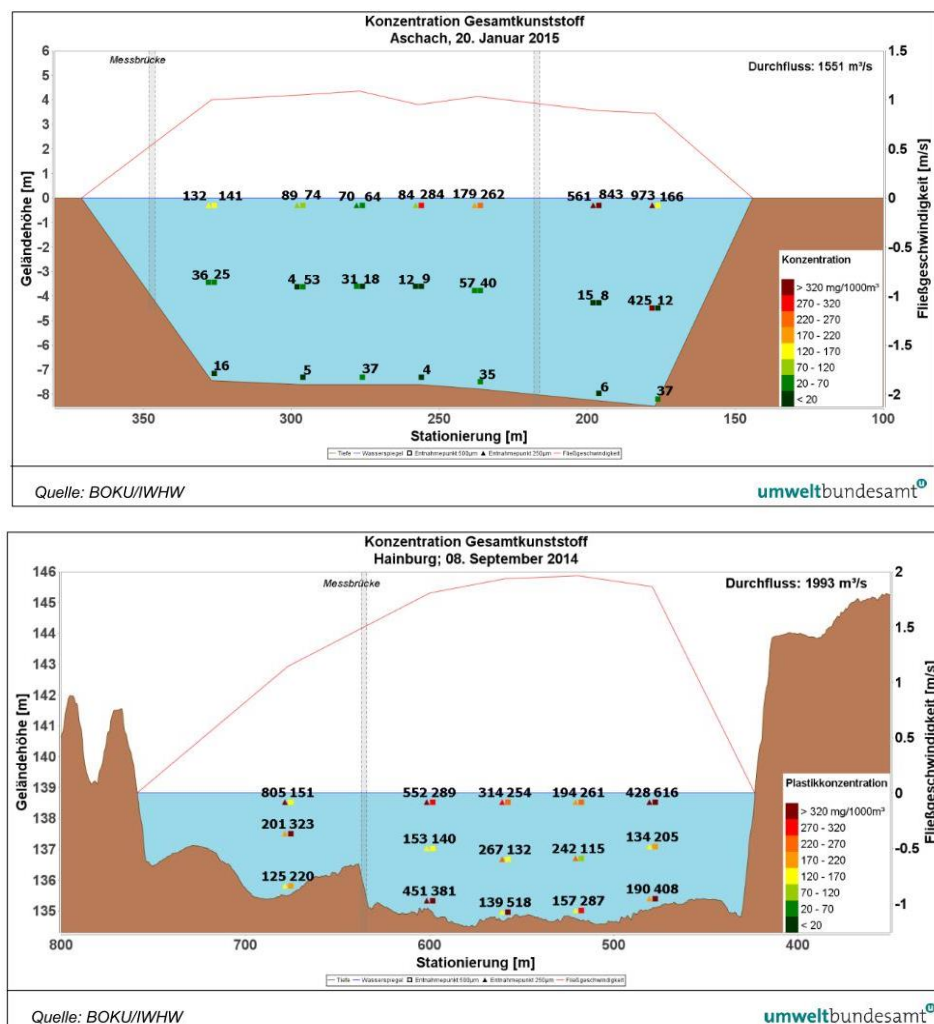


Fig. 5: Multispot measurements of concentration of plastic (both micro and macro) in the Danube at Aschach (above) and Hainburg (Below). The site of Aschach showed less turbulent flow than Hainburg. (Hohenblum et al., 2015).

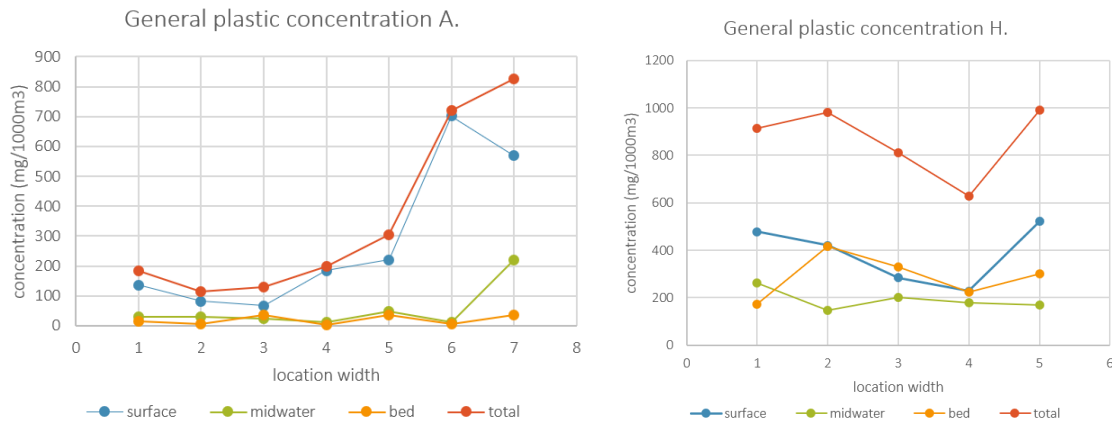


Fig. 6: Own analysis: Concentration of plastic (both micro and macro) at Aschach (left) and Hainburg (right).

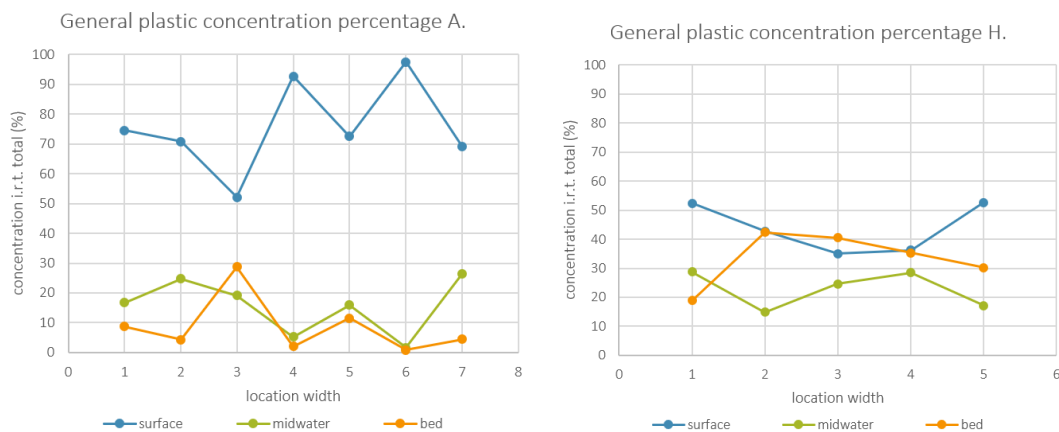


Fig. 7: Own analysis: Relative concentrations with respect to total sampled plastic at Aschach (left) and Hainburg (right). On average, the surface-share at Aschach is about 75%, at Hainburg about 45%.

A.3. Thames: Samples near the riverbed

A study to the presence of plastic near the river bed is conducted in the Thames River, London (Morritt et al., 2014). Samples of the water up till 40 cm above the water bed were taken with eel-fykes. Within 87 days of measuring, a total of 8490 items of rubbish were counted, of which about 1.50% plastic bags (127 bags). The plastic sampled could both originate from the bed, eroded and brought in suspension, or positive buoyant plastics that are mixed over the water-depth. No additional measurements were conducted to other water-depths, such as the surface-share. Therefore, no comparison over depth can be made. In Fig. 8, the composition of litter found near the river bed at multiple sites is given. Even though the share of the bags is small with respect to other plastics, the presence does substantiate the hypothesis that marginal positive buoyant plastics can be found over the entire water depth. Food wrappers are also often made of materials with a lower density than water and therefore positive buoyant. From the classification used it is however not possible to get information on the buoyancy of the plastics found.

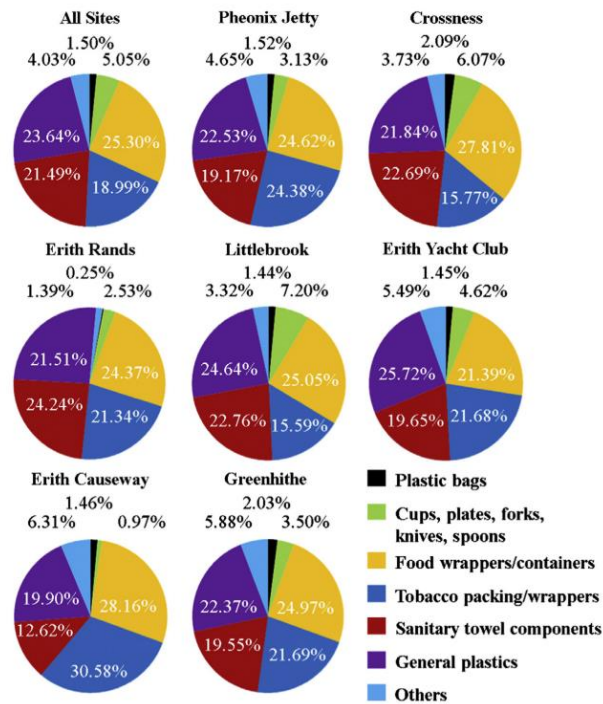


Fig. 8: Results of the Thames sampling campaign. Composition of litter intercepted in fyke nets at different sites in the Upper Thames estuary (Morritt et al., 2014)

Additional Experiments

B.1. Density determination of the plastic

Sheets of the size 10 x 10 cm (± 0.1 mm) are tested for their material density. 10 sheets were weighted (Mettler AE 240 ± 0.001 g) of both the HDPE and LDPE material. The thickness was determined with a digital caliper (± 0.01 mm), by stacking of 4, 8 and 16 sheets. From this thickness measurement it was clearly seen the HDPE material is thinner. This plastic was found more flexible. The range of densities is determined by including the uncertainties of each measurement (mass, thickness and size). Even though the range indicates both positive and negative buoyant properties, it was found that when the sheets, both HDPE and LDPE, lost all air bubbles attached, the floating ability would be eliminated. All sheets would sink. For the HDPE plastic it was however found that the air attachment is an average condition, intensive stirring was needed to get rid of all air.

Table 1: Densities as found in experiment

	HDPE	LDPE	Water
average density (g/cm³)	1.01	1.03	
min density	0.85	0.95	
max density	1.21	1.12	
Average thickness (mm)	0.001	0.004	
Average mass (g)	0.15	0.41	
Estimated density (g/cm³)	0.93-0.97	0.92-0.93	0.98-1.0
Density difference with water	0.03-0.07	0.05-0.08	

B.2. Time of submergence: changing properties

In a tank of 2 x 2 m, with a water depth of 1 m, the rise time of 'old' plastic was compared to the rise time of the new plastic. In these experiments as well, the plastics are stirred under water before released from the bottom, to get rid of the bigger air bubbles trapped inside the bag or folds of the sheets. Plastic bags and sheets are submerged for 5 weeks, in order to investigate the influence of watering time on the floating ability. It is very clearly from this experiment that air attachment gets less (Fig. 10). Also, it could be that there are changes on molecular levels. This is not further investigated. The probability density graphs are plotted in Fig. 9.

	HDPE	HDPE_5weeks	LDPE	LDPE_5weeks
average rise velocity (cm/s)	6.9	4.1	5.1	2.4

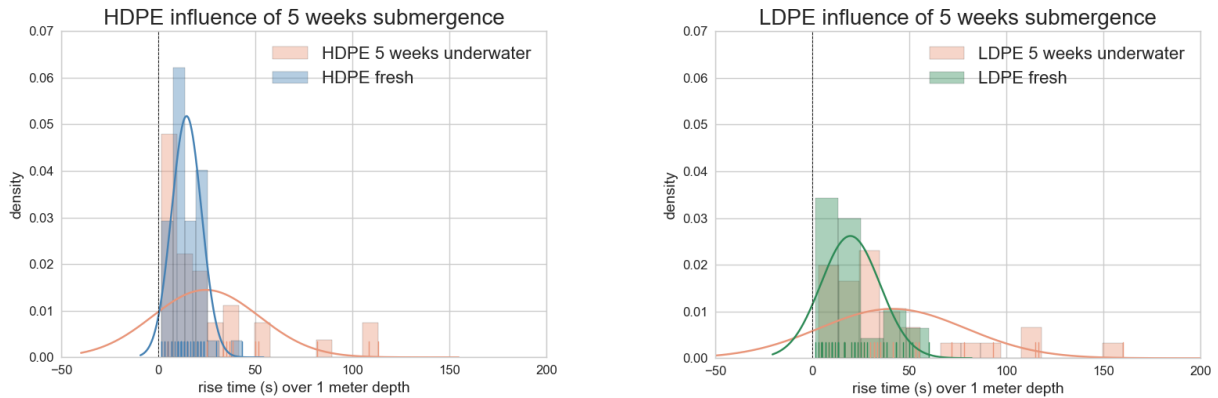


Fig. 9: rise times of fresh bags versus wetted bags (5 weeks submerged), left = HDPE, right = LDPE

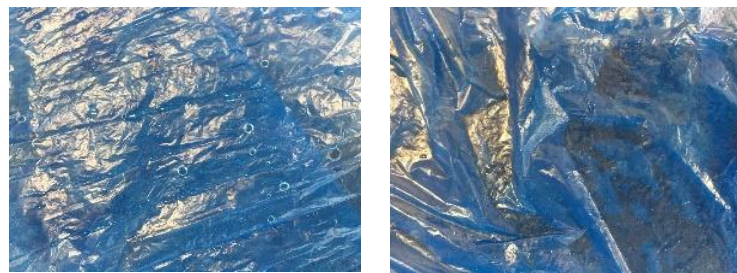


Fig. 10: Observed difference between fresh bag (left) and a bag that has been submerged for 5 weeks (right). Almost no air bubbles are attached to the material.

Other influencing factors on the floating ability of plastic

Volume: The volume of a particle is a key characteristic determine the buoyancy force. Since the plastic was downsized without decreasing the thickness of the material, the volume was constant. A small experiment was conducted with different thicknesses of the plastic sheet. A greater volume resulted in higher rise velocities. Sheets are melted together under low temperature (ironing)

Temperature influence: In a first set of experiments, it became clear that the ambient water temperature has an influence on the rise time of the plastic when using a small container. The average times differed over days in which the temperature differed greatly due to a heatwave. It appeared that the marginal positive buoyant plastics is sensitive for such small changes. Alternating ambient conditions can occur in reality, due to tidal flows, sediment currents, pollution etc.

Orientation of the plastic: It was observed that the orientation of the rectangular, flat sheet, was of importance as well. Higher rise velocities were noticed when the frontal area was smallest, and the sheet would ascend vertically through the water. For bigger sheets, the material would fold and the horizontal versus vertical orientation is of less interest. However, this indicates the complexity of the movement of arbitrary shaped plastics, with respect to spherical sediments and other particles.

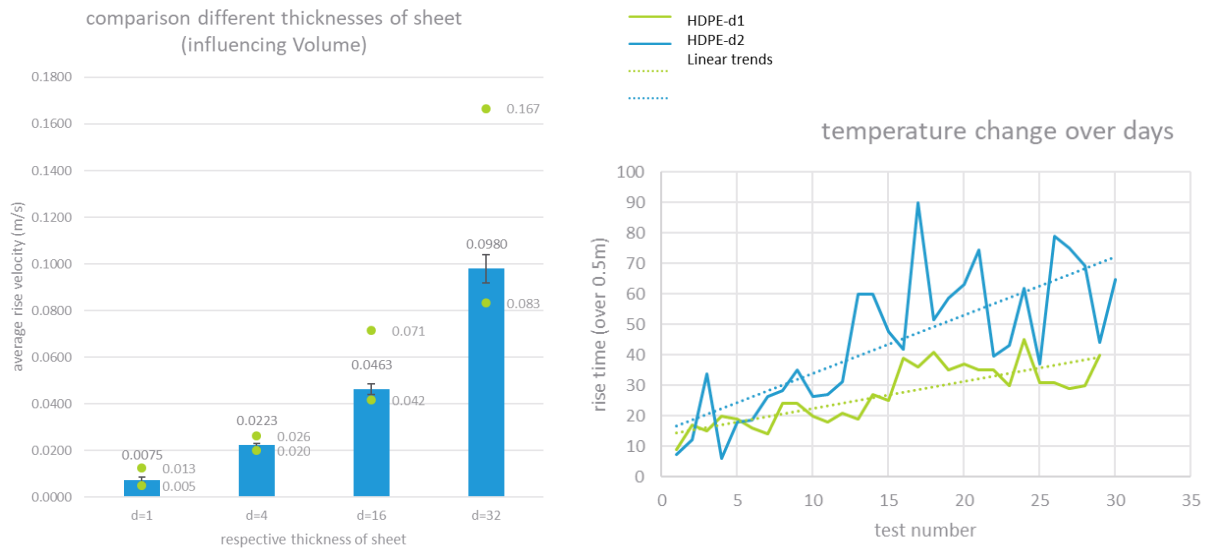


Fig. 11: Left: The thickness is multiplied, d=1 represents a single sheet, d=4 means 4 layers. With this, the volume of the plastic particle is increased (without changing the frontal area). Right: when repeating the rise velocity experiments with the same sheets, the rise time increases (rise velocity decreases). This indicates the effect of watering. Thereby, measurements of two different days show different results, this could be due to the heat wave at day 1

B.3. Additional experiments Gate structure

Two other factors of the gate structure are investigated under an approach flow velocity of 0.34 m/s (experiment number 3). Those factors are:

1. The angle of the gate with respect to the water surface (0 degrees).
2. The influence of the gate on the distribution downstream of the gate.

Results on the first factor are showed in Fig. 12. Results on the second factor are described below. It was seen that for all three orientations of the gate, the distribution in front of the gate only differs slightly. The surface share is about equal (72, 64 and 63% respectively). What is noteworthy, is the difference observed underneath the gate. In case of the 70 degrees gate, which is oriented opposite of the flow direction, more plastic is passing through deeper sections below the gate structure. However, behind the gate it can be seen that plastic is taken in the wake-flow and stirred over the entire water depth. Only for the lowest velocity and 90° orientation, some trapping in front and behind the gate was observed (20% in front, 14% behind). Also, some temporal trapping was observed, in which the plastic was trapped in the wake in front and/or behind the gate but released from the wake during the experiment. For the higher velocities, no trapping or temporarily trapping was observed, irrespective of some stirring behind the gate, in each orientation.

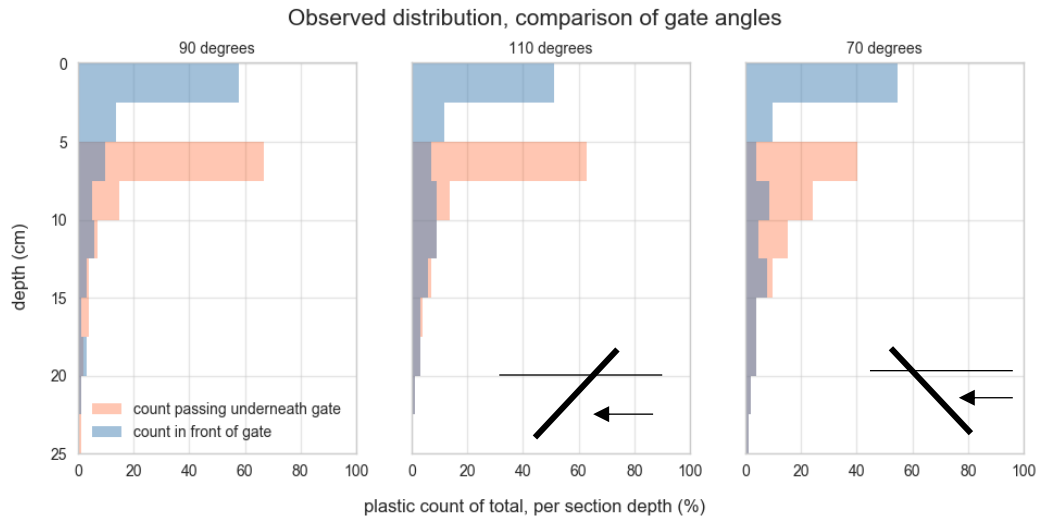


Fig. 12: The gate structure (0-5 cm below water depth) is placed perpendicular to the water, under 110 degrees with the current and under 70 degrees against the current direction. With this last orientation, more plastic is passing via deeper water layers.

Additionally, the development of the vertical distribution behind the gate is monitored. To do so, the setup was changed so that there was enough length behind the gate. It can be seen from Fig. 13 that there is no positive effect on the surface share behind the gate. Plastic is mixed over the water depth behind the gate and most probably develops to an average distribution profile as was found from the experiments in section 5.2. The length however is not enough to develop to a constant distribution, and we cannot use these results as comparison.

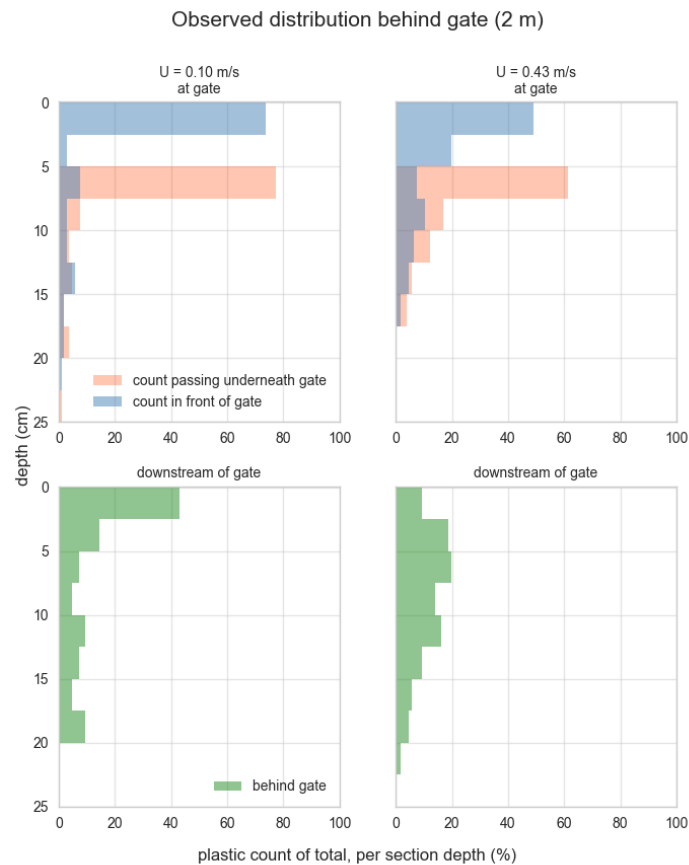


Fig. 13: Behind the gate, plastic is brought in suspension. With higher flow velocities, plastic passes through deeper depths.

B.4. Flume roughness: additional experiment

Plates with gravel were placed in the flume and experiments were conducted as described in this report in Chapter 3.2. The results were not as expected. It was hypothesized that with an increased bed roughness, the resulting shear velocity would increase and therefore, with the same average flow velocities, more mixing of plastic would be observed. From Table 2 it can be seen that this was not the case. For the HDPE plastic, the surface share is lower at 0.2 m/s flow velocity and then shows higher shares for increasing velocities with respect to the ‘smooth’ flow conditions. For the LDPE plastic there is no trend, but also relatively high surface-shares are found. In Fig. 14 the vertical velocity series can be seen. It may be observed that the vertical fluctuation does increase in case of the rougher bed. The observed results for the plastic distribution cannot be explained. These results can be dictated by other processes in the flume setup rather than the influence of an increased friction coefficient. Therefore, these results are neglected in the main report.

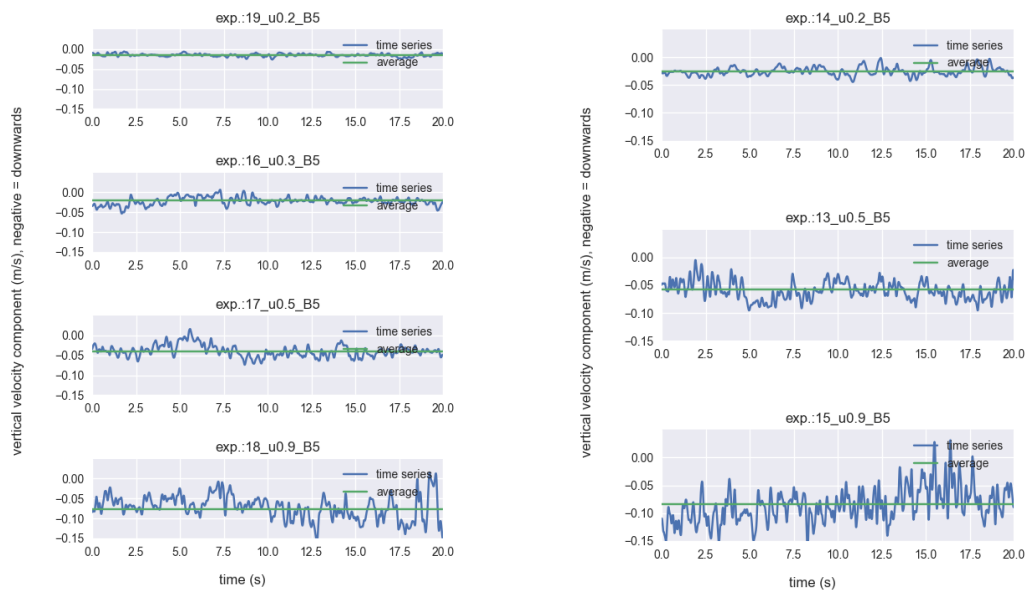


Fig. 14: Vertical fluctuations of velocity at half-depth for a smooth bed (left) and rough bed (right), for a stream velocity of 0.2 to 0.9 m/s. For the rough bed, greater fluctuations are seen and we can expect higher shear velocities.

Table 2: Surface shares for increased bed roughness scenarios

Experiment number	1	2	3	4	5	6	7
U_{da} flow velocity (m/s)	0.10	0.20	0.35	0.45	0.55	0.65	0.95
U_* shear velocity (cm/s)	0.5	1.1	1.6	2.2	2.7	3.3	4.9
HDPE Smooth Surface share (%)	95	74	52	34	28	25	17
HDPE Rough Surface share (%)		51			45		21
LDPE Smooth Surface share (%)	28	15	33	22	10	15	25
LDPE Rough Surface share (%)		13			43		17

Experiment setup and considerations

C.1. Flume setup

A more elaborate description of the flume setup used for the experiments is given in this section, belonging to Chapter 3.2.1. The setup is schematically shown in Fig. 15.

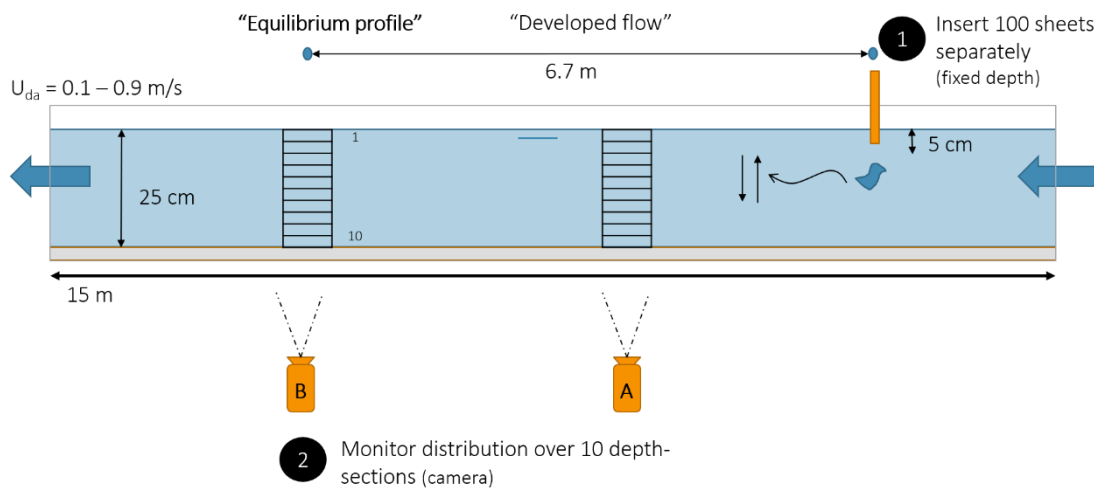


Fig. 15: Flume setup for vertical distribution observations. Location B serves as measurement location, location A as reference.

Dimensions flume: The flume has a length of 15 m and width of 0.40 m (figure). The water depth in the flume is kept constant for every velocity experiment to create equally scaled distribution profiles. Based on the dimensions of the flume and desired range of flow velocities, the depth is set on 0.25 m. The setup is schematically visualized in figure X, in which distances and dimensions are given. For the sake of developed flow and a possibility for an equilibrium distribution of plastics, length scales are of importance. There must be a considerable distance between measuring location and flume in- and outlet. In addition, there must be a considerable distance between the inlet of plastic and measuring location; taking into account both the longitudinal flow velocity, vertical shear velocity and the rise velocity, it must be possible for the plastic to be distributed over the entire water depth.

Velocity range: The velocity range in the flume is from 0.10 m/s up till 0.90 m/s, under a constant water depth of 25 cm. Based on the bed friction coefficient of the flume in relation to a prototype river, 0.003 and 0.005 respectively, this range is applicable for the experiments to be compared to prototype conditions of 0.1 – 0.5 m/s.

Geometrically scaling: Based on the plastic sheets and flume dimensions, a geometrical scaling factor of 1:10 is chosen. The 'water surface' equals 50 cm (as described in the introduction, section 1.2). In the flume, this equals 5 cm. The influence of water depth on the distribution of plastic is not further investigated. The sheets are cut out of the two prototype bags, the thickness (and elasticity/ deformability) of the sheets is therefore not scaled. This is neglected for simplicity.

Plastic inlet: At 2.5 meters from the inlet of the flume, plastic is released through a pipe (diameter = 2 cm) at 5 cm below the water surface ($1/5^{\text{th}}$ of total depth). This depth is mostly based on a set of preliminary trial and error experiments: Plastic is not released at the surface, because suspension is prevented due to surface tension. Releasing plastic just under the surface gives the plastic the opportunity to move over the entire depth before it reaches the measuring location (based on the average rise velocity and the flow velocities in the flume). Since we want to indicate mixing, and therefore especially downward movement, releasing plastic near the flume bed is not ideal.

Measuring the distribution (camera): At two locations, A and B, cameras are used to capture the position of the plastic sheet over depth. The depth is divided in 10 sections, of each 2.5 cm. The times that a sheet is present in each section is count. After a pre-analysis, only location B is considered as reliable measuring location. This is because of the distance between the inlet of the plastic and the camera location A, in relation to the rise velocity and average flow velocities used; The distance should be great enough to ensure a developed distribution, which is assumed for location B. The data retrieved from location A is used to check whether a downward movement, and therefore mixing, does occur. A threshold of 10 % is chosen to indicate mixing, meaning that if less than 10 % of the tested sheets shows downward movement between location A and B, the distribution of the plastic at location B may be due to effects of the inlet method rather than mixing ability of the flow. In that case the shear-velocity is considered as 'below mixing threshold'.

Number of experiments: Each velocity experiment (7 experiments) is conducted once (for the sake of time), in which 100 sheets of both plastics are released one by one.

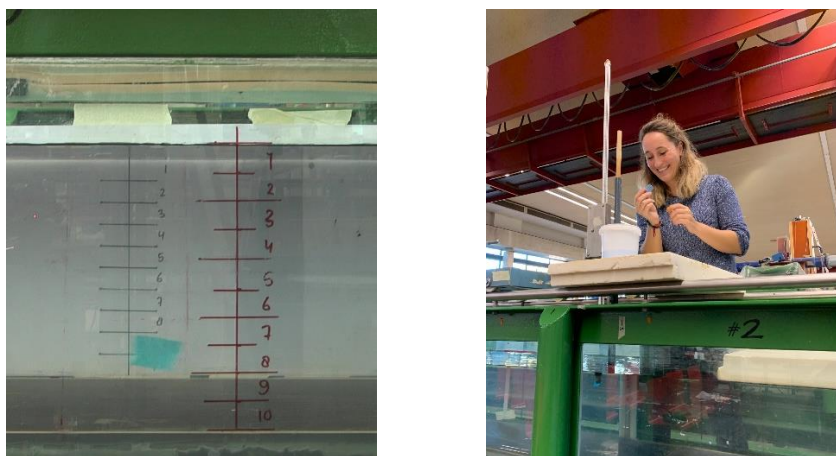


Fig. 16: Flume setup for vertical distribution observations. Location B serves as measurement location, location A as reference. Plastic is manually put in the flume at a constant location.

C.2. Flow development over flume

The flow profile was investigated in order to setup the experiment. Measurement location A and B were compared to see if both of them could be used as measurement location for the plastic distribution. This would only be possible for lower flow velocities, because the length until measurement location must be long enough for the plastic sheet to find an 'equilibrium position over depth'. With too high flow velocities, the rise velocity of 0.010 m/s would be too low to be able to bring the sheet to the surface. It was found that the velocity profiles differ between A and B, especially for higher flow velocities. It is decided to only use location B as measurement location and A as reference. Secondly, it is checked if there is a certain influence of the inlet (height) and the foam plate used to smoothen the flow at the inlet. From Fig. 17 it can be seen there is no influence noticed. In Fig. 18 it may be observed there is a decrease of the flow velocity near the surface. The measurement equipment is sensitive for interfering signals, the vertical differences in flow velocities could partly be an effect of this sensitiveness since the measurements are manually done per height. However, a 'velocity-dip' at the surface is also a more often seen phenomenon in channel flow.

Lastly, the vertical component of the flow is investigated. Due to the sensitivity of the equipment, the found flow is not considered as absolute information. The average vertical velocity should equal 0. The fluctuation

around the average however can be compared for increasing velocities. In Fig. 19 it may be observed that with increasing velocities, the vertical fluctuation increases and therefore so does the shear velocity.

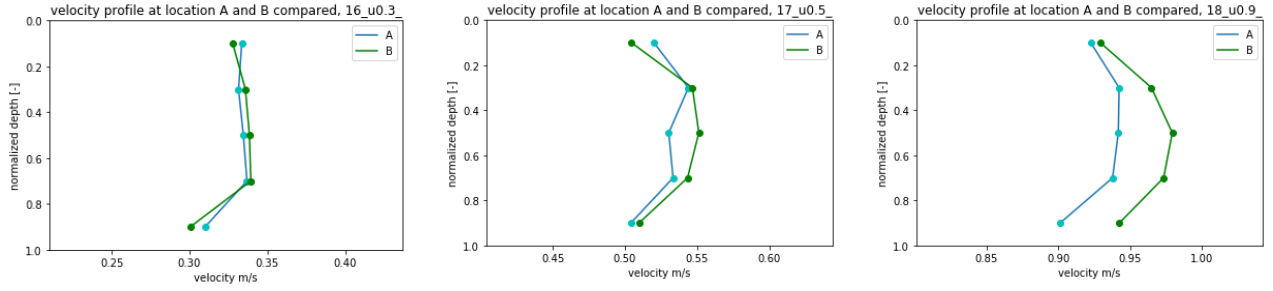


Fig. 17: Stream flow velocity measurements in flume at (1) 0.3 m/s, (2) 0.5 m/s and (3) 0.9 m/s average flow velocity, at location A and B in flume. With higher velocities, the profiles diverge more from each other. B is considered as ‘developed flow’

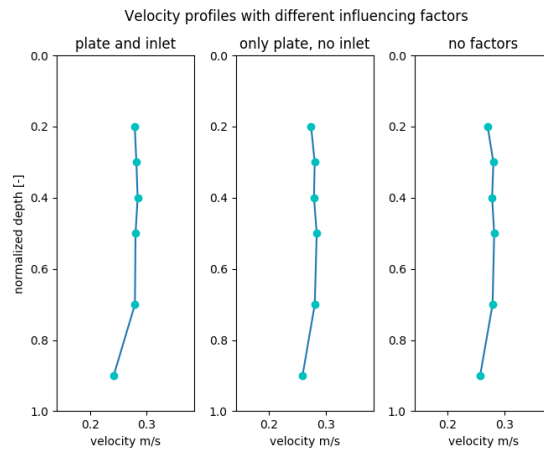


Fig. 18: Influence of the setup components in the flume are examined. These are a (foam) plate at the inlet, decreasing waves, and the inlet pipe through which plastic is inserted. These components do not influence the flow

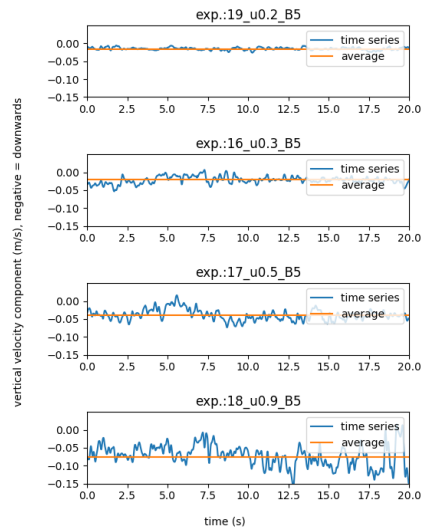


Fig. 19: Velocity fluctuation over depth, at half water depth for 0.2, 0.3, 0.5 and 0.9 m/s (above to below). With an increasing flow velocity, the fluctuation around the average increases.

C.3. Impression of lab experiments



Fig. 20: A: HDPE bag and different sizes of sheets, B: the container used for rise velocity experiments with different scales, C: the tank used for the rise velocity experiments with bags and foils, D: an obstruction placed in the flume. In this scenario it is a bottom sill (5 cm).

Fieldwork: Borgharen Sluice

The ambition during this master thesis was to compare the lab results in with findings from the field. Field measurements are however difficult, no general method exist for the sampling of plastics, especially not over the entire water depth. During this research, I was brought in contact with Rijkswaterstaat. The Borgharen sluice in Maastricht is not in use anymore, and the plan existed to develop a 1:1 scale river test facility. Together with Rinze de Vries of the startup Noria, I have investigated the possibility of research to the vertical distribution of plastic in this sluice. Unfortunately, the conclusion after a week of testing flow conditions was that this possibility is not yet there. The sluice is too turbulent due to the inlet method. A study to the distribution of plastic would only represent the motion of plastic in this specific sluice and could therefore not be compared to lab results. The developments around the sluice are however promising. Because more startups and projects are involved, Rijkswaterstaat is exploring opportunities to improve the flow conditions in this sluice, in order to create more uniform flow. The sluice doors and inlet gates will be altered by the coming year (2020). This offers great opportunities for students of the TU Delft (and other universities) in cooperation with relevant startups and organizations. In this appendix, a short overview of the measurements conducted in the flume is given, indicating the complex situation that was not suitable for further research. For more information and contacts, please contact me (the author of the report).

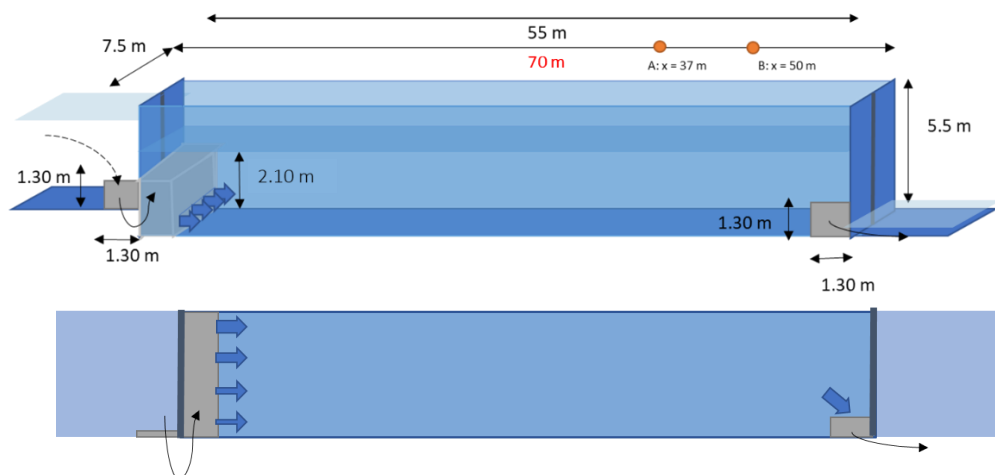


Fig. 21: Borgharen sluice schematically. Below: top view.

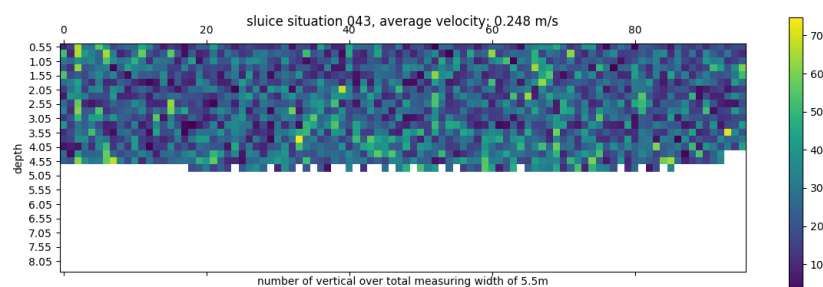


Fig. 22: flow velocity measurements with ADCP catamaran. Average flow velocity = 0.25 m/s. There is no uniform profile in the sluice, the flow velocity varies greatly, both temporal as spatial.

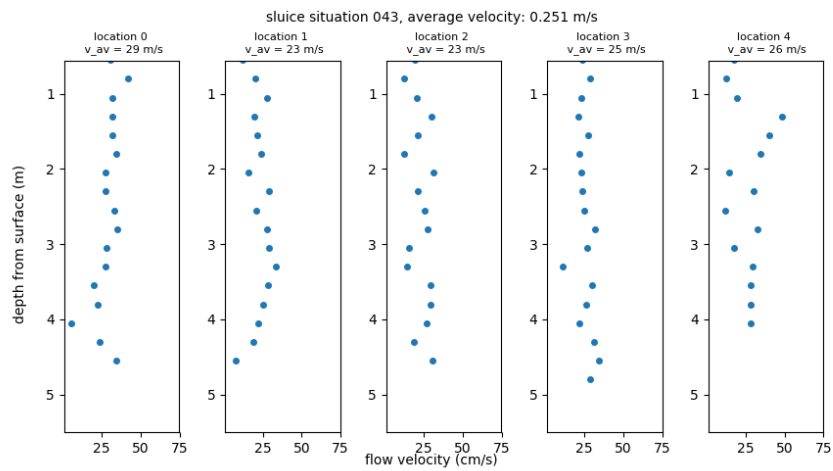


Fig. 23: Vertical profiles of flow velocities over transect. The datapoints are averaged over



Fig. 24: Impression of Borghare Sluice measurements. A: sluice next to Grensmaas, B: inlet doors and inlet sewers below, C: flow measurements with ADP flow meter, D: flow measurements with ADCP catamaran, executed by RWS.

Plastic Problem in figures

For plastic classification, different approaches are used. In Table 3 a combination of classifications as found in literature is shown, including remarks on the buoyancy, based on the found material density. However, due to the use of multilayered plastic, additives and dye, the density can differ from factory-specifications. Plastic bags form a great part of the plastic litter found in rivers, natural water bodies and on beaches (Fig. 25). These plastics are very harmful because of their form. They are often confused for food by marine wildlife and are a cause of suffocation. These plastic bags are presumed to be buoyant because of their material density and expected to float at the surface (Fig. 26). However, as was found in this MSc research, this (marginally) positive buoyant plastic can be brought in suspension and therefore missed when focusing on the surface plastics. This is part of an explanation to the “**Missing plastic question**” that is growing in publicity (Lebreton et al., 2019). The balance of production and observation is not closed. Other explanations are e.g. degradation and circulation dynamics on a great scale. While conducting this MSc research, more studies and reviews were published considering the transport mechanism of plastic. Something that was found to be missing. In yet unpublished work, Sebille et al, (2019) made a review of the existing literature on transport of floating marine plastic debris, referring to insights from neighboring fields. As was stated as underlying goal of this thesis. Fig. 27 shows an overview of processes defined in the ocean.



Fig. 25: Top 10 trash found during the International Coastal Cleanup 2017 (Ocean Conservancy). Plastic bags were abundantly found

Which plastics float and which sink in seawater?

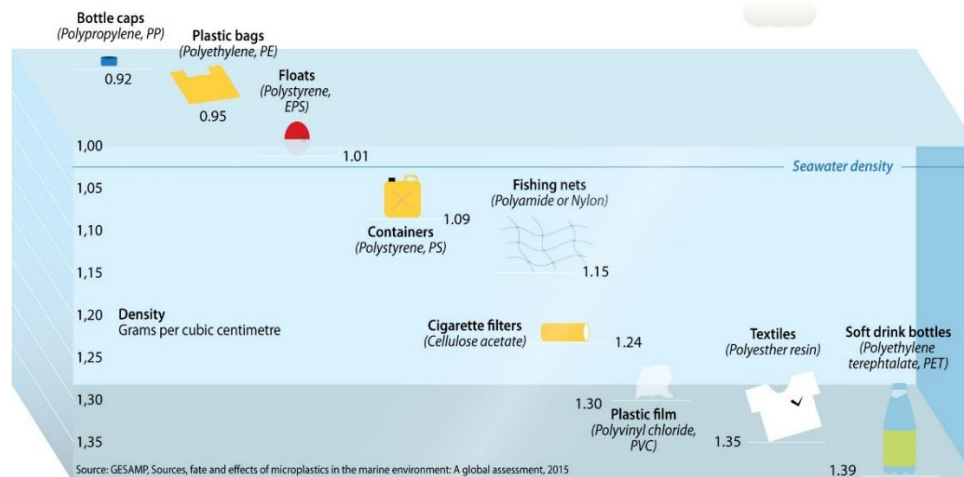


Fig. 26: Classification of plastics by their floating ability in sea water ($\rho=1.02-1.03 \text{ g/cm}^3$)

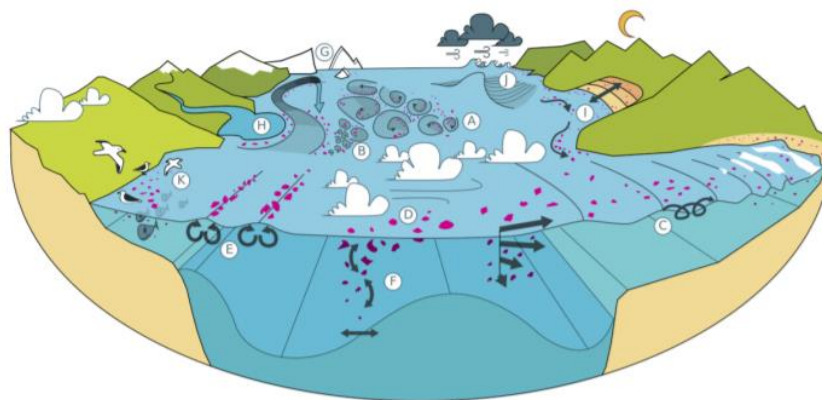


Fig. 27: Schematic of the physical processes that effect the transport of plastic the ocean (Sebille et al., 2019).

Table 3: classification of plastic types (based on a combination of different classes found in literature)

Type	Sub	Sub2	Name	Product	Buoyant/density
PET			Polyethylene terephthalate	Bottles soft drinks, salad containers	Non buoyant 1.38-1.39 g/cm ³
PS			Polystyrene	Plastic cutlery, cups, casings, toys	Non buoyant 1.05 g/cm ³
		EPS	Expanded polystyrene	Foams, packing material, foam cups, meat trays	buoyant
PO			Polyolefin		
		PP	Polypropylene	Plastic furniture, jerry cans, bottle tops, straws, chips bags, ice cream tubs	Buoyant 0.90 g/cm ³
		PE	Polyethylene		buoyant
		LDPE	Low-density polyethylene	Soft plastics, cling film, carry bags	0.92-0.93 g/cm ³
		HDPE	High-density polyethylene	Containers, pipes, shampoo bottles, milk bottles	0.94-0.97 g/cm ³
PVC			Polyvinylchloride	Sewage pipes, window frames	Non buoyant 1.29-1.44 g/cm ³
O			Other		



MEDASSET

**Mediterranean Association
to Save the Sea Turtles**

Fig. 28: example of a campaign against plastic bags. Bags are often confused for food and cause entanglement and suffocation of marine life (Medasset, n.d.)

F

Photo impressions



Fig. 29: A: Press day at Borgharen Sluice with team RWS and Noria. B: With the help of RWS testing in the sluice. C: Competition of Dopper, for the best thesis award (unfortunately there was no best proposal price). D: Pitching my research proposal at the Dopper challenge.

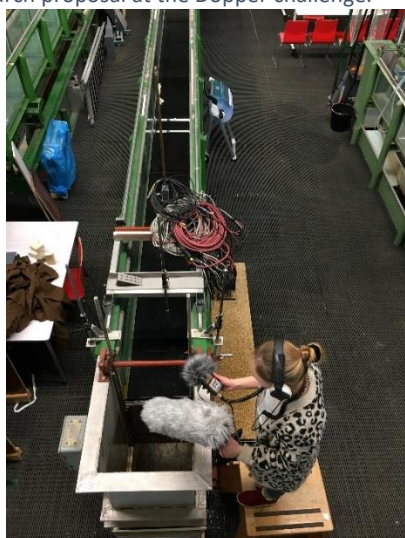


Fig. 30: Interview for artist (sound artist) about plastic research.